

241

0-315-12552-7

 National Library of Canada

Bibliothèque nationale du Canada

Canadian Theses Division / Division des thèses canadiennes

Ottawa, Canada
K1A 0N4

60463

PERMISSION TO MICROFILM — AUTORISATION DE MICROFILMER

• Please print or type — Écrire en lettres moulées ou dactylographier

Full Name of Author — Nom complet de l'auteur

Artur Semftleben

Date of Birth — Date de naissance | Country of Birth — Lieu de naissance

May, 12, 1982

Germany

Permanent Address — Résidence fixe

Am Hornbusch 23
4132 Kamp-Lintfort
Federal Republic of Germany

Title of Thesis — Titre de la thèse

Geometric Nonlinear Analysis of Circular Cylindrical Shells

University of Alberta, Edmonton, Alberta
University — Université

Master of Science
Degree for which thesis was presented — Grade pour lequel cette thèse fut présentée

1982
Year this degree conferred — Année d'obtention de ce grade

Dr. Terry Hrudex
Name of Supervisor — Nom du directeur de thèse

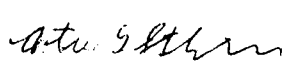
Permission is hereby granted to the NATIONAL LIBRARY OF CANADA to microfilm this thesis and to lend or sell copies of the film.

L'autorisation est, par la présente, accordée à la BIBLIOTHÈQUE NATIONALE DU CANADA de microfilmer cette thèse et de prêter ou de vendre des exemplaires du film.

The author reserves other publication rights, and neither the thesis nor extensive extracts from it may be printed or otherwise reproduced without the author's written permission.

L'auteur se réserve les autres droits de publication; ni la thèse ni de longs extraits de celle-ci ne doivent être imprimés ou autrement reproduits sans l'autorisation écrite de l'auteur.

Date
June, 10, 1982

Signature


CANADIAN THESES ON MICROFICHE

I.S.B.N.

THESES CANADIENNES SUR MICROFICHE



National Library of Canada
Collections Development Branch

Canadian Theses on
Microfiche Service

Ottawa, Canada
K1A 0N4

Bibliothèque nationale du Canada
Direction du développement des collections

Service des thèses canadiennes
sur microfiche

NOTICE

The quality of this microfiche is heavily dependent upon the quality of the original thesis submitted for microfilming. Every effort has been made to ensure the highest quality of reproduction possible.

If pages are missing, contact the university which granted the degree.

Some pages may have indistinct print especially if the original pages were typed with a poor typewriter ribbon or if the university sent us a poor photocopy.

Previously copyrighted materials (journal articles, published tests, etc.) are not filmed.

Reproduction in full or in part of this film is governed by the Canadian Copyright Act, R.S.C. 1970, c. C-30. Please read the authorization forms which accompany this thesis.

THIS DISSERTATION
HAS BEEN MICROFILMED
EXACTLY AS RECEIVED

AVIS

La qualité de cette microfiche dépend grandement de la qualité de la thèse soumise au microfilmage. Nous avons tout fait pour assurer une qualité supérieure de reproduction.

S'il manque des pages, veuillez communiquer avec l'université qui a conféré le grade.

La qualité d'impression de certaines pages peut laisser à désirer, surtout si les pages originales ont été dactylographiées à l'aide d'un ruban usé ou si l'université nous a fait parvenir une photocopie de mauvaise qualité.

Les documents qui font déjà l'objet d'un droit d'auteur (articles de revue, examens publiés, etc.) ne sont pas microfilmés.

La reproduction, même partielle, de ce microfilm est soumise à la Loi canadienne sur le droit d'auteur, SRC 1970, c. C-30. Veuillez prendre connaissance des formules d'autorisation qui accompagnent cette thèse.

LA THÈSE A ÉTÉ
MICROFILMÉE TELLE QUE
NOUS L'AVONS REÇUE

THE UNIVERSITY OF ALBERTA

GEOMETRIC NONLINEAR ANALYSIS OF CIRCULAR CYLINDRICAL SHELLS

by

©

ARTUR SENFTLEBEN

A THESIS

SUBMITTED TO THE FACULTY OF GRADUATE STUDIES AND RESEARCH
IN PARTIAL FULFILMENT OF THE REQUIREMENTS FOR THE DEGREE
OF MASTER OF SCIENCE

IN

CIVIL ENGINEERING

DEPARTMENT OF CIVIL ENGINEERING

EDMONTON, ALBERTA

FALL, 1982

THE UNIVERSITY OF ALBERTA

RELEASE FORM

NAME OF AUTHOR

ARTUR SENFTLEBEN

TITLE OF THESIS

GEOMETRIC NONLINEAR ANALYSIS OF CIRCULAR CYLINDRICAL
SHELLS

DEGREE FOR WHICH THESIS WAS PRESENTED MASTER OF SCIENCE

YEAR THIS DEGREE GRANTED 1982

Permission is hereby granted to THE UNIVERSITY OF ALBERTA LIBRARY to reproduce single copies of this thesis and to lend or sell such copies for private, scholarly or scientific research purposes only.

The author reserves other publication rights, and neither the thesis nor extensive extracts from it may be printed or otherwise reproduced without the author's written permission.

(SIGNED) *Artur Senftleben*

PERMANENT ADDRESS:

Am Hornbusch 23

4132 Kamp-Lintfort

Federal Republic of Germany

DATED 9th of June, 1982

THE UNIVERSITY OF ALBERTA
FACULTY OF GRADUATE STUDIES AND RESEARCH

The undersigned certify that they have read, and recommend to the Faculty of Graduate Studies and Research, for acceptance, a thesis entitled GEOMETRIC NONLINEAR ANALYSIS OF CIRCULAR CYLINDRICAL SHELLS submitted by ARTUR SENFTLEBEN in partial fulfilment of the requirements for the degree of MASTER OF SCIENCE in CIVIL ENGINEERING.

T. Hardy

.....
Supervisor

Gay Faulkner

J. Hammond

Date. 4th June, 1982

Abstract

A modification to a previously developed finite element for circular cylindrical shells is presented and its linear and nonlinear stiffness matrices are defined. The element is tested on various linear and nonlinear problems and shows good agreement for cases which have already been investigated with finite elements. The linear bending of circular cylinders is extensively discussed and the element displacement field is checked for its approximations towards the linear bending theory. The induced stresses for rigid body motions are studied for the element and it is successfully tested on the nonlinear problems of a pinched barrel vault and a circular arch. This work concludes with the geometric nonlinear bending analysis of circular cylinders. Recommendations for further studies are given.

Acknowledgement

The author wishes to thank Dr. Terry Hrudehy for his interest and support for this project and acknowledges the financial support by the National Science and Engineering Research Council.

The author also extends his thanks to Thomas Casey and various staff members of the Department of Computing Services for their invaluable help with textformatting and programming problems.

Table of Contents

Chapter	Page
1. Introduction	1
2. Literature Review	4
2.1 Analytical Approaches	4
2.2 Finite Elements for Cylindrical Shells	7
2.3 Finite Elements Based on Strain Functions	13
3. Formulation of a New Strain Element	19
3.1 Displacement Function	19
3.2 Formulation of the Strain Energy Expression	22
3.3 Derivation of the Stiffness Matrices	25
3.4 Newton-Raphson Method Solution Procedure	27
4. Linear Solutions	32
4.1 Pinched Cylinder Problem	32
4.2 Cylinder under Bending	36
4.2.1 Boundary Conditions and Theoretical Results	36
4.2.2 Element Approximation of Cylinder under Bending	40
4.2.3 Results of Linear Tests	43
5. Nonlinear Problems	59
5.1 Introduction	59
5.2 The Circular Arch	60
5.3 The Barrel Vault Problem	66
5.4 Nonlinear Strains and Rigid Body Motions	70
5.4.1 Rotation around the \bar{x} -Axis	70
5.4.2 Rotation around the \bar{y} -Axis	71
5.4.3 Rotation around the \bar{z} -Axis	74
5.4.4 Summary of the Rigid Body Rotations	77

5.5 Cylinder under Bending	80
5.5.1 Review of Earlier Investigations	80
5.5.2 Boundary Conditions and Their Representation	81
5.5.3 Prescribed Displacements at the Cylinder Ends	82
5.5.3.1 Shortening of Cylinder due to Bending	83
5.5.3.2 Nonlinear Boundary Conditions for End Rotation	85
5.5.4 Discussion of Test Results	88
5.5.4.1 Rigid and Semi-Rigid Cylinder Ends ..	88
5.5.4.2 The Short Cylinder	91
5.5.4.3 The Long Cylinder	96
6. Summary and Conclusions	104
References	107
Appendix A.1: Inverse of the Matrix [T]	113
Appendix A.2: Linear Strain Fields in Terms of Nodal Displacements	115
Appendix B.1: Listing of the Finite Element Program	117
Appendix B.2: Input Description	157

List of Tables

Table	Description	Page
4.1	Deflection of Thick Pinched Cylinder under Load.	34
4.2	Deflection of Thin Pinched Cylinder under Load.	.35
4.3	Approximations of the Element Displacement Field.	41
4.4	Cylinder Data for Linear Bending Tests.	43
4.5	Ratio of Bottom Fibre Centre Deflections to Beam Theory for Long Cylinder with Rigid Ends.	45
4.6	Ratio of End Moment to Beam Theory for Long Cylinder with Rigid Ends.	45
4.7	Ratio of Computed Δv to Donnell Solution for Long Cylinder with Rigid Ends.	46
4.8	Ratio of End Moment to Beam Theory for Long Cylinder with Semi-Rigid Ends.	49
4.9	Ratio of Computed Δv to Donnell Solution for Long Cylinder with Semi-Rigid Ends.	49
4.10	Ratio of Bottom Fibre Deflection to Beam Theory for Short Cylinder with Rigid Ends.	50
4.11	Ratio of Computed Δv to Donnell Solution for Short Cylinder with Rigid Ends.	51
4.12	Ratio of End Moment to Beam Theory for Short Cylinder with Rigid Ends.	51
4.13	Ratio of Computed Δv to Donnell Solution for Short Cylinder with Semi-Rigid Ends.	55
4.14	Ratio of Cylinder Moment to Beam Moment for Short Cylinder with Semi-Rigid Ends.	55
5.1	Loads (lbs) for Prescribed Deflections of Two Cylindrical Arches.	65
5.2	Loads for Prescribed Deflections of a Hinged Barrel Vault under Single Load.	69
5.3	Circumferential Strain Induced by Rotation around the \bar{y} -Axis.	74

5.4	Circumferential Strain Induced by Rotation around the z -Axis.	77
5.5	Maximum of Induced Strains from Rigid Body Motions.	77
5.6	Ratio of $\max \bar{\epsilon} / \bar{\epsilon}_{cr}$ for Three Cylinders.	84
5.7	Effects of Axially Fixed Ends and Prescribed Circumferential Strain on the Long Cylinder by Stephens <i>et al.</i> with 4×2 Elements and $\beta = \beta_{cr}$. ..	89
5.8	Nonlinear Results of Short Cylinder under Bending.	91
5.9	Nonlinear Results of Long Cylinder under Bending.	97
5.10	Ovalization of Long Cylinder under Bending.	98

List of Figures

Figure	Description	Page
2.1	Local Coordinate System for a Thin Cylindrical Shell.	8
2.2	Shell Element with Local and Global Axes.	16
3.1	Element with Centre Coordinate System and Corner Nodes.	21
3.2	The Newton-Raphson Method for a One-Degree-of-Freedom System.	30
4.1	Pinched Cylinder under Load with Element Mesh for One Octant.	32
4.2	Left Half of Cylinder under Bending with Linearized Boundary Conditions.	36
4.3	Slope Variation of Long Cylinder with Rigid Ends.	47
4.4	Variation of Parameter Δv for Long Cylinder with Rigid Ends.	48
4.5	Deflection of Short Cylinder with Rigid Ends.	52
4.6	Variation of Δv of Short Cylinder with Rigid Ends.	54
5.1	Circular Arch under Concentrated Load.	60
5.2	Load Deflection Curve for Cylindrical Arch (R=250 in.) under Concentrated Load.	63
5.3	Load Deflection Curve for Cylindrical Arch (R=150 in.) under Concentrated Load.	64
5.4	Hinged Barrel Vault under Single Load.	66
5.5	Load Deflection Curve of a Hinged Barrel Vault under Single Load.	68
5.6	Stresses for Short Cylinder at Mid-Section for $\beta = 0.4 \beta_{cr}$	94
5.7	Incremental Deflections of Long Cylinder under Bending.	100
5.8	Stresses of Long Cylinder at $\beta = 0.3 \beta_{cr}$	102

List of Symbols

Special Symbols

$\langle \rangle, \{ \}^T$	denotes row vectors
$\{ \}, \langle \rangle^T$	denotes column vectors
$[]$	denotes a matrix
$[]^{-1}$	denotes a matrix inverse
$[]^T$	denotes a transposed matrix
$ $	denotes a determinant of a matrix or a vector norm
\cdot	denotes differentiation of preceding expression with respect to the following variables
<u> </u>	underlined term includes nonlinear parts
<u> </u>	underlined strain term includes in-plane and out-of-plane strain contributions

Roman Symbols

A	area described by middle surface of shell element
$\langle B_x \rangle$, $\langle B_\theta \rangle$, $\langle B_u \rangle$, $\langle B_v \rangle$	displacement derivatives defined in Eq. 3.16
c	$\cos(p)$
C	in-plane plate stiffness $Et/(1-\nu^2)$
D	plate bending stiffness $Et^3/12(1-\nu^2)$,
E	Young's modulus
[E]	elasticity matrix
I	moment of inertia
[I]	identity matrix
$[K^T]$	tangent stiffness matrix
K^2_{ij} , K^3_{ijk} , K^4_{ijkl}	stiffness coefficient of second, third and fourth order, respectively
k_x	curvature in x-direction
k_θ	curvature in θ -direction
$k_{x\theta}$	twisting curvature
l	half length of element
L	length of cylinder
Le	distance from left end of cylinder
\bar{L}	cylinder length after bending with fixed ends
m	number of buckles in longitudinal direction
M	cylinder end moment

M_B	critical cylinder moment by Brazier (Eq. 2.4)
M_{cr}	cylinder moment causing δ_{cr}
N	axial force in cylinder
N_{cr}	axial force in cylinder causing δ_{cr}
NP	number of elements in the circumferential direction
NX	number of elements in the longitudinal direction
$2 p$	angle prescribed by cylindrical shell element
P	magnitude of a single concentrated load
$\{q\}$	nodal displacement vector
$\{q^i\}$	nodal displacement vector after i -th equilibrium iteration
$\{Q\}$	nodal force vector
$\{Q^i\}$	nodal force vector after i -th equilibrium iteration
R	radius of cylinder or cylindrical element
\bar{R}	radius of curvature of cylinder under bending
s	$\sin(p)$
t	shell thickness
$[T]$	coefficient matrix relating generalized degrees of freedom α_i to nodal displace- ments
U	strain energy

u, v, w displacements in x-y-z coordinate
directions, respectively
 W potential of external forces
 x, \bar{y}, z local element coordinates
 $\bar{x}, \bar{y}, \bar{z}$ global element coordinates
[0] zero-matrix

Greek Symbols

α_i	i-th parameter of displacement function (Eq. 3.1)
$\{\alpha\}$	vector of displacement parameters α_i
$\langle \alpha x \rangle, \langle \alpha \phi \rangle,$ $\langle \alpha x \phi \rangle$	bending strain field defined by Eq. 3.16.
β	end rotation of cylinder
β_{cr}	end rotation causing δ_{cr}
$\beta_{x_1}, \beta_{x_2},$ $\beta_{x_3}, \beta_{\phi_1},$ $\beta_{\phi_2}, \beta_{\phi_3}$	displacement derivatives defined by Eq. 3.13
β_x, β_ϕ	rotation of the tangent to the mid-surface about the local x and ϕ axes, respectively
$\gamma_{x\phi}$	linear shear strain
$\underline{\gamma}_{x\phi}$	nonlinear shear strain
Δ	as a prefix denotes an increment, alone denotes a rigid body rotation
ΔL	elongation of cylinder due to bending with fixed ends
Δv	vertical deflection of cylinder side due to circumferential stretching
Δw	ovalization of cross-section of cylinder under bending
$\{\epsilon\}$	vector of strain components
ϵ_x	linear strain in x-direction
$\underline{\epsilon}_x$	nonlinear strain in x-direction

ϵ_θ	linear strain in θ -direction
$\underline{\epsilon}_\theta$	nonlinear strain in θ -direction
ϵ_θ^*	circumferential strain induced by rigid body motions
$\langle \theta_x \rangle, \langle \theta_\theta \rangle$	in-plane strain fields defined by Eq. 3.16
$\langle \theta_{x\theta} \rangle$	
ν	Poisson's ratio
Π	potential energy
$\{\sigma\}$	stress vector
σ_B	Brazier's critical stress
σ_{cr}	classical elastic buckling stress for axially loaded cylinder
σ_x	longitudinal stress
σ_θ	circumferential stress
$\bar{\sigma}$	longitudinal stress of cylinder with axially fixed ends under bending
$\tau_{x\theta}$	shear stress
θ	circumferential element coordinate = y/R
$\bar{\theta}$	cylinder angle, measured from the top fibre
θ°	cylinder angle, measured from the side edge downwards

1. Introduction

Since the development of shell theories around 1900, an increasing interest has been shown in the behaviour of circular cylinders under various loads.

Flügge¹ solved the linear elastic buckling problem of circular cylinders under compression and bending by using a simplified shell theory. The discrepancy between his theoretical results and the loads from structural tests activated researchers to study the effect of initial imperfections and residual stresses, which may significantly reduce the load. Another problem of comparing analytical loads with test results is the definition of appropriate boundary conditions at the cylinder ends, which are often selected to facilitate the analysis. In structural tests similar difficulties are encountered with boundary conditions. The appropriate assessment of flexible or rigid boundaries is a necessity to avoid unexpected collapse loads.

As opposed to the failure of a thin-walled cylinder under compression, the buckling of a cylinder under bending occurs after large elastic deformations take place. The deflections, even for moderate dimensions, can be in the order of 20 times the wall thickness. Analysis of this problem requires a large displacement formulation. Short thin-walled cylinders under bending show a buckling mode with longitudinal wrinkles, whereas cylinders with a high length-to-radius ratio fail due to ovalization of the cross-

section. With increasing moment the bending stiffness and the section modulus are reduced. Cylinders with moderate dimensions may exhibit a combination of these two modes (Stephens *et al.*²³, Flügge²⁴) which complicates the analysis. With the assumption of particular displacement functions or buckling modes the limit load is easily overestimated which explains the somewhat scattered data from analytical studies.

In the last few decades, thin-walled cylinders have been used extensively in off-shore drilling platforms and aerospace vehicles. With the use of cylinders in space structures there was a need to reduce the weight as much as possible. This led to very thin-walled structures. As a consequence the elastic buckling problem has been emphasized since the inelastic buckling prevails in thicker-walled structures. One of the latest achievements in the analysis and design of thin cylinders are to be seen in the Skylab and Space Shuttle programs of the National Aeronautics and Space Administration.

The motivation for this study lies in the design of circular steel cylinders for the use as long-span beams. Such cylinders are often used for surface pipelines which are subject to large bending moments. Another application are galleries which support conveyor systems for the transport of loose materials. These long-span cylinders are primarily stressed by bending moments so that the present

study deals mainly with cylinders under pure bending and excludes torsional moments, shear forces, and axial loads.

Following this introduction a review of analytical studies in circular cylinders and finite elements for cylindrical shells is given. Then a modification to a previous finite element is presented whose displacement functions are based on an assumed strain field. The stiffness matrices are defined and the solution procedure is described. After the linear test problem of a pinched cylinder the linear bending of circular cylinders is discussed and the approximations of the element displacement field are investigated. Next the element is applied to the geometric nonlinear problems of a pinched barrel vault and a circular arch under single load. Then the strains induced by rigid body motions of a cylinder under bending are discussed. The strains caused by axially fixed ends of a cylinder under bending are computed and the nonlinear boundary conditions for rigid cylinder ends are given. After a discussion of the circumferential stretching associated with the linear Donnell solution for cylinders under bending, various boundary conditions are tested. Finally the results for the geometrically nonlinear bending of two cylinders are presented and compared with results from previous studies.

2. Literature Review

2.1 Analytical Approaches

The buckling moment for a cylindrical shell under bending was, in early studies, correlated to the buckling stress of a cylinder under compression. The classical solution for the latter case was derived by Flügge²⁵. The displacement function he used was a combination of trigonometric functions in the longitudinal and circumferential direction. With the assumption that the stresses do not change during initial deformations, his analysis can be described as a linear elastic buckling problem. He assumed that the displacements are infinitesimally small and derived a stability criterion using the principle of minimum potential energy. Neglecting certain strain terms, he obtained the critical stress $\bar{\sigma}_{cr}$ for an axially compressed cylinder:

$$\bar{\sigma}_{cr} = Et/R \cdot [3(1-\nu^2)]^{-0.5} \quad (2.1)$$

$$= 0.605 Et/R \quad \text{for } \nu=0.3, \quad (2.2)$$


where E denotes Young's modulus of elasticity, ν is Poisson's ratio, and R and t are the radius of the cylinder and its wall thickness, respectively. The corresponding critical moment for $\nu = 0.3$ is:

$$M_{cr} = 0.605 \pi Et^2 R. \quad (2.3)$$

Brazier¹⁰ studied the flattening of long cylinders under bending and derived an expression for the potential energy of an infinite cylinder under bending. By minimizing the strain energy he found the critical moment to occur when the flattening of the cross-section reached $2/9 R$.

The critical moment is:

$$M_B = 2 \times 2^{0.5} / 9 E t^2 R (1 - \nu^2)^{-0.5}. \quad (2.4)$$

 Assuming an undeformed cross-section and ν equal to 0.3 this corresponds to a buckling stress of

$$\sigma_B = 0.329 E t / R. \quad (2.5)$$

Flügge²⁵ investigated the buckling behaviour of cylinders with a Poisson's ratio of $1/6$ and a radius to thickness ratio R/t of 289. He assumed a failure mode with a longitudinal wave-length ratio

$$m = L/R\pi,$$

with m being the number of longitudinal waves and L the length of the cylinder. The analysis thus considered longitudinal waves only with a wave-length equal to half the circumference. The buckling stress found was 30 % higher than the solution for axial compression (Eq. 2.2). Supported by various results of moment tests, which indicated somewhat higher stresses than for the equivalent compression problem,

and overlooking the restrictions due to the assumed buckling mode, a performance factor of 1.3 was accepted and has been used subsequently to estimate the elastic buckling load of cylinders under bending.

Seide and Weingarten¹⁴ investigated the buckling of circular cylinders using a modified form of the Donnell equations and the Galerkin method. Using four different R/t ratios they demonstrated that for most practical length to radius ratios the critical bending stress is insignificantly higher than the stress for pure compression.

Stephens *et al.*¹⁵ used the computer code STAGS, a two-dimensional, energy formulation, finite difference program, and analyzed cylinders under bending with an R/t ratio of 100 and various length to radius ratios. By introducing imperfections in the order of $t/1000$, they were able to follow the nonlinear loading path and determine a limit point that for practical purposes can be assumed to be a bifurcation point. Their results indicate that the critical buckling stress of cylinders coincides with the classical stress σ_{cr} for very short cylinders and decreases with increasing L/R . For an L/R ratio of 20 the buckling moment was approximately that predicted by Brazier and occurred at a cross-section flattening of 0.22 times the radius.

Fabian¹⁶ studied the behaviour of infinite cylinders using the finite difference technique. By prescribing the possible deformation modes he separated the ovalization effect from longitudinal wrinkling. For a cylinder with

$R/t=60$ and $\nu=1/3$ he found the moment to be about 53 % of M_{cr} , which is slightly below Brazier's solution.

2.2 Finite Elements for Cylindrical Shells

Thin shell theories, as opposed to three-dimensional theory, are based on the Love-Kirchhoff hypothesis that straight lines normal to the middle surface remain straight and unchanged in length during deformation. This implies that the deformation of the shell can be described by the deformation of its middle surface and that there are no transverse strains. With decreasing shell thickness t the transverse stresses become negligibly small compared to all other stresses and allow the assumption of plane stress.

The first complete set of kinematic relations for cylindrical shells was developed by Flügge²⁵. Because of the awkward nonlinearities involved, various approximations and simplifications were suggested. Further approximations based on the negligibility of certain strain terms led to a variety of shell theories, of which the three major ones are reviewed below.

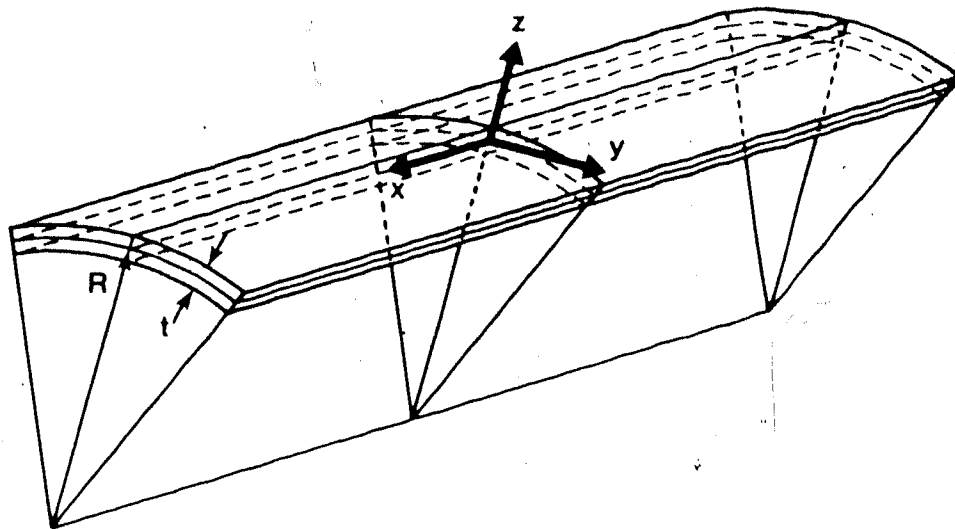


Fig. 2.1: Local Coordinate System for a Thin Cylindrical Shell.

Donnell obtained the following strain displacement expressions.

$$\epsilon_x = U, x, \quad (2.6a)$$

$$\epsilon_\phi = (v, \phi + w)/R, \quad (2.6b)$$

$$\gamma_{x\phi} = U, \phi/R + v, x, \quad (2.6c)$$

$$k_x = -w, xx, \quad (2.6d)$$

$$k_\phi = - (w, \phi\phi)/R^2, \quad (2.6e)$$

$$k_{x\phi} = - (w, x\phi)/R. \quad (2.6f)$$

The comma denotes the differentiation with respect to the following coordinates, and U , v , and w are displacements along the x - y - z coordinate axes, shown in Fig. 2.1.

In comparison with the classical plate theory, the y -coordinate is replaced by $R\theta$ and the normal displacement w contributes to the circumferential strain ϵ_θ .

Timoshenko and Woinoisky-Kreiger's¹⁰ formulation differs for the circumferential and twisting curvature by considering the influence of circumferential displacements. The resulting curvature expressions are

$$k_\theta = (v, \theta - w, \theta\theta) / R^2, \quad (2.7a)$$

$$k_{x\theta} = (v, x - w, x\theta) / R. \quad (2.7b)$$

A third set of strain expressions are the equations by Koiter and Sanders. These are regarded by some as the 'best' linear shell theory, because they satisfy strainless rigid body motions.

$$\epsilon_x = u, x, \quad (2.8a)$$

$$\epsilon_\theta = (v, \theta + w) / R, \quad (2.8b)$$

$$\gamma_{x\theta} = u, \theta / R + v, x, \quad (2.8c)$$

$$k_x = -w, xx, \quad (2.8d)$$

$$k_\theta = (v, \theta - w, \theta\theta) / R^2, \quad (2.8e)$$

$$k_{x\theta} = (3v, x - 4w, x\theta - u, \theta / R) / 4R. \quad (2.8f)$$

The only difference from Timoshenko and Woinoisky-Kreiger's equations is in the expression for the twisting curvature.

A detailed discussion of the approximations in these shell theories is given by Dym²³.

During the continuing development of the finite element method many attempts have been made to model shells with finite elements. Besides the curved finite strip (Cheung¹⁶, Dawe²¹) and various hybrid formulations (e.g. Horrigmoe²⁸), most elements can be categorized as either flat, three-dimensional (degenerated), or 'true' curved shell elements.

The modelling of shells as an assembly of flat elements was the first and probably is still the easiest approach. It is however a crude approach. The elements are derived by superposition of the independent in-plane (stretching) and out-of-plane behaviour (bending) of plates. With increasing mesh refinement they can represent a curved surface.

The coupling of the bending and stretching effects occurs during the assembly of the elements and with the transformation of the nodal degrees of freedom from the local element coordinates to a global coordinate system. One of the latest developments with flat finite elements is that of Argyris and Dunne² who employed a triangular plate element for postbuckling studies of cylindrical panels.

The three-dimensional brick element was originally developed for structures with thick walls and was later used for shells with a low R/t ratio. For thin shells the element showed an overemphasized shear stiffness, and caused numerical accuracy problems. Zienkiewicz and Hinton⁴⁵ eliminated this problem by using a reduced order of integration for the shear strain.

Kanok-Nukulchai³⁰ and Ramm³² developed procedures for degenerating three-dimensional isoparametric elements to thin shells and obtained promising results in general shell analysis.

One of the first elements derived directly from a shell theory was a nonconforming rectangular element formulated by Connor and Brebbia⁷. They used a linear polynomial for the in-plane displacement function with a quadratic polynomial for the shear strain and an incomplete quartic polynomial function for the out-of-plane displacements. This element used the geometrical degrees of freedom

$$u, v, w, w,x \text{ and } (w, \phi - v)/R$$

at each of the four corner nodes.

Gallagher²⁷ added the twisting curvature $w, x\phi$ as an internal degree of freedom to obtain a conforming element. Later Bogner *et al.*⁹ increased the degree of the polynomial expressions with Hermitian polynomials. This resulted in 12 degrees of freedom per node, of which 7 represented derivatives proportional to various strains and changes of curvature. To avoid an overstiffening of the structure due to enforcing continuity of internal degrees of freedom, these non-geometric degrees of freedom were assembled at a single artificial node or were eliminated by static condensation.

Curved shell elements based on polynomial displacement functions can represent strainless rigid body motions only approximately. Except for the rotation and translation around the axis of revolution, trigonometric terms are needed to represent rigid motions exactly (compare Eq. 2.11). If the element does not have these functions, rigid body motions induce strains which are normally a higher order in the rigid body displacements. A general criterion, ensuring that a displacement function is capable of representing rigid body motions is not available. This depends on the structure considered, the displacement function chosen, and the strain formulation used.

Dawe²⁰ showed that high order polynomials can approximate rigid body motions quite well. He employed quintic polynomials for all three displacement fields and constrained the functions at the edges of the element to be cubic, thereby enforcing compatibility between elements. His element has 54 degrees of freedom (18 per node) and shows considerable success for various arch and shell problems. The only disadvantage is the larger bandwidth due to its triangular shape.

Cantin¹³ included strainless rigid body motions for polynomial displacement functions using certain matrix operations. A further discussion of this technique is found in Reference 3.

In order to avoid the difficulties in only approximating rigid body motions by polynomials, several researchers have explicitly included the rigid body displacements in their displacement fields. One of the first attempts was made by Cantin and Clough¹⁴, who modified Gallagher's element. This gave rise to trigonometric terms in the displacement field and also to a coupling of u , v , and w .

Sabir and Lock¹⁵ simplified Cantin and Clough's displacement functions by omitting the highest order terms and eliminating the internal degree of freedom w, x_0 . Despite giving a smaller stiffness matrix and violating the compatibility requirements, the element showed no apparent loss of accuracy when compared to the original element.

It should be mentioned here, that the displacements defining the rigid body motions discussed above are based on the strain displacement equations from the linear theory and may cause significant strains in nonlinear shell formulations.

2.3 Finite Elements Based on Strain Functions

By studying finite element solutions for cylindrical rings and arches Ashwell, Sabir and Roberts¹⁶ found that a particular arch element, whose strain functions are simple expressions in the element coordinates, showed very good convergence when compared to all other preceding elements.

Sabir and Ashwell⁴ concluded that the success of the arch element is due to the smoothness of the strain field:

"... strain energy is calculated from squares and products of the strains, and imposing local variations on an initially smooth distribution without altering the local mean values, increases the value of the squares when they are integrated over the element."

With the results of this arch element in mind Sabir and Ashwell⁴ developed an assumed strain element for cylindrical shells.

Using the strain displacement expressions of Timoshenko and Woinoisky-Kreiger, (Eq. 2.6 and 2.7) the following compatibility equations are obtained:

$$\epsilon_{\theta,xx} + k_x/R + (\epsilon_{x,\theta\theta})/R^2 - (\gamma_{x\theta,\theta x})/R = 0, \quad (2.9a)$$

$$k_{x\theta,x} - (k_{x,\theta})/R + (\epsilon_{x,\theta})/R^2 - (\gamma_{x\theta,x})/R = 0, \quad (2.9b)$$

$$k_{\theta,x} - (k_{x\theta,\theta})/R = 0. \quad (2.9c)$$

With the assumption that $(\epsilon_{x,\theta})/R$ equals $\gamma_{x\theta,x}$ the following more restrictive equations are used.

$$(\epsilon_{x,\theta})/R = \gamma_{x\theta,x}, \quad (2.10a)$$

$$\epsilon_{\theta,xx} = -k_x/R, \quad (2.10b)$$

$$(k_{x,\theta})/R = k_{x\theta,x}, \quad (2.10c)$$

$$k_{\theta,x} = (k_{x\theta,\theta})/R. \quad (2.10d)$$

In the first step for the derivation of the displacement function, the strain expressions (Eq. 2.6 a-d, 2.7) are integrated to give the strainless rigid body motions. †

$$U = (\alpha_2 \cos\theta + \alpha_4 \sin\theta)R + \alpha_5, \quad (2.11a)$$

$$V = (\alpha_1 + \alpha_2 x) \sin\theta - (\alpha_3 + \alpha_4 x) \cos\theta + \alpha_6, \quad (2.11b)$$

$$W = -(\alpha_1 + \alpha_2 x) \cos\theta - (\alpha_3 + \alpha_4 x) \sin\theta. \quad (2.11c)$$

The parameters α_i may be identified with the following rigid modes of the element in Fig. 2.2.

α_1 : translation in the \bar{z} direction,

α_2 : rotation around the \bar{y} -axis,

α_3 : translation in the \bar{y} direction,

α_4 : rotation around the \bar{z} -axis,

α_5 : translation in the \bar{x} direction,

α_6 : rotation around the \bar{x} -axis.

† The displacements due to rotations are derived from the assumption that the rotations are 'small'. A further discussion of the 'exact' displacements is given in section 5.4.

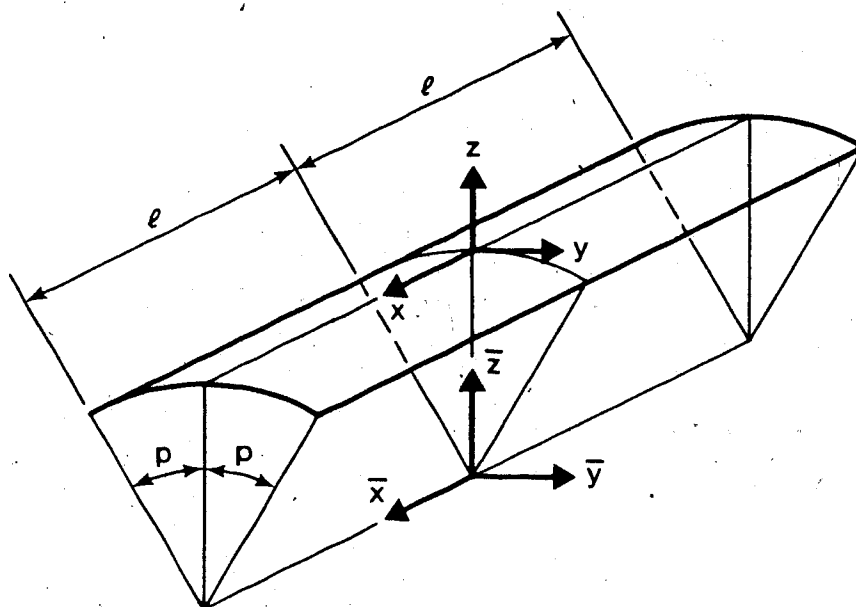


Fig. 2.2: Shell Element with Local and Global Axes.

With 20 nodal degrees of freedom wanted, 14 parameters are left for the strain functions and are distributed as follows:

$$\epsilon_x = \alpha_1 + \alpha_2 \theta, \quad (2.12a)$$

$$\epsilon_\theta = \alpha_3 + \alpha_4 x - (\alpha_5 x^2 / 2R + \alpha_6 x^3 / 6R + \alpha_7 x^2 \theta / 2R + \alpha_8 x^3 \theta / 6R), \quad (2.12b)$$

$$\gamma_{x\theta} = \alpha_9 + (\alpha_{10} x / R), \quad (2.12c)$$

$$k_x = \alpha_{11} + \alpha_{12} x + \alpha_{13} \theta + \alpha_{14} x \theta, \quad (2.12d)$$

$$k_\theta = \alpha_{15} + \alpha_{16} x + \alpha_{17} \theta + \alpha_{18} x \theta, \quad (2.12e)$$

$$k_{x\theta} = \alpha_{19} + (\alpha_{20} x / R + \alpha_{21} x^2 / 2R + R\alpha_{22} \theta + R\alpha_{23} \theta^2 / 2). \quad (2.12f)$$

After the unbracketed terms are written, the terms in

parentheses are added to satisfy the compatibility equations (Eq. 2.10).

The displacement functions are obtained by integration of the above equations. The integration constants depend on the choice of location of the origin of the local coordinate system. For simplicity this is chosen to be at the middle of the element as shown (Fig. 2.1).

$$U = \alpha_7 x + \alpha_8 x\phi + R\alpha_{1,0} - 0.5R^2\alpha_{1,1}\phi^2 + R^2(\phi - \phi^3/6)\alpha_{1,2} - R^2\alpha_{2,0}\phi, \quad (2.13a)$$

$$V = R^2\alpha_{1,3}\phi + R^2\alpha_{1,4}x\phi + 0.5R^2\alpha_{1,5}\phi^2 + (x\phi\phi/2 - 1)R^2\alpha_{1,6} + R\alpha_{2,0}x, \quad (2.13b)$$

$$W = (R\alpha_{1,7} + R\alpha_{1,8})x - \alpha_{1,2}x^2/2 - \alpha_{1,3}x^3/6 - \alpha_{1,4}x^2\phi/2 - \alpha_{1,5}x^3\phi/6 - R^2\alpha_{1,6} - R^2\alpha_{1,7}x - R^2\alpha_{1,8}\phi - R^2\alpha_{1,9}x\phi. \quad (2.13c)$$

The complete displacement field consists of the equations above plus the rigid body motions (Eq. 2.11).

Ashwell and Sabir obtained very good convergence for their element for the problem of a barrel vault under gravitational load. In section 4.1 its performance is compared to that of the element used in this study for the problem of a pinched cylinder.

Ashwell made the argument that a finite element should be capable of representing the known solutions of certain test problems and therefore altered the strain functions (Eq. 2.12) so as to better represent the stresses in a cylinder under bending. These stresses are functions of the

circumferential coordinate only. This requires a $\sin\theta$ term in the expressions for the strains ϵ_x and k_x , and also requires $\gamma_{x\theta}$ to be independent from all the other strains.

$$\epsilon_x = \alpha_7 + \alpha_8 \sin\theta, \quad (2.14a)$$

$$\epsilon_\theta = \alpha_9 + \alpha_{10}x - (\alpha_{11}x^2/2R + \alpha_{12}x^3/6R + \alpha_{13}x^2\theta/2R + \alpha_{14}x^3\theta/6R), \quad (2.14b)$$

$$\gamma_{x\theta} = \alpha_{15}, \quad (2.14c)$$

$$k_x = \alpha_{16} \sin\theta/R + \alpha_{17} + \alpha_{18}x + \alpha_{19}\theta + \alpha_{20}x\theta, \quad (2.14d)$$

$$k_\theta = \alpha_{21} + \alpha_{22}x + \alpha_{23}\theta + \alpha_{24}x\theta, \quad (2.14e)$$

$$k_{x\theta} = \alpha_{25} + (\alpha_{26}x/R + \alpha_{27}x^2/2R + R\alpha_{28}\theta + R\alpha_{29}\theta^2/2). \quad (2.14f)$$

In the displacement function for U , ' $\alpha_8 x\theta$ ' becomes ' $\alpha_8 x \sin\theta$ ' and v and w are supplemented by the terms ' $-\alpha_{11}x^2 \cos\theta/2R^2$ ' and ' $-\alpha_{12}x^2 \sin\theta/2R$ ', respectively. With the altered displacement field appreciable improvement is obtained for the barrel vault problem if compared to the element of Ashwell and Sabir⁴. Both strain elements converge to solutions of the 'deep shell' theory.

3. Formulation of a New Strain Element

3.1 Displacement Function

The element in this study is derived from the Koiter-Sander's strain expressions (Eq. 2.8). With the constants α_i defined as for the Sabir-Ashwell element (Eq. 2.11), the displacement functions are developed using the procedure described in section 2.3 and are given in the equations below.

$$U = (\alpha_2 \cos \theta + \alpha_4 \sin \theta)R + \alpha_5 + \alpha_7 x + \alpha_8 x \sin \theta + 0.75 R \alpha_{11} \theta - 0.5 R^3 \alpha_{17} \theta^2 + R^3 (\theta - \theta^3/6) \alpha_{11} - R^2 \alpha_{20} \theta, \quad (3.1a)$$

$$V = (\alpha_1 + \alpha_2 x) \sin \theta - (\alpha_3 + \alpha_4 x) \cos \theta + \alpha_6 - \alpha_8 x^2 \cos \theta / 2R + x \alpha_{11} / 4 + R^2 \alpha_{16} \theta + R^2 \alpha_{17} x \theta + 0.5 R^2 \alpha_{18} \theta^2 + R^2 (\theta^2/2 - 1) \alpha_{11} x + R^2 \alpha_{20} x, \quad (3.1b)$$

$$W = -(\alpha_1 + \alpha_2 x) \cos \theta - (\alpha_3 + \alpha_4 x) \sin \theta - \alpha_8 x^2 \sin \theta / 2R + R \alpha_{10} + R \alpha_{11} x - \alpha_{12} x^2 / 2 - \alpha_{13} x^3 / 6 - \alpha_{14} x^2 \theta / 2 - \alpha_{15} x^3 \theta / 6 - R^2 \alpha_{16} - R^2 \alpha_{17} x - R^2 \alpha_{18} \theta - R^2 \alpha_{19} x \theta. \quad (3.1c)$$

The only differences from the improved element of Ashwell³ are the change from ' $R \alpha_{11} \theta$ ' to ' $0.75 R \alpha_{11} \theta$ ' in the expression for U , and the addition of ' $x \alpha_{11} / 4$ ' to the expression for v . The resulting assumed strains are:

$$\epsilon_x = \alpha_7 + \alpha_8 \sin \theta, \quad (3.2a)$$

$$\epsilon_\theta = \alpha_6 + \alpha_{10} x - (\alpha_{12} x^2 / 2R + \alpha_{13} x^3 / 6R + \alpha_{14} x^2 \theta / 2R + \alpha_{15} x^3 \theta / 6R),$$

$$(3.2b)$$

$$\gamma x \theta = \alpha_{11}, \quad (3.2c)$$

$$kx = \alpha_8 \sin \theta / R + \alpha_{12} + \alpha_{13} x + \alpha_{14} \theta + \alpha_{15} x \theta, \quad (3.2d)$$

$$k\theta = \alpha_{16} + \alpha_{17} x + \alpha_{18} \theta + \alpha_{19} x \theta, \quad (3.2e)$$

$$kx\theta = (\alpha_{14} x / R + \alpha_{15} x^2 / 2R + R\alpha_{17} \theta + R\alpha_{19} \theta^2 / 2) + \alpha_{20}. \quad (3.2f)$$

The vector of the displacement parameters $\{\alpha\}$ is related to the nodal displacement vector $\{q\}$ by the matrix $[T]$, the inverse of which is given in Appendix A.1.

$$\{q\} = [T] \{\alpha\}, \quad (3.3a)$$

$$= \langle U_1, V_1, W_1, \beta x_1, \beta \theta_1, U_2, V_2, W_2, \beta x_2, \beta \theta_2, U_3, V_3, W_3, \beta x_3, \beta \theta_3, U_4, V_4, W_4, \beta x_4, \beta \theta_4 \rangle^T. \quad (3.3b)$$

The indices denote the node number. With the explicit form of the inverse of $[T]$ it is possible to write the element shape functions explicitly for each of the 20 degrees of freedom. This is not done here due to the lengthiness of the resulting expressions.

The Eqs. 3.2 and 3.3a define the strain functions in terms of nodal displacements. Instead of using the explicit shape functions, the strain functions are used directly for the formulation of the stiffness matrices.

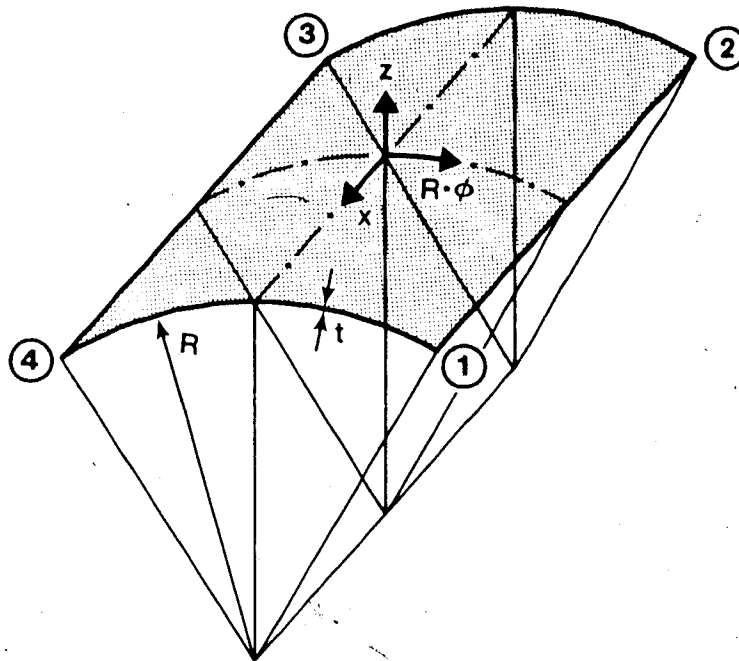


Fig. 3.1: Element with Centre Coordinate System and Corner Nodes.

The degrees of freedom U , V , and W are the displacements along the local x , y , and z coordinate directions, respectively, and β_x and β_ϕ are the rotations of the normal about the local x and ϕ axes, respectively. In terms of the displacements, these rotations are given by

$$\beta_x = w, x, \quad (3.4a)$$

$$\beta_\phi = (w, \phi - v) / R. \quad (3.4b)$$

3.2 Formulation of the Strain Energy Expression

The element used in this study is based on a displacement field (Eqs. 3.1) derived from an assumed strain field. Following the usual steps in the classical displacement method, the stiffness matrices for the element are derived using the Principle of the Stationary Potential Energy. The potential energy Π is the difference of the strain energy U and the potential W of the external loads Q_i with respect to the corresponding displacements q_i .

$$\Pi = U - W. \quad (3.5)$$

The strain energy is defined as

$$U = 1/2 \int_V \{\delta\}^T \{\epsilon\} dv, \quad (3.6)$$

with V being the volume of the structure considered.

The strain and stress vectors $\{\delta\}$ and $\{\epsilon\}$ for the assumed plane stress state in thin shells take the form

$$\{\delta\} = \langle \delta_x \ \delta_\theta \ \gamma_{x\theta} \rangle^T, \quad (3.7a)$$

$$\{\epsilon\} = \langle \epsilon_x \ \epsilon_\theta \ \gamma_{x\theta} \rangle^T. \quad (3.7b)$$

For a linear elastic structure, the stress vector is expressed by the product of the elasticity matrix $[E]$ and the strain vector.

$$\{\sigma\} = [E] \cdot \{\epsilon\}, \quad (3.8)$$

$$\text{with } [E] = E/(1-\nu^2) \begin{bmatrix} 1 & \nu & 0 \\ \nu & 1 & 0 \\ 0 & 0 & (1-\nu)/2 \end{bmatrix}, \quad (3.9)$$

and the Poisson's ratio ν .

Using Eq. 3.6 the strain energy becomes:

$$U = 1/2 E/(1-\nu^2) \int_V [\underline{\epsilon}_x^2 + \underline{\epsilon}_\theta^2 + 2\nu \underline{\epsilon}_x \underline{\epsilon}_\theta + (1-\nu)/2 \gamma_{x\theta}^2] dV. \quad (3.10)$$

For later convenience the strains are separated into an in-plane and an out-of-plane part.

$$\begin{bmatrix} \underline{\epsilon}_x \\ \underline{\epsilon}_\theta \\ \gamma_{x\theta} \end{bmatrix} = \begin{bmatrix} \underline{\epsilon}_x \\ \underline{\epsilon}_\theta \\ \gamma_{x\theta} \end{bmatrix} + z \cdot \begin{bmatrix} k_x \\ k_\theta \\ 2k_{x\theta} \end{bmatrix}. \quad (3.11)$$

Substituting Eq. 3.11 into Eq. 3.10 and performing the integration over the shell thickness t the strain energy is:

$$U = C/2 \int_A [\underline{\epsilon}_x^2 + \underline{\epsilon}_\theta^2 + 2\nu \underline{\epsilon}_x \underline{\epsilon}_\theta + (1-\nu)/2 \gamma_{x\theta}^2] dA + D/2 \int_A [k_x^2 + k_\theta^2 + 2\nu k_x k_\theta + 2(1-\nu)k_{x\theta}^2] dA, \quad (3.12)$$

$$\text{with } C = Et/(1-\nu^2),$$

$$D = Et^3/12(1-\nu^2),$$

and A is the middle surface area of the element.

Before the strain equations by Koiter-Sanders are substituted into Eq. 3.12, the strain expressions are divided into linear and nonlinear parts.

$$\begin{aligned}
 \underline{\epsilon}_x &= \epsilon_x + 1/2(\beta_{x_1}^2 + \beta_{x_2}^2 + \beta_{x_3}^2), \\
 \underline{\epsilon}_\theta &= \epsilon_\theta + 1/2(\beta_{\theta_1}^2 + \beta_{\theta_2}^2 + \beta_{\theta_3}^2), \\
 \underline{\gamma}_{x\theta} &= \gamma_{x\theta} + \beta_{x_1}\beta_{\theta_1} + \beta_{x_2}\beta_{\theta_2} + \beta_{x_3}\beta_{\theta_3}, \\
 k_x &= -\beta_{x,x}, \\
 k_\theta &= -\beta_{\theta,\theta}/R, \\
 k_{x\theta} &= -\beta_{\theta,x} - \gamma_{x\theta}/4R, & \gamma_{x\theta} &= \beta_{x_2} + \beta_{\theta_1}, \\
 \beta_{x_1} &= \epsilon_x = u_{,x}, & \beta_{\theta_1} &= u_{,\theta}/R, \\
 \beta_{x_2} &= v_{,x}, & \beta_{\theta_2} &= \epsilon_\theta = (v_{,\theta} + w)/R, \\
 \beta_{x_3} &= \beta_x = w_{,x}, & \beta_{\theta_3} &= \beta_\theta = (w_{,\theta} - v)/R. \quad (3.13)
 \end{aligned}$$

Since the strain energy consists of products of the above strains, it is separated into a quadratic, a cubic, and a quartic part.

$$U = U_2 + U_3 + U_4. \quad (3.14a)$$

$$\begin{aligned}
 U_2 &= c/2 \int_A [\epsilon_x(\epsilon_x + \nu\epsilon_\theta) + \epsilon_\theta(\epsilon_\theta + \nu\epsilon_x) + (1-\nu)/2 \gamma_{x\theta}^2] dA \\
 &+ D/2 \int_A [k_x(k_x + \nu k_\theta) + k_\theta(k_\theta + \nu k_x) + 2(1-\nu) k_{x\theta}^2] dA, \quad (3.14b)
 \end{aligned}$$

$$\begin{aligned}
 U_3 = C/2 \int_A [& \epsilon_x (\beta_{x_1}^2 + \beta_{x_2}^2 + \beta_{x_3}^2 + \nu \{ \beta_{\theta_1}^2 + \beta_{\theta_2}^2 + \beta_{\theta_3}^2 \}) \\
 & + \epsilon_{\theta} (\beta_{\theta_1}^2 + \beta_{\theta_2}^2 + \beta_{\theta_3}^2 + \nu \{ \beta_{x_1}^2 + \beta_{x_2}^2 + \beta_{x_3}^2 \}) \\
 & + (1-\nu) \gamma x_{\theta} (\beta_{x_1} \beta_{\theta_1} + \beta_{x_2} \beta_{\theta_2} + \beta_{x_3} \beta_{\theta_3})] dA,
 \end{aligned} \tag{3.14c}$$

$$\begin{aligned}
 U_4 = C/8 \int_A [& (\beta_{x_1}^2 + \beta_{x_2}^2 + \beta_{x_3}^2)^2 + (\beta_{\theta_1}^2 + \beta_{\theta_2}^2 + \beta_{\theta_3}^2)^2 \\
 & + 2\nu (\beta_{x_1}^2 + \beta_{x_2}^2 + \beta_{x_3}^2) (\beta_{\theta_1}^2 + \beta_{\theta_2}^2 + \beta_{\theta_3}^2) \\
 & + 2\nu (\beta_{x_1} \beta_{\theta_1} + \beta_{x_2} \beta_{\theta_2} + \beta_{x_3} \beta_{\theta_3})^2] dA.
 \end{aligned} \tag{3.14d}$$

3.3 Derivation of the Stiffness Matrices

In order to formulate the stiffness matrices the stiffness coefficients have to be defined by the components of the strain energy and the nodal displacements.

$$U = U_2 + U_3 + U_4,$$

$$U_2 = 1/2 K^{ij} q_i q_j,$$

$$U_3 = 1/6 K^{ijkl} q_i q_j q_k q_l,$$

$$U_4 = 1/12 K^{ijkl} q_i q_j q_k q_l, \quad (i, j, k, l = 1 \dots 20). \tag{3.15}$$

In the above, q_i is the i -th term of the nodal displacement vector $\{q\}$. With Eqs. 3.2 and 3.13 the strain fields are expressed in the form:

$$\begin{bmatrix} \epsilon_x \\ \epsilon_\theta \\ \gamma_{x\theta} \\ k_x \\ k_\theta \\ k_{x\theta} \\ \beta_{x_3} \\ \beta_{\theta_3} \\ \beta_{x_2} \\ \beta_{\theta_1} \end{bmatrix} = \begin{bmatrix} \langle \theta_x \rangle \\ \langle \theta_\theta \rangle \\ \langle \theta_{x\theta} \rangle \\ \langle \alpha_x \rangle \\ \langle \alpha_\theta \rangle \\ \langle \alpha_{x\theta} \rangle \\ \langle B_x \rangle \\ \langle B_\theta \rangle \\ \langle B_u \rangle \\ \langle B_v \rangle \end{bmatrix} \{q\}. \quad (3.16)$$

The linear strain functions ($\langle \theta \rangle$ and $\langle \alpha \rangle$) are given in Appendix A.2. Introducing Eq. 3.16 into Eq. 3.14 the stiffness matrices can be computed. The linear stiffness matrix is:

$$\begin{aligned}
 [K^2] = & CR \int_{-p}^p \int_{-l}^l [\{ \theta_x \} \langle \theta_x + \nu \theta_\theta \rangle + \{ \theta_\theta \} \langle \theta_\theta + \nu \theta_x \rangle \\
 & + (1-\nu)/2 \{ \theta_{x\theta} \} \langle \theta_{x\theta} \rangle] d\theta dx \\
 & + DR \int_{-p}^p \int_{-l}^l [\{ \alpha_x \} \langle \alpha_x + \nu \alpha_\theta \rangle + \{ \alpha_\theta \} \langle \alpha_\theta + \nu \alpha_x \rangle \\
 & + 2(1-\nu) \{ \alpha_{x\theta} \} \langle \alpha_{x\theta} \rangle] d\theta dx, \quad (3.17)
 \end{aligned}$$

In the above equations, R is the radius of the cylinder, p is half of the angle subtended by the element and l is half of its longitudinal dimension.

The nonlinear stiffness terms of third and fourth order as defined in Eqs. 3.15, are computed in a similar manner.

3.4 Newton-Raphson Method Solution Procedure

An elastic structure follows the principle of stationary potential energy:

Of all kinematically admissible displacement fields, the actual equilibrium displacements make the potential energy have a stationary value.

The term kinematically admissible means that the displacements are continuous within the structure and that they satisfy the kinematic boundary conditions.

A stationary value for the potential energy requires that the first partial derivatives of the potential energy with respect to the nodal displacements are zero. Taking the first derivative of Eq. 3.5 the equilibrium conditions can be written:

$$\begin{aligned} \Pi, q_i = 0 = & K^{2ij} q_j + 1/2 K^{3ijk} q_j q_k \\ & + 1/3 K^{4ijkl} q_j q_k q_l - Q_i. \end{aligned} \quad (3.18)$$

It may be further stated that the equilibrium state that makes Π stationary (first variation equal to zero) is stable if the second variation of Π is positive.

This means that the determinant of the Jacobian matrix of Π

has to be positive. Using Eq. 3.5 this can be expressed as:

$$\begin{aligned}
 & | \prod, q_i q_j | > 0, \text{ or} \\
 & | K^2_{ij} + K^3_{ijk} q_k + K^4_{ijkl} q_k q_l | = | [K^T] | > 0, \\
 & \hspace{20em} (3.19)
 \end{aligned}$$

where $| \quad |$ denotes the determinant.

The matrix $[K^T]$ is referred to as the tangent stiffness matrix and is positive definite for a stable equilibrium configuration. For an unstable equilibrium configuration the determinant of $[K^T]$ becomes negative. At a bifurcation point or a limit point (a horizontal tangent in the load-deflection curve), the determinant of $[K^T]$ is zero.

To first order in the incremental displacement Δq_i , the incremental form of the equilibrium equation 3.18 is

$$K^T_{ij} \Delta q_j = \Delta Q_i.$$

In order to be able to prescribe both displacement and force type boundary conditions, the above equation must be modified. In the new equations below a Δ denotes increments in forces or displacements and a star (*) indicates prescribed values. For easier representation the equations have been reordered so that the prescribed incremental forces are grouped together as are the prescribed incremental displacements.

$$\begin{bmatrix} [K^T_{1,1}] & [K^T_{1,2}] \\ [K^T_{2,1}] & [K^T_{2,2}] \end{bmatrix} \begin{bmatrix} \{\Delta q_1\} \\ \{\Delta q_{2*}\} \end{bmatrix} = \begin{bmatrix} \{\Delta Q_{1,*}\} \\ \{\Delta Q_2\} \end{bmatrix}. \quad (3.20)$$

The first equation resulting from this partitioning is then re-arranged so that the unknown displacements may be solved for.

$$[K^T_{1,1}] \{\Delta q_1\} = \{\Delta Q_{1,*}\} - [K^T_{1,2}] \{\Delta q_{2*}\}.$$

After $\{\Delta q_1\}$ is known, the unknown forces $\{\Delta Q_2\}$ can be calculated from the stiffness matrix and the displacements. In the finite element program used, the nodal forces are not needed, and the stiffness matrix and the right hand side are changed for easier application of the equation solver and to obtain a full incremental displacement vector.

$$\begin{bmatrix} [K^T_{1,1}] & [O] \\ [O] & [I] \end{bmatrix} \begin{bmatrix} \{\Delta q_1\} \\ \{\Delta q_{2*}\} \end{bmatrix} = \begin{bmatrix} \{\Delta Q_{1,*}\} - [K^T_{1,2}] \cdot \{\Delta q_{2*}\} \\ \{\Delta q_{2*}\} \end{bmatrix}. \quad (3.21)$$

In the above, $[I]$ denotes the identity and $[O]$ the zero-matrix.

After the new displacements of the structure are found, the equilibrium of the deformed structure can be checked with Eq. 3.18. If the equilibrium equation is not satisfied, the displacements have to be changed until they satisfy Eq. 3.18. One well established procedure for this problem is

the Newton-Raphson method which is described in the algorithm given below.

Figure 3.2 shows the Newton-Raphson method for a load step from $\{Q^0\}$ to $\{Q\}$. The corresponding deformations are the vectors $\{q^0\}$ and $\{q\}$.

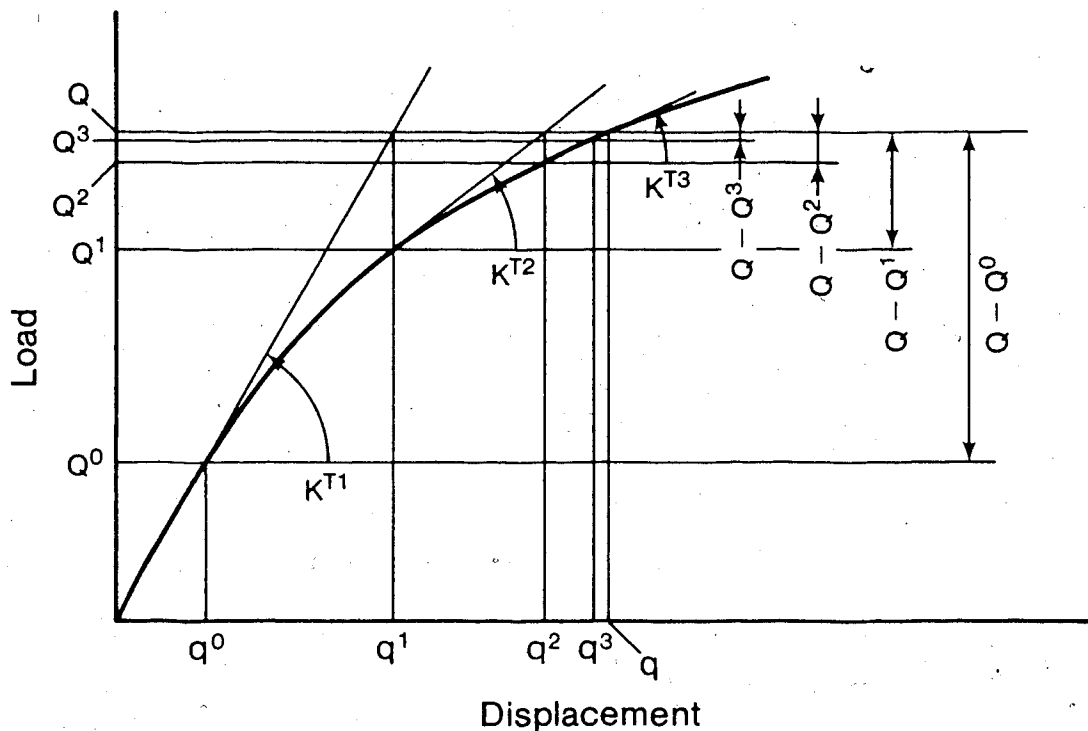


Fig. 3.2: The Newton-Raphson Method for a One-Degree-of-Freedom System.

Algorithm for the Newton-Raphson Method:

- 1) Start of new load step,
set i as superscript of $\{q^i\}$, $\{Q^i\}$, and $[K^T{}^i]$ to one.
- 2) Form the tangent stiffness matrix,

$$K^T{}^i{}_{ij} = K^2{}_{ij} + K^3{}_{ijk} q^i{}^k + K^4{}_{ijkl} q^i{}^k q^j{}^l.$$

- 3) If superscript i is greater than one, go to step 5.
- 4) Modify the tangent stiffness matrix and the incremental load vector as shown in Eq. 3.21 by including the prescribed incremental loads and displacements for this load step.
- 5) Calculate the incremental displacements from Eq. 3.21, and update the displacement vector,

$$\{q^i\} = \{q^{i-1}\} + [K^T{}^i]^{-1} \{Q - Q^{i-1}\}.$$
- 6) Check if the displacements have converged, (if $|q^i - q^{i-1}| < \text{tolerance}$), go to step 10.
- 7) Compute the internal nodal forces from the equilibrium equation,

$$Q^i{}^i = K^2{}_{ij} q^i{}^j + 1/2 K^3{}_{ijk} q^i{}^j q^i{}^k + 1/3 K^4{}_{ijkl} q^i{}^j q^i{}^k q^j{}^l.$$
- 8) Compute the vector $\{Q - Q^i\}$ as a new right hand side of Eq. 3.21.
- 9) Increase superscript i of $\{q^i\}$, $\{Q^i\}$, and $[K^T{}^i]$ by one, return to step 2.
- 10) End of load step.

4. Linear Solutions

4.1 Pinched Cylinder Problem

In order to study the convergence behaviour of cylindrical shell finite elements, various sample problems have been utilized. The most often used problem for cylindrical shells is a pinched cylinder as shown in Fig. 4.1.

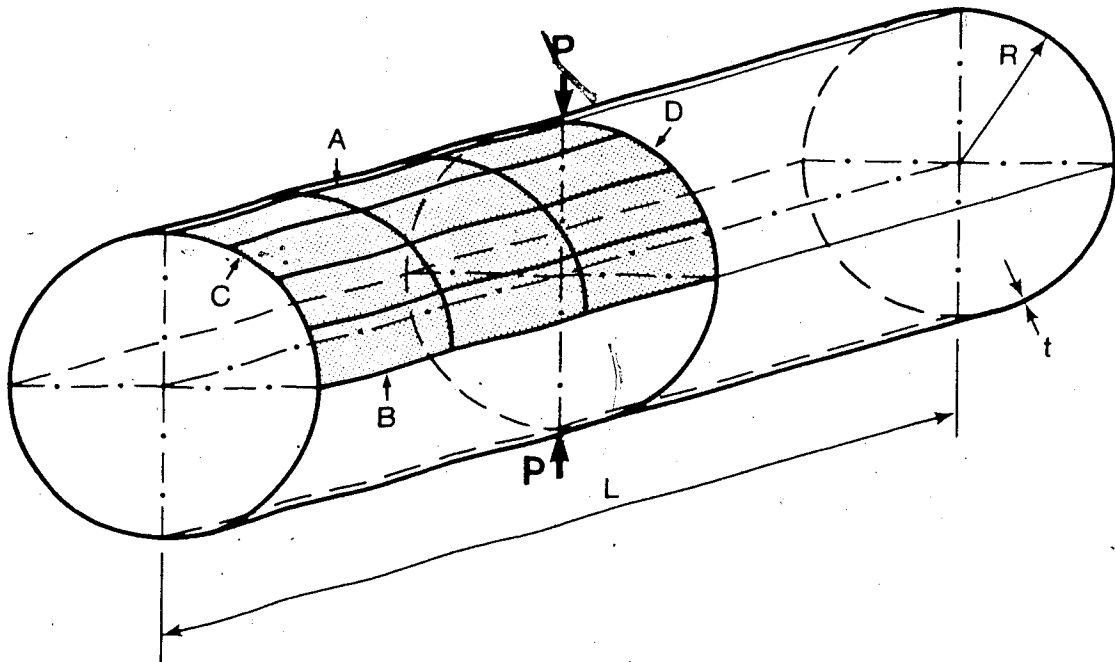


Fig. 4.1: Pinched Cylinder under Load with Element Mesh for One Octant.

The data for this cylinder are:

$$R = 4.953 \text{ in.},$$

$$L = 10.35 \text{ in.},$$

$t = 0.094$ in. for the thick and 0.01548 in. for the thin cylinder,

$E = 1.05 \times 10^6$ lbs/in.²,

$\nu = 0.3125$.

The load P is 100 lbs for the thick cylinder and 0.1 lbs for the thin one.

Because of symmetry, only one octant needs to be analyzed, with the appropriate boundary conditions applied as described in the following. The nodal degrees of freedom v and $\beta\theta$ along the top fibre A and the side edge B, are set to zero. No displacements are prescribed at end C. Symmetry about the vertical plane and the mid-section D requires u and βx to be zero.

Ashwell and Sabir calculated the deflection under the load for the thick cylinder. Their solution in Reference 4 converges to a value of 0.1137 inches. For the mesh sizes chosen by Ashwell and Sabir no difference could be found between their results and the present results. It would be interesting to compare their solution with more significant figures to determine if there are any differences.

For comparison the results of Cantin¹³ are also shown.

The latter is believed by Ashwell and Sabir to be the most accurate solution. It converges to a deflection of 0.1139 inches.

Table 4.1: Deflection of Thick Pinched Cylinder under Load.

Mesh size NX × NP	present study, Ashwell and Sabir	Cantin
1×1	0.1041	-
2×2	0.1103	0.0931
4×4	0.1129	0.1126
6×6	0.1135	0.1137
8×8	0.1137	0.1139
10×10	0.1137	0.1139

Despite having 20 % fewer degrees of freedom than the Cantin element, the elements of Ashwell and Sabir and the present study show a similar convergence. The two strain formulation elements give better results for mesh sizes up to 4×4 and converge to a deflection of 99.8 % of Cantin's solution.

For the thin pinched cylinder problem better or worse behaviour can be obtained, depending on the simplifications and assumptions of the shell theory used. In the appendix of Reference 4 Ashwell and Sabir estimate the exact solution to be 0.02439 in., which they believe to be correct to four significant figures.

Table 4.2: Deflections of Thin Pinched Cylinder under Load.

Mesh size NX × NP	Ashwell and Sabir	present study
1×1	0.02301	0.02327
2×1	0.02300	0.02336
3×1	0.02302	0.02337
1×4	0.02403	0.02432
2×4	0.02409	0.02448
3×4	0.02414	0.02452
1×8	0.02406	0.02436
2×8	0.02414	0.02443
3×8	0.02418	0.02448

Despite giving the same results as Ashwell and Sabir for the thick cylinder ($R/t=53$), the thin cylinder problem ($R/t=320$) shows a significant difference. For all mesh sizes chosen, the present study gives deflections, that are 1.0 to 1.5 % larger and which are closer to the 'exact' solution of 0.02439 in. than the Ashwell and Sabir solution. Except for the 2×1 mesh, the Sabir Ashwell model softens with increasing number of elements in the circumferential and longitudinal direction and seems to converge to a solution below the 'exact' solution. The present element converges nonmonotonically with respect to grid refinement in the θ -direction to a value above the 'exact' solution.

4.2 Cylinder under Bending

4.2.1 Boundary Conditions and Theoretical Results

With the symmetry of a cylinder under bending only one quarter needs to be analyzed. The symmetry about the central vertical longitudinal plane requires that v and $\beta\theta$ at the top and bottom fibre be zero. Symmetry about the cross-section plane at the mid-cylinder requires that u and βx be zero at that plane.

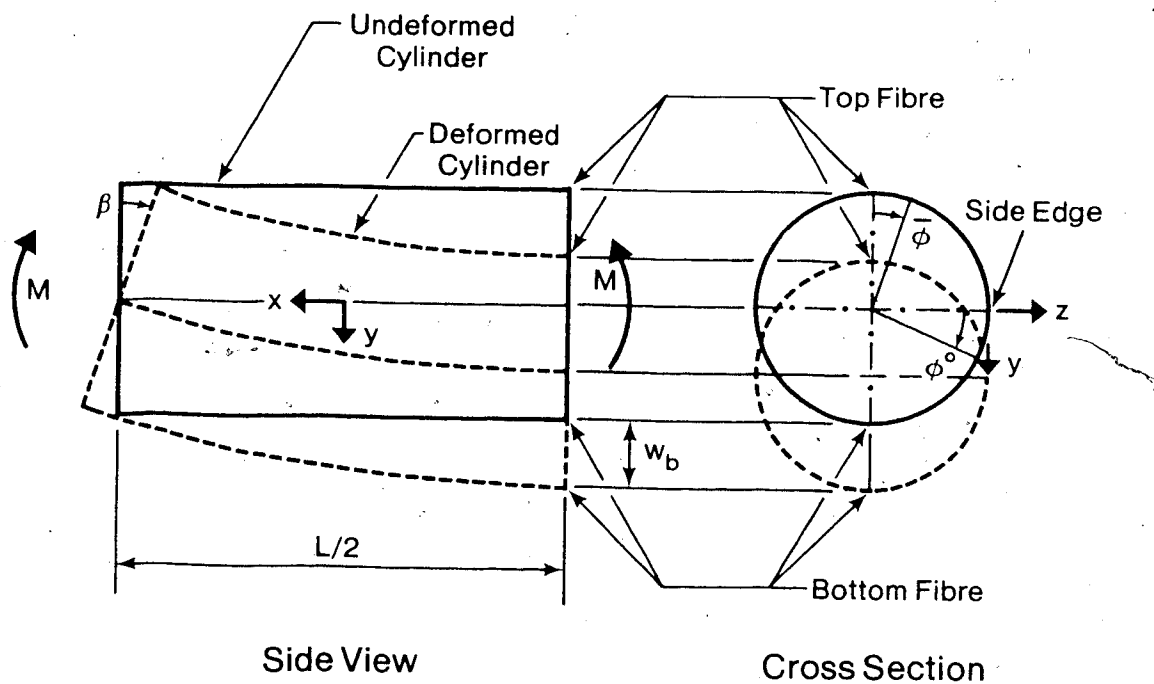


Fig. 4.2: Left Half of Cylinder under Bending with Linearized Boundary Conditions.

The boundary condition at the left cylinder end is determined by the end rotation β . The cylinder cross-section

at the end is taken to be rigid and rotates as a plane without change in the circular shape. It is assumed that higher orders in the rotation β are negligibly small for a linearized theory. The resulting displacements and rotations at the end section are shown below to first order in β .

$$\begin{aligned} u &= -R \beta \cos(\bar{\theta}), \\ v &= 0, \\ w &= 0, \\ \beta x &= \beta \cos(\bar{\theta}), \\ \beta \theta &= 0. \end{aligned} \tag{4.1}$$

The exact end conditions, including nonlinear terms, are discussed in section 5.5.3.

A closed form solution for the linear bending problem is given by Donnell²². After transformation to the coordinate system in Fig. 4.2, it becomes

$$u = 0.50 \beta R \sin(\theta^0) (1 + 4x/L), \tag{4.2a}$$

$$v = 0.25 \beta L \cos(\theta^0) (3/4 - 2x/L - 4x^2/L^2 + 8vR^2/L^2), \tag{4.2b}$$

$$w = 0.25 \beta L \sin(\theta^0) (3/4 - 2x/L - 4x^2/L^2). \tag{4.2c}$$

For this solution the top and bottom points at the cylinder end are fixed vertically. The cross-section at the cylinder end is no longer rigid since the last term in

Eq. 4.2b causes displacements tangential to the local circumferential coordinate $\bar{\theta}$.

The corresponding strains are computed using Eq. 2.8:

$$\epsilon_x = 2 \beta R/L \sin(\theta^\circ), \quad (4.3a)$$

$$\epsilon_\theta = -2 \nu \beta R/L \sin(\theta^\circ), \quad (4.3b)$$

$$\gamma_{x\theta} = 0, \quad (4.3c)$$

$$k_x = 2 \beta/L \sin(\theta^\circ), \quad (4.3d)$$

$$k_\theta = -2 \nu \beta/L \sin(\theta^\circ), \quad (4.3e)$$

$$k_{x\theta} = 0. \quad (4.3f)$$

The stresses are then defined with Eq. 3.8.

$$\sigma_x = 2 E \beta (R+z)/L \sin(\theta^\circ), \quad (4.4a)$$

$$\sigma_\theta = 0, \quad (4.4b)$$

$$\tau_{x\theta} = 0. \quad (4.4c)$$

The relationship between Donnell's solution and the common beam stresses can be clearly seen in the equations above. The stresses are the same as those predicted by beam theory. With $\nu=0$ in the displacement function (Eq. 4.2) the cylinder behaves like a simple beam. That is, the circular cross-section is not deformed.

With zero circumferential stress, the circumferential strain ϵ_θ is $-\nu \epsilon_x$. The strain ϵ_θ has its maximum values at the top and bottom of the cylinder and is zero at the

cylinder side. The positive circumferential strain in the upper cylinder half and the negative strain in the lower half cause individual points of the cross-section to move circumferentially towards the bottom. These circumferential displacements are zero at the top and bottom fibre and have their maximum value at the side of the cylinder.

For later convenience a measure of the effect of the circumferential stretching is defined. This is the difference between the vertical movement of the cylinder side and the deflection of the top fibre. This difference is denoted as Δv . The Donnell solution predicts the circumferential stretching as

$$\Delta v = (8 \nu R^2/L^2) w_b,$$

$$w_b = \beta L/4.$$

For long cylinders Δv is quite small, but it is significant for relatively short cylinders. For a cylinder with the geometry of the cylinder being tested by Stephens³⁷ ($R/L = 764.5/1829$), Δv is 42 % of w_b . A better insight into the effects of Δv is gained if it is expressed as a function of the end rotation β . The rotation at which the classical buckling stress σ_{cr} occurs, assuming linear bending theory, is

$$\beta_{cr} = t L/2R^2 [3(1-\nu^2)]^{-1/2}. \quad (4.5)$$

$$\Delta v = (2 \nu R^2/L) \beta,$$

$$= (\nu t [3(1-\nu^2)]^{1/2}) (\beta/\beta_{cr}). \quad (4.6)$$

For $\nu=0.3$ and $\beta=\beta_{cr}$, Δv is equal to 0.182 t .

The circumferential strain ϵ_{θ} for this Δv is $0.182 t/R$ at the top fibre when the elastic buckling moment M_{cr} has been reached. If Δv is prevented at the ends due to rigid plates then a circumferential compressive stress equal to ν times the longitudinal stress develops. In a structural test this can lead to an outward buckle along the end plate of the cylinder.

4.2.2 Element Approximation of Cylinder under Bending

In the preceding section it was shown that the linear solution for the displacements of a cylinder under bending consists of products of simple trigonometric functions in the coordinate θ° (Fig. 4.2) and quadratic polynomials in the longitudinal coordinate x . If the semi-circumference is divided into several elements, the coordinate θ° can be expressed by the local element coordinate θ and the angle α between the side edge and the origin of the element coordinate:

$$\theta^{\circ} = \alpha + \theta$$

With above expression introduced into Eq. 4.2, the addition formulas of trigonometry result in there being a combination of $\sin\theta$ and $\cos\theta$ terms in the displacement fields. Some of these terms in the displacement function

cannot be represented exactly by the assumed displacement field (Eqs. 3.1) of the element. A list of terms occurring in the Donnell solution is given in Table 4.3 and compared with the available parameters of the element displacement functions.

Table 4.3: Approximations of the Element Displacement Field.

Displacement	terms in Donnell solution	terms in the element displacement field	Nature of the approximation
U	$\sin\theta$ $x\sin\theta$ $\cos\theta$ $x\cos\theta$	$\alpha_1\sin\theta$ $\alpha_2x\sin\theta$ $\alpha_3\cos\theta$ α_4x	exact exact exact o.k. for $\cos\theta \approx 1$
V	$\cos\theta$ $x\cos\theta$ $x^2\cos\theta$ $\sin\theta$ $x\sin\theta$ $x^2\sin\theta$ $v\cos\theta$ $v\sin\theta$	$\alpha_1\cos\theta$ $\alpha_2x\cos\theta$ $\alpha_3x^2\cos\theta$ $\alpha_4\sin\theta$ $\alpha_5x\sin\theta$ † $\alpha_6 \ddagger$ ‡	exact exact exact exact exact o.k. for $x \ll L$ o.k. for $\cos\theta \approx 1$ o.k. for $\sin\theta \approx 0$
W	$\sin\theta$ $x\sin\theta$ $x^2\sin\theta$ $\cos\theta$ $x\cos\theta$ $x^2\cos\theta$	$\alpha_1\sin\theta$ $\alpha_2x\sin\theta$ $\alpha_3x^2\sin\theta$ $\alpha_4\cos\theta$ $\alpha_5x\cos\theta$ α_6x^2	exact exact exact exact exact o.k. for $\cos\theta \approx 1$

 † No term appears, because there is no term in the displacement field for v which has a factor of $x^2\sin\theta$.
 ‡ ' $v\cos\theta$ ' and ' $v\sin\theta$ ' represent the circumferential strain predicted by Donnell which is independent of the displacements for U and W . The parameters α_1 and α_3 occur as rigid motions in the displacement function for W too, and are therefore not suitable for these two terms.

Table 4.3 indicates that the exact functions for U and w are well represented by the element displacement fields for small angles, and the term ' $v \cos \theta$ ' for v can be approximated for shallow elements by the rigid element rotation around the revolution axis. For one element per half circumference the element coordinate θ coincides with 0° , and U and w are exactly represented. The boundary conditions for this case force α to zero which thereby causes Δv to be zero.

The approximations of $\cos \theta$ with 1 and $\sin \theta$ with 0 are worst for two elements per semi-circumference ($p = 45^\circ$) and improve with grid refinement.

For the terms ' $v \sin \theta$ ' and ' $x^2 \sin \theta$ ' in v , there are no corresponding terms in the element displacement functions. This suggests that a large number of elements is needed to keep the error by the approximation for $\sin \theta$ and $\cos \theta$ in an reasonable range. An element refinement in the longitudinal direction reduces the errors arising from the approximation of displacement terms involving x and x^2 .

Summarizing the above discussion it can be said that the element should work well for the linear problem of a cylinder under bending. However, one must be careful in selecting an element gridwork to keep the approximations of the displacement field in an reasonable range.

4.2.3 Results of Linear Tests

In order to evaluate the performance of the present finite element and the influence of the boundary conditions, two cylinders are chosen for the linear bending problem. The two different boundary conditions considered are:

1. rigid ends, as described in section 4.2.1 with
 $v = w = \beta\theta = 0,$
2. semi-rigid ends, which allow the stretching predicted by the Donnell solution to occur at the cylinder end. That is, $v, w,$ and $\beta\theta$ are free which allows a distortion of the cross-section.

Nevertheless, the circular cross-section remains plane since out-of-plane forces do not apply.

In addition to a cylinder of the same geometry as that tested (Stephens³⁷) another cylinder was also examined. The large L/R ratio was chosen in order to study whether the effects of the boundary conditions at the cylinder end would be less than those of the short cylinder. The data is given in Table 4.4.

Table 4.4: Cylinder Data for Linear Bending Test.

	Long cylinder	Short cylinder
Length (mm)	2500	1829
Radius (mm)	90	764.5
Wall thickness (mm)	1.1	5.13
Ratio L/R	27.7	2.39
Ratio R/t	81.8	149
Young's modulus (MPa)	200000	202016
Poisson's ratio	0.3	0.3
End rotation	0.01	0.000485808
Beam deflection (mm)	6.25	0.222136
Donnell solution Δv (mm)	0.01944	0.093145
Beam moment (kNm)	4.03079	802290

The element meshes chosen for the quarter cylinder modelled range from 1×1 to 10×10 elements, but were concentrated on even numbers, for the circumferential division (NP) in order to facilitate calculation of the parameter Δv .

In all cases for NP=1, the results obtained are as indicated earlier in the last chapter. That is, the boundary conditions at the top and bottom prevent any circumferential stretching. If the displacements computed are expressed in terms of the parameters α_i , the deflections can be shown to correspond to the Donnell solution with $\nu=0$. The latter coincides with the beam theory. The moment calculated is found to be 9.89 % higher than the beam theory would predict. This reflects a factor of $1/(1-\nu^2)$, caused by the restriction of Δv . A solution for the long cylinder was also obtained with $\nu=0$ and it gives a bending moment equal to that from beam theory thus verifying the factor of $1/(1-\nu^2)$. The moments calculated are accurate to 5 digits, and for the

deflections no difference could be detected from the beam theory.

The first cylinder investigated is the long cylinder, whose maximum bottom fibre deflection, stretching at the mid-section and end moment are shown for different mesh sizes in Tables 4.5 to 4.7.

Table 4.5: Ratio of Bottom Fibre Centre Deflection to Beam Theory for Long Cylinder with Rigid Ends.

NP \ NX	2	4	6	8	10
2	1.18	1.24	1.26	1.27	1.27
4	1.033	1.051	1.052	1.054	1.054
6	1.008	1.014	1.014	1.014	1.014
8	1.0024	1.0050	1.0050	1.0051	1.0051
10	1.0006	1.0019	1.0018	1.0017	1.0017

Table 4.6: Ratio of End Moment to Beam Theory
for Long Cylinder with Rigid Ends.

NX \ NP	2	4	6	8	10
2	0.724	0.539	0.510	0.496	0.481
4	0.801	0.828	0.843	0.849	0.851
6	0.857	0.940	0.963	0.971	0.976
8	0.875	0.978	1.004	1.013	1.018
10	0.882	0.994	1.021	1.032	1.035

Table 4.7: Ratio of Computed Δv to Donnell Solution
for Long Cylinder with Rigid Ends.

NX \ NP	2	4	6	8	10
2	-6.7	20	20	20	20
4	3.6	4.5	4.6	4.7	4.7
6	2.2	2.4	2.5	2.5	2.5
8	1.6	1.7	1.8	1.8	1.8
10	1.3	1.5	1.5	1.5	1.5

Table 4.5 shows that the deflection for the cylinder middle converges to the beam deflection with an increasing number of elements in the longitudinal direction. A similar convergence is found for the stretching of the mid-section of the cylinder, shown in Table 4.7. The moment converges with finer element divisions in both x and ϕ direction to a

value above the beam moment, which reflects the stiffening effect of the rigid ends. As mentioned earlier, this restraint results in circumferential stresses, which are relieved by an upward moving of the cylinder and an emphasized stretching near the cylinder ends. Figure 4.3 shows the difference of the variation of slope between the 10×10 element mesh and the beam theory (the differences in deflections are less illustrative), and the variation of circumferential stretching versus the distance from the cylinder end in the longitudinal direction is plotted in Fig. 4.4.

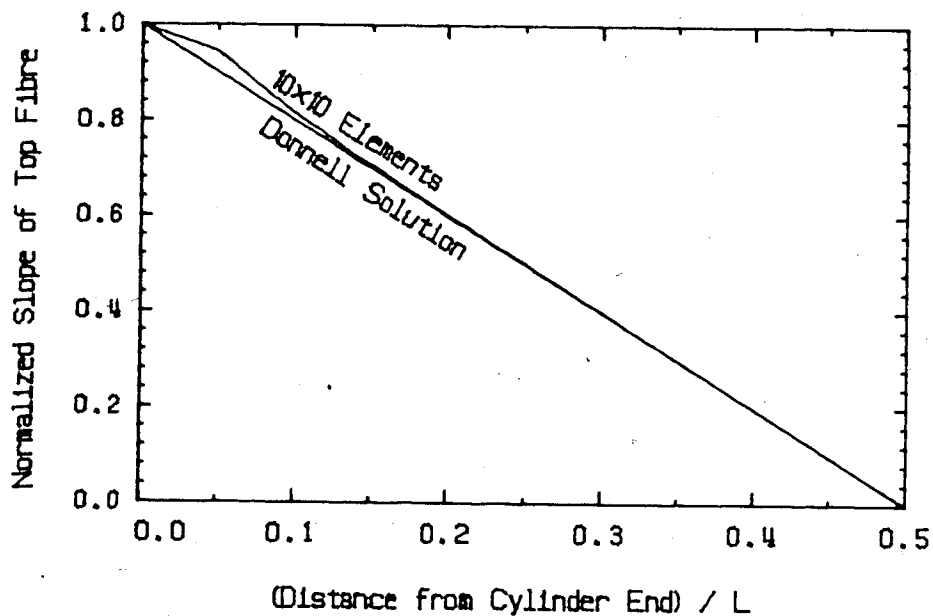


Fig. 4.3: Slope Variation of Long Cylinder with Rigid Ends.

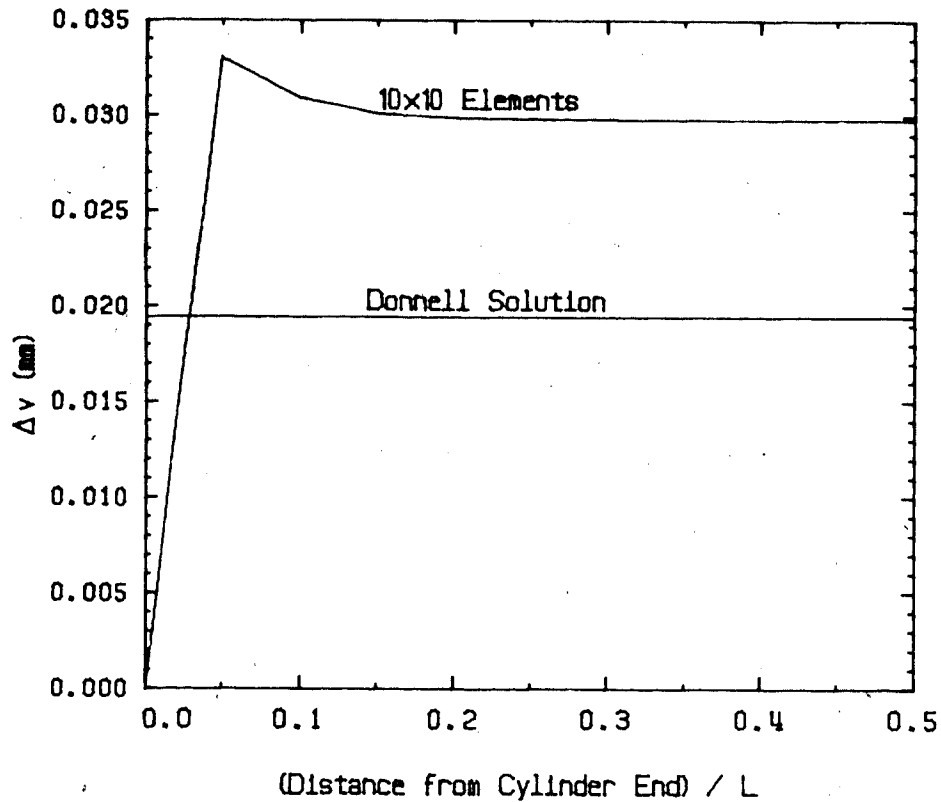


Fig. 4.4: Variation of Parameter Δv for Long Cylinder with Rigid Ends.

The second boundary conditions, referred to earlier as semi-rigid ends, were introduced to see if these boundary conditions would better represent the cylinder behaviour associated with the Donnell solution. The ratios of the resulting end moment and the parameter Δv for the long cylinder are shown in Table 4.8 and 4.9.

Table 4.8: Ratio of End Moment to Beam Theory
for Long Cylinder with Semi-Rigid Ends.

NP \ NX	2	4	6	8	10
2	-0.020	-0.200	-0.245	-0.262	-0.269
4	0.632	0.666	0.673	0.676	0.671
6	0.746	0.827	0.844	0.850	0.852
8	0.785	0.883	0.903	0.910	0.914
10	0.804	0.909	0.931	0.939	0.942

Table 4.9: Ratio of Computed Δv to Donnell Solution
for Long Cylinder with Semi-Rigid Ends.

NP \ NX	2	4	6	8	10
2	12	14	14	14	14
4	3.6	4.1	4.3	4.3	4.3
6	2.1	2.4	2.4	2.5	2.5
8	1.53	1.75	1.80	1.81	1.82
10	1.28	1.46	1.50	1.52	1.52

A similar table for deflections is not given for this case since the top and bottom fibre deflections are the same as predicted by the beam theory and the Donnell solution. The stretching is found to be constant along the cylinder length as predicted by Donnell and is a little better estimated than for the cylinder with rigid ends. The moment

convergences towards the beam solution, but shows quite unexpectedly poor values for less than 6 elements in the longitudinal direction.

For the second cylinder, which has a much lower L/R ratio than the first (2.4 versus 27.8), the circumferential stretching is expected to be more significant than for the long cylinder. The results for deflection, the parameter Δv , and moment of the cylinder with the rigid ends are given in Tables 4.10 to 4.12.

Table 4.10: Ratio of Bottom Fibre Deflection to Beam Theory for Short Cylinder with Rigid Ends.

NP \ NX	2	4	6	8	10
2	2.455	0.621	0.549	0.535	0.528
4	1.454	0.640	0.607	0.594	0.588
6	0.998	0.632	0.606	0.596	0.591
8	0.857	0.629	0.605	0.596	0.591
10	0.808	0.627	0.604	0.596	0.592

Table 4.11: Ratio of Computed Δv to Donnell Solution for Short Cylinder with Rigid Ends.

NP \ NX	2	4	6	8	10
2	-5.67	1.070	1.192	1.197	1.201
4	-1.83	1.000	1.010	1.021	1.025
6	-1.05	0.967	0.994	1.004	1.009
8	0.368	0.961	0.989	0.999	1.003
10	0.546	0.958	0.986	0.996	1.001

Table 4.12: Ratio of End Moment to Beam Theory for Short Cylinder with Rigid Ends.

NP \ NX	2	4	6	8	10
2	0.902	1.029	1.058	1.069	1.074
4	0.892	1.021	1.049	1.060	1.064
6	0.887	1.015	1.041	1.050	1.055
8	0.883	1.010	1.033	1.042	1.046
10	0.880	1.007	1.027	1.034	1.038

The bending moment is found to converge in a manner similar to that for the long cylinder, to a value above the beam moment. The stretching tends to a value near Donnell's prediction. The deflections appear at first to be unusually small since they converge to around 0.585 times the beam deformation. The reason for the relatively small

displacements becomes clear from inspection of the deflected shape of the cylinder, shown in Fig. 4.5.

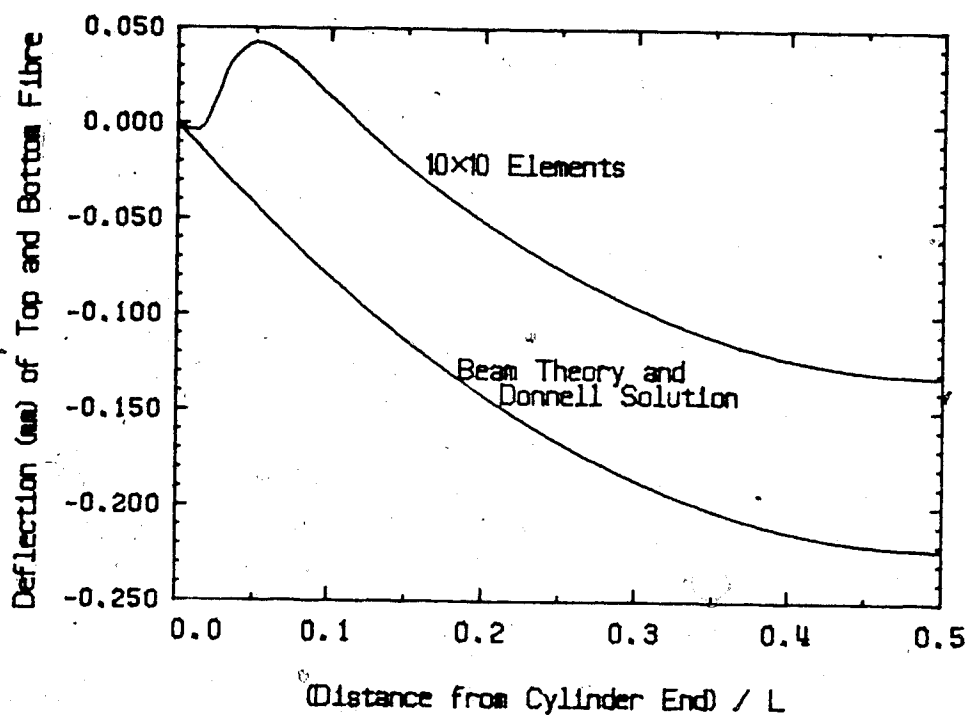


Fig. 4.5: Deflection of Short Cylinder with Rigid Ends.

In addition to the deflection predicted by the beam theory the inner part of the cylinder undergoes essentially a rigid body motion in the direction opposite to the bending deflection. This upward displacement is 0.091 mm and can be attributed to the circumferential stress caused by the restraint of the rigid ends. The similar numerical values for this displacement and for Δv (0.093 mm in Table 4.4) suggests that as the element grid is refined, the magnitude

of this rigid body displacement should approach the value of Δv from the Donnell solution. Flügge²⁵ predicted a similar outward deformation for the ends of rigidly compressed cylinders. He showed this disturbance to occur within a distance of circa $(Rt)^{1/2}$, which for the short cylinder is 62 mm. Since for the finest element mesh used, the shell element length is 91 mm, the displacement fields can only approximate the localized curvature. In order to study the upward movement in detail, the end region should be modelled with at least one or two elements. The deflections of the long cylinder are less affected by the rigid ends. However, the induced strains and stresses cannot be neglected. The use of long elements (125 mm long for a 10x10 element mesh) is not adequate for the region affected by the end constraint (ca. 10 mm). The long elements force the stretching to develop farther away from the cylinder end and therefore influence the deflections of the cylinder over a larger region and increase the rotational stiffness.

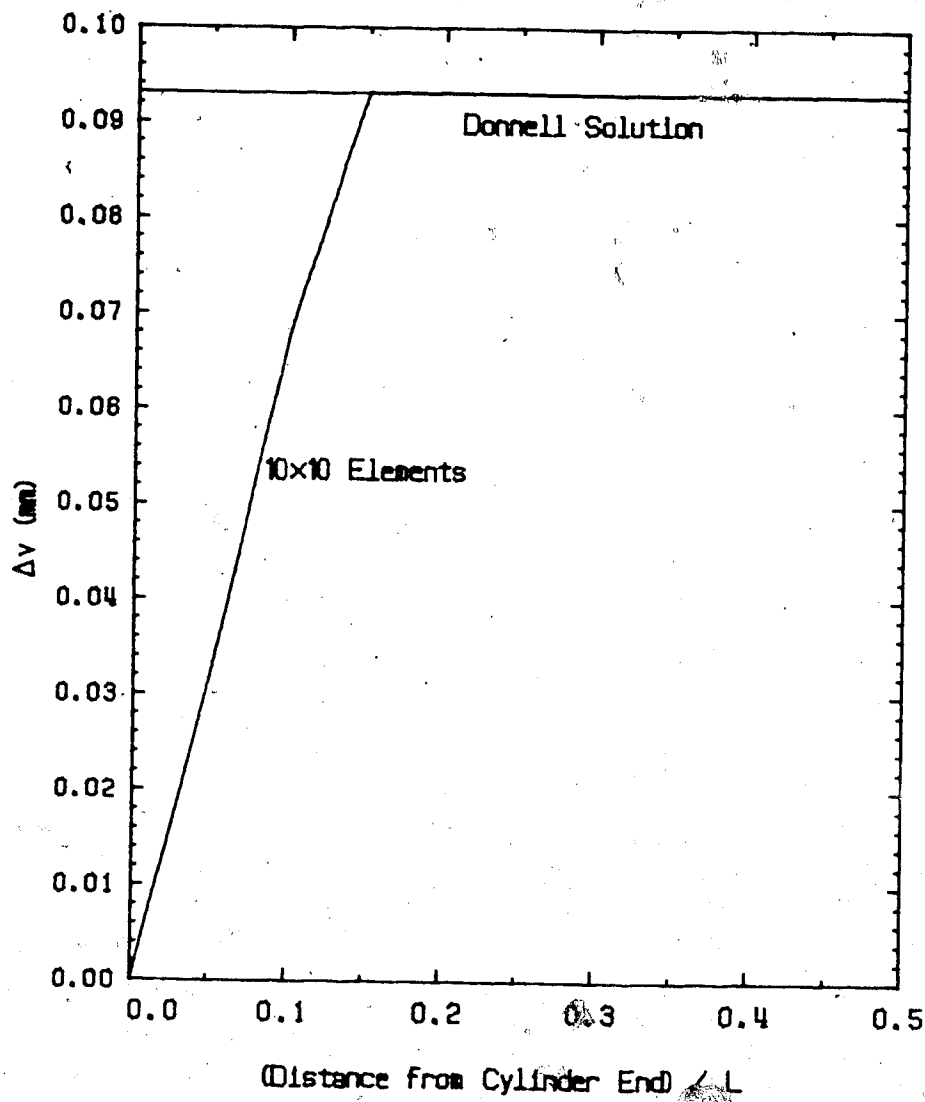


Fig. 4.6: Variation of Δv of Short Cylinder with Rigid Ends.

Fig. 4.6 shows the convergence of Δv to Donnell's prediction: At the cylinder ends Δv is zero and the transition region for Δv encompasses the first three elements in the axial direction.

With the application of the semi-rigid boundary conditions, results similar to those for the long cylinder are obtained: Δv is constant over the cylinder length and

the deflections correspond exactly to the beam theory.

The variation of Δv and the end moment with the element mesh are given in Tables 4.13 and 4.14.

Table 4.13: Ratio of Computed Δv to Donnell Solution for Short Cylinder with Semi-Rigid Ends.

NP \ NX	2	4	6	8	10
2	0.917	1.045	1.075	1.085	1.090
4	0.856	0.974	1.002	1.012	1.016
6	0.845	0.961	0.988	0.998	1.003
8	0.841	0.957	0.984	0.993	0.998
10	0.839	0.955	0.982	0.991	0.996

Table 4.14: Ratio of Cylinder Moment to Beam Moment for Short Cylinder with Semi-Rigid Ends.

NP \ NX	2	4	6	8	10
2	.8302	.9465	.9706	.9792	.9833
4	.8348	.9529	.9774	.9862	.9903
6	.8356	.9551	.9787	.9875	.9916
8	.8359	.9546	.9791	.9879	.9920
10	.8360	.9547	.9793	.9881	.9923

As opposed to the long cylinder, the moment, Δv , and the deflections converge to the values of Donnell's solution with an increasing number of elements in the circumferential direction. For a given total number of elements the long and the short cylinders have different 'optimal' mesh sizes. For the long cylinder the best ratio of NX to NP is 10:2, and for the short cylinder NX:NP is around 4:10. For both cases a good mesh seems to be that one when the curved sides of the elements are as long as the longitudinal dimension. The exact mesh-ratios for equilateral elements would be for the long cylinder (NX:NP) 10:2.26 and for the short cylinder 3.81:10.

It is interesting to note that the so called 'optimal' meshes discussed above have the least total inter-element boundary length for a fixed number of elements. If one could assume that the effects of element nonconformity are contributed similarly for circumferential and longitudinal inter-element boundaries and that the total effect is dependent on the total inter-element boundary length, then it follows that meshes with equilateral elements would suffer the least due to nonconformity.

The results discussed above show that grid meshes with equilateral elements give the best results for a given number of elements. Rigid ends cause the circumferential strain predicted by Donnell to be developed by the elements near the cylinder end. Thereby the cylinder undergoes an upward lifting equal to Δv . For short cylinders this effect

is large compared with the deflections from beam theory, whereas the deflections of long cylinders are less affected. Unfortunately, the circumferential stretching has not been reported yet from structural tests, so that it could be compared to the results obtained in this study.

In the preceding section it is shown that the element displacement field of the present element approximates the displacements of a cylinder under bending for sufficiently small element dimensions. The best results for the linear bending problem were obtained with about equilateral elements. It is shown that the cylinder is significantly influenced by the boundary conditions at the cylinder end. If the nodal points at the circumference between the top and bottom fibre are free to move along the circumference and to rotate around the local longitudinal axis (semi-rigid cylinder end) the top and bottom fibre deflections of the cylinder correspond exactly to the beam theory and the circumferential stretching is constant with respect to the cylinder length.

Rigid cylinder ends prevent circumferential strain at the cylinder end and thereby cause circumferential stresses which are relieved towards the cylinder middle by an upward movement of the cylinder in a direction opposite to the bending deflections.

In real cylinders, boundary conditions are neither rigid nor 'semi-rigid' but lie somewhere in between and one

has to decide which boundary condition comes nearest to structural reality.

5. Nonlinear Problems

5.1 Introduction

The geometric nonlinear behaviour of circular shell elements has been studied mostly using cylindrical arch, panel, and barrel vault problems ^{24, 27-29, 35}. The pure bending of finite cylinders, which represents the main part of this chapter, has been analyzed mostly by using half-analytical methods and finite difference techniques ^{24, 25, 36, 38}.

In order to test ~~the~~ the program developed for this study and to evaluate the performance of the shell element it is first tested on cylindrical arches and barrel vaults. For simplicity only concentrated loads are considered. Then the rigid body motions occurring in a cylinder under bending are examined and the resulting induced strains for the present element are discussed. Finally the problem of a cylinder under bending is examined and results obtained with the present shell element are discussed.

5.2 The Circular Arch

Sabir and Lock^{3,4} investigated the geometric nonlinear behaviour of a circular arch element on arches with R/t ratios ranging from 43 to 500. The other data for the arches studied are:

$$L = 100 \text{ in.},$$

$$E = 10^7 \text{ psi.},$$

$$A = 1 \text{ in.}^2 \text{ as area of cross-section,}$$

$$I = 1 \text{ in.}^4 \text{ as moment of inertia of cross section,}$$

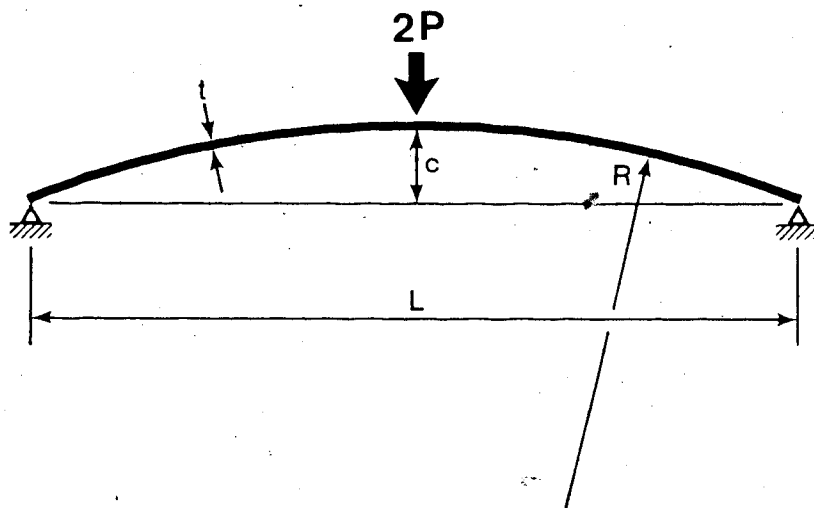


Fig. 5.1: Circular Arch under Concentrated Load.

For one particular arch Sabir and Lock expected horizontal and vertical tangents in the load-deflection curve. In order to follow the equilibrium path through these regions, they employed a procedure which switched automatically from load to displacement control and vice versa. For an arch

with $R/t=500$ Sabir and Lock demonstrated that an increasing number of elements reduces the load significantly. A reason for this is that the element can only represent a linear change of curvature (compare Eq. 3.2e). Localized changes in slope for deep arches (the maximum deflection for the deepest arch was 10 % of the radius) might require a very fine mesh.

In the present study the shell thickness and the element length were chosen to give the same cross-section properties as the arches of Sabir and Lock¹⁴. In order to simulate the displacement field used by Sabir and Lock the displacements corresponding to the longitudinal axis and Poisson's ratio are set to zero. Neglecting the parameters corresponding to the x-coordinate, the displacement field used by Sabir and Lock is obtained.

For the nonlinear strains Sabir and Lock assumed

$$\begin{aligned} \epsilon_{\theta} &= (v, \theta + w)/R + 1/2 \beta_{\theta}^2, \\ \beta_{\theta} &= w, \theta / R. \end{aligned} \quad (5.1)$$

Compared with $\beta_{\theta} = (w, \theta - v)/R$ used in the present study, the expressions above correspond to a more 'shallow' theory. As done by Sabir and Lock, the nonlinear strain terms involving β_{θ} , and β_x , are set to zero. Since the circular arch is a plane structure, the strain terms β_{x_2} , β_{x_3} , and

β_0 , should be zero. However, the displacement field (Eqs. 3.1) causes these strain terms to have nonzero values that are assumed to be negligibly small.

The program developed for this study allows either displacement control or load control. For the arch problem prescribed displacements are used. Thus only part of the equilibrium path can be obtained. The recalculation of the tangent stiffness matrix during the equilibrium iteration is found to take about the same time as the computation of the equilibrium forces, so that the full Newton-Raphson method is used.

Using symmetry, only one half of the arch needs to be modelled for which ten elements were used. The load-deflection curves obtained are given in Fig. 5.2 and 5.3.

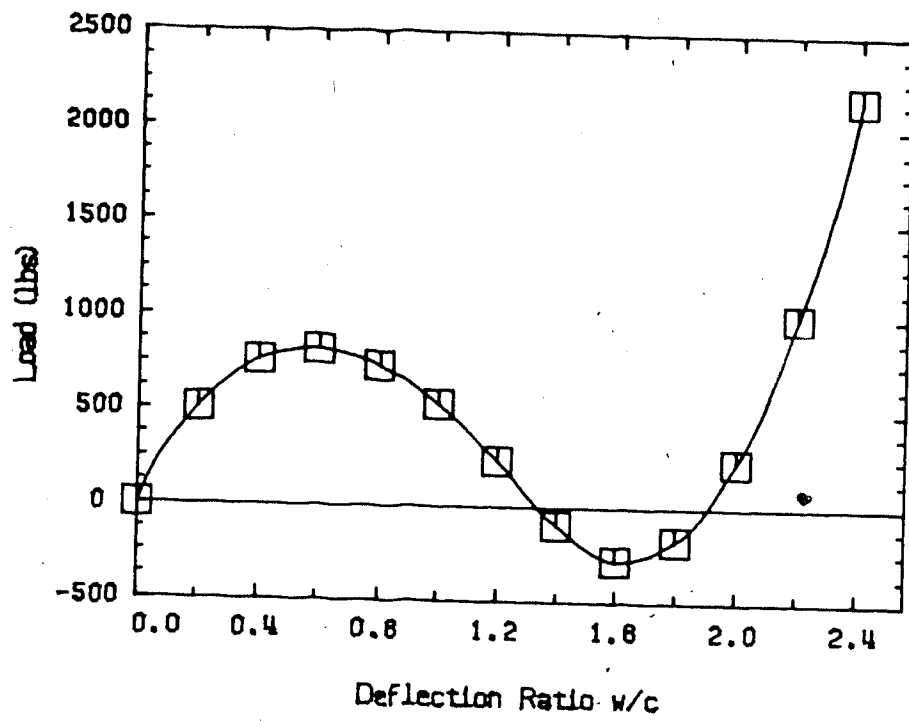


Fig. 5.2: Load Deflection Curve for Cylindrical Arch ($R=250$ in.) under Concentrated Load.

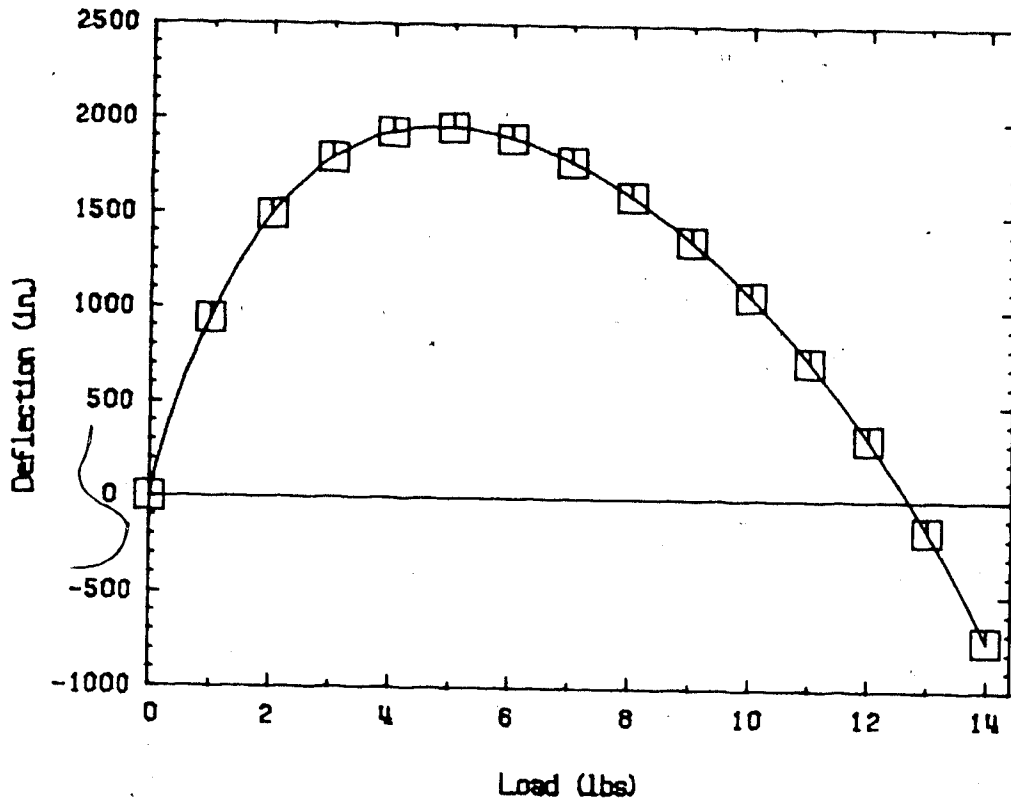


Fig. 5.3: Load Deflection Curve for Cylindrical Arch (R=150 in.) under Concentrated Load.

The results obtained are similar to those of Sabir and Lock except that the equilibrium path is slightly above theirs. This difference can be attributed not only to the more general strain expressions used herein but also to a different element mesh. Unfortunately a conclusive comparison is not possible because Sabir and Lock do not identify the element gridwork used. Due to the high computing costs associated with nonlinear problems, a convergence study with finer element meshes is not done. That study would be necessary to determine the influence,

if any, of the different strain displacement expression used here.

Table 5.1: Loads (lbs) for Prescribed Deflections of Two Cylindrical Arches.

Δ (in.) or $5w/c$	R=250 in.	R=150 in.
1	939.6	507.8
2	1489	759.7
3	1789	819.3
4	1927	734.3
5	1954	535.0
6	1898	241.2
7	1776	- 94.83
8	1596	-281.1
9	1362	-174.8
10	1074	242.1
11	730.0	1003.6
12	323.2	2159.0
13	-157.6	—
14	-734.5	—

5.3 The Barrel Vault Problem

After Sabir and Lock³⁴ applied the geometric nonlinear theory to arches, they tested various cylindrical shell formulations for a barrel vault under external pressure. Since the strain element by Ashwell and Sabir⁴ showed the best convergence, the element was subsequently used for the problem of a point loaded barrel vault as shown in Fig. 5.4.

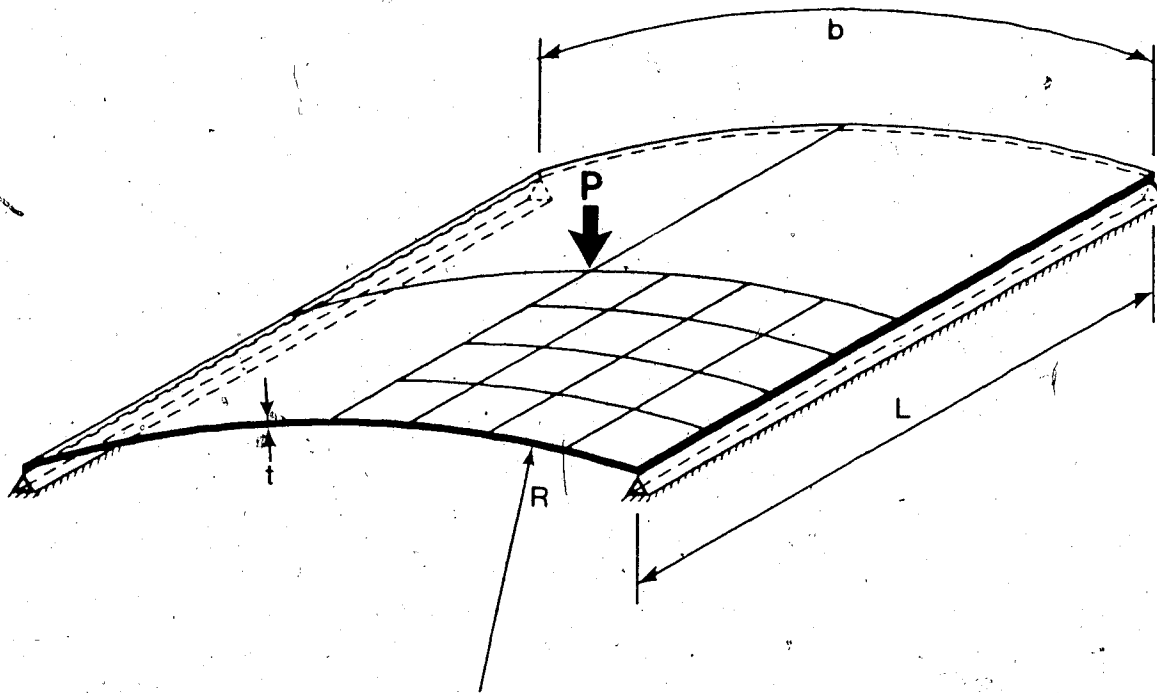


Fig. 5.4: Hinged Barrel Vault under Single Load.

The data for the cylindrical panel are:

$$E = 20 \text{ in.},$$

$$R = 100 \text{ in.},$$

$$b = 20 \text{ in.},$$

$t = 1$ or 0.5 in.,

$E = 450000$ psi,

$\nu = 0.3$.

For the computation, one quarter of the panel is divided into 4×4 elements. The curved edges are free and the longitudinal edges are hinged, with rotation about the longitudinal axis the only movement allowed. Since the load-deflection curve is expected to exhibit horizontal tangents, the vertical displacement under the load P is prescribed in steps of 0.1 inches as in Ref. 35.

As in their study, the nonlinear strain terms β_{x_1} , β_{x_2} , β_{θ_1} , and β_{θ_2} are assumed to be negligibly small. The load-deflection curves obtained follow the published curves of Sabir and Lock³⁵. A more detailed comparison is difficult since the actual numerical results obtained by Sabir and Lock were not published. The results of the present study are given in Table 5.2.

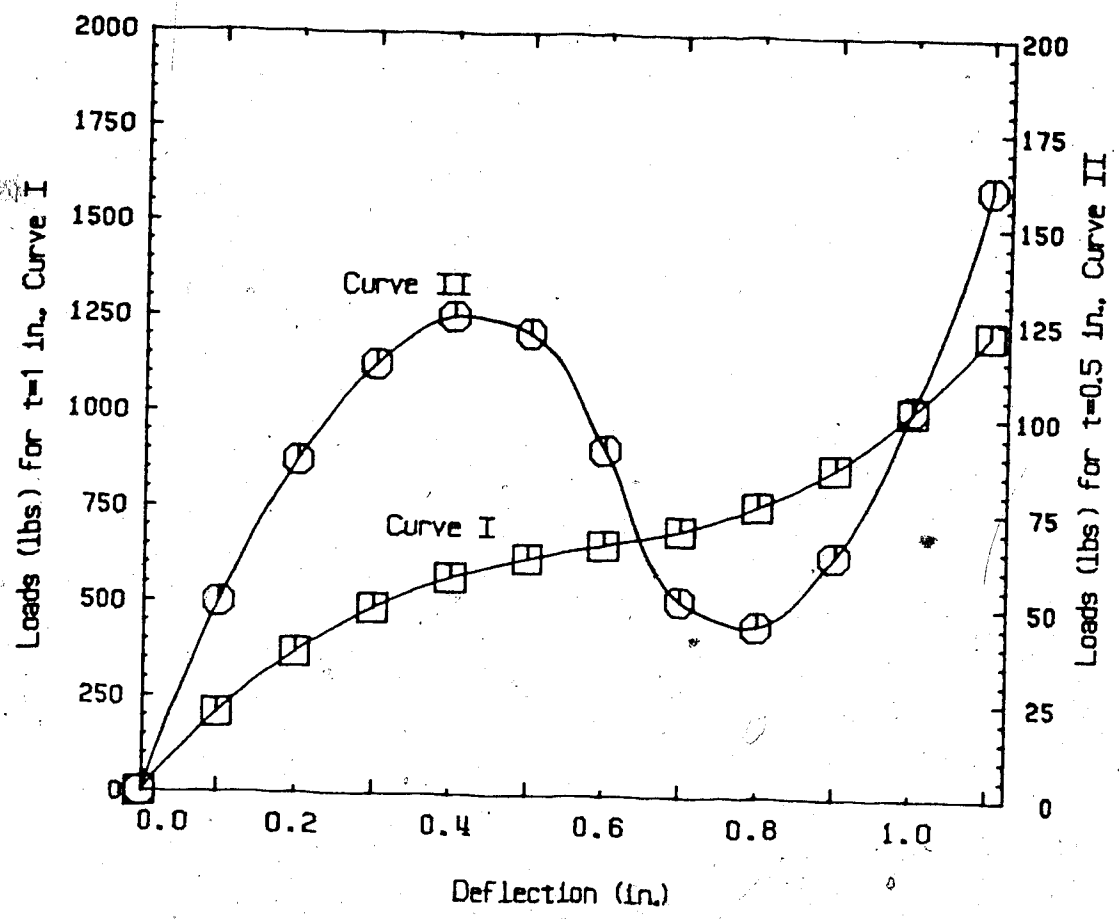


Fig. 5.5: Load Deflection Curve of a Hinged Barrel Vault under Single Load.

Table 5.2: Loads for Prescribed Deflections of a Hinged Barrel Vault under Single Load.

Deflection Δ (in.)	Load P (lbs)	
	t=1 in.	t=0.5 in.
0.1	207.8	49.84
0.2	369.7	87.17
0.3	488.7	112.6
0.4	569.5	125.2
0.5	621.0	121.0
0.6	657.7	90.60
0.7	698.6	51.44
0.8	762.9	44.78
0.9	865.5	63.56
1.0	1016	102.3
1.1	1219	160.1

5.4 Nonlinear Strains and Rigid Body Motions

As shown in the previous chapters the finite element displacement fields used include rigid body motions associated with the linear strain displacement equations. With the inclusion of the nonlinear strain terms certain rigid body motions are no longer properly represented. Introducing rigid translations along any of the \bar{x} , \bar{y} , or \bar{z} axes (see Fig. 2.2) into Eq. 3.13 gives zero strains. These motions are therefore properly represented.

The rotations around the \bar{x} , \bar{y} , and \bar{z} axes are discussed for small rotations in section 2.3. With the introduction of the exact displacements some of the rotations cannot be exactly represented by the element and may cause significant strains for even relatively small rotations. This problem is analyzed in further detail below.

5.4.1 Rotation around the \bar{x} -Axis

A rotation about the \bar{x} -axis occurs for elements at the side of a cylinder under bending, since the vertical movement of the sides is larger than that at the top or bottom of the cylinder. If the magnitude of the rotation is Δ , then the corresponding displacements are given by

$$u = 0, \quad (5.2a)$$

$$v = R \sin \Delta, \quad (5.2b)$$

$$w = -R(1 - \cos \Delta). \quad (5.2c)$$

This motion is represented exactly by the element displacement field and therefore does not induce any strains.

5.4.2 Rotation around the \bar{y} -Axis

A rotation about the \bar{y} -axis occurs at the top and bottom fibre of a cylinder under bending and is largest at the ends of the cylinder.

The theoretical displacements for a rigid body motion of a cylindrical element are given below for a rotation of magnitude Δ .

$$U = R \sin\Delta \cos\theta - x (1 - \cos\Delta) , \quad (5.3a)$$

$$V = x \sin\Delta \sin\theta + R(1 - \cos\Delta) [\sin\theta \cos\theta] , \quad (5.3b)$$

$$W = - x \sin\Delta \cos\theta - R(1 - \cos\Delta) [\cos^2\theta] . \quad (5.3c)$$

The terms in square brackets cannot be represented by the element displacement fields, since neither v nor w have the required trigonometric terms. The finite element displacement fields determined by setting the nodal displacements to values consistent with Eqs. 5.3, are

$$U = R \sin\Delta \cos\theta - x (1 - \cos\Delta) , \quad (5.4a)$$

$$V = x \sin\Delta \sin\theta + R (1 - \cos\Delta) [\cos(p)\{2\sin\theta - \theta\sin(p)/p\}] , \quad (5.4b)$$

$$W = - x \sin\Delta \cos\theta - R (1 - \cos\Delta) [\cos(p)\{2\cos\theta - \cos(p)\}] . \quad (5.4c)$$

It is seen that u is exactly represented, and v and w are quite well approximated for a larger number of elements in the circumferential direction.

With Eqs. 3.13 we obtain for the induced strains:

$$\begin{aligned}
 \epsilon_x &= -(1-\cos\Delta) + 1/2(1-\cos\Delta)^2 + 1/2 \sin^2\Delta \\
 &= 0, \\
 \epsilon_\theta &= (1-\cos\Delta)f + 1/2 \sin^2\Delta \sin^2\theta + 1/2 [(1-\cos\Delta)f]^2 \\
 &\quad + 1/2 [(1-\cos\Delta)\sin(p) \cos(p) \theta/p]^2, \\
 \gamma_{x\theta} &= (1-\cos\Delta)\sin\Delta [1 - 2/3 p^2 \sin\theta - \sin(p) \cos^2(p)\theta/p], \\
 k_x &= 0, \\
 k_\theta &= (1-\cos\Delta)\sin(p)\cos(p)/pR, \\
 k_{x\theta} &= 0,
 \end{aligned} \tag{5.5}$$

$$\text{with } f = \cos(p)[p \cos(p) - \sin(p)]/p.$$

With the assumption that higher terms in Δ are negligibly small relative to other terms the strain expressions are simplified:

$$\epsilon_\theta \cong \Delta^2 d,$$

where d is a function of θ and p .

$$\gamma_{x\theta} = O(\Delta^3),$$

$$k_\theta = O(\Delta^2).$$

The strain $\gamma_{x\theta}$ is of higher order in Δ and can be therefore neglected if compared to ϵ_θ . The curvature k_θ gives a

maximum circumferential strain of about $t \cdot \Delta^2 / 4R'$, which can be neglected for large R/t ratios.

Taking the centre rotation of the finite element as the rigid body rotation, the rotation for the top element at the cylinder end is:

$$\Delta = \beta_{cr} \cos(\pi/2NP) (1 - 1/2NX). \quad (5.6)$$

For a fine element mesh the factor $(1 - 1/2NX)$ can be approximated by 1.

The strain ϵ_{θ} induced by the rigid body motion is denoted by ϵ_{θ}^* . It is compared to the longitudinal strain which causes the classical buckling stress σ_{cr} .

$$\epsilon_{\theta}^* \cong d/2 [\beta_{cr} \cos(\pi/2NP)]^2. \quad (5.7)$$

Assuming ν as 0.3, ϵ_{θ}^* can be expressed in terms of the critical buckling strain:

$$\epsilon_{\theta}^* \cong d (tL^2 \epsilon_{cr} / 13.22R^3) [\cos(\pi/2NP)]^2. \quad (5.8)$$

The induced strain ϵ_{θ}^* is largest for $\theta = \pm \theta$ and is computed below for various numbers of elements in the circumferential direction.

Table 5.3: Circumferential Strain Induced by Rotation around the \bar{y} -Axis.

NP	2	4	6	8	10
$\frac{-\epsilon_{\theta}^+ \cdot R^3}{\epsilon_{cr} \cdot tL^2}$	0.0239	0.0106	0.0054	0.0032	0.0021

As shown in Table 5.3 the strain ϵ_{θ}^+ tends to zero for a large number of elements in the circumferential direction. For a thick, long cylinder the longitudinal strain may become so large that a large number of elements is necessary to ensure reasonable results. However, these spurious strains are very localized at the top or bottom of the ends of the cylinder and decay rapidly with increased longitudinal and circumferential distance due to the term ' Δ^2 '.

5.4.3 Rotation around the \bar{z} -Axis

Rotations about the \bar{z} -axis occur at the sides of the cylinder and are largest for the side elements at the cylinder ends. The theoretical rigid body displacements associated with this motion are given below for a rotation of magnitude Δ .

$$U = R \sin\Delta \sin\theta - x (1 - \cos\Delta), \quad (5.9a)$$

$$V = -x \sin\Delta \cos\theta - R (1 - \cos\Delta) [\sin\theta \cos\theta], \quad (5.9b)$$

$$W = -x \sin\Delta \sin\theta - R (1 - \cos\Delta) [\sin^2\theta]. \quad (5.9c)$$

The element displacement functions approximate the above

functions as shown below.

$$U = R \sin \Delta \sin \theta - x (1 - \cos \Delta), \quad (5.10a)$$

$$V = -x \sin \Delta \cos \theta - R (1 - \cos \Delta) [\cos(p) \{2 \sin \theta - \theta \sin(p)/p\}], \quad (5.10b)$$

$$W = -x \sin \Delta \sin \theta - R (1 - \cos \Delta) [\sin^2(p) + 2 \cos \theta \{\cos(p) - \cos \theta\}]. \quad (5.10c)$$

Substituting the element displacement field into the strain expressions gives

$$\begin{aligned} \epsilon_x &= -(1 - \cos \Delta) + 1/2 (1 - \cos \Delta)^2 / 2 + 1/2 \sin^2 \Delta, \\ &= 0, \\ \epsilon_\theta &= -(1 - \cos \Delta)(1 + f) + 1/2 (1 - \cos \Delta)^2 (1 + f)^2 \\ &\quad + 1/2 [(1 - \cos \Delta) \sin(p) \cos(p) \theta / p]^2 \\ &\quad + 1/2 \sin^2 \Delta \cos^2 \theta, \\ \gamma_{x\theta} &= (1 - \cos \Delta) \sin \Delta [-\cos \theta + \cos \theta (1 + f) \\ &\quad + \sin(p) \cos(p) \theta \sin \theta / p], \\ k_x &= 0, \\ k_\theta &= (1 - \cos \Delta) \sin(p) \cos(p) / p R, \\ k_{x\theta} &= 0. \end{aligned} \quad (5.11)$$

For small rotations Δ , only the lowest powers of Δ for each strain component need to be considered.

$$\begin{aligned} \epsilon_\theta &= -(\Delta^2/2) [\sin^2 \theta + \cos(p) \{\cos(p) - \sin(p)/p\}], \\ \gamma_{x\theta} &= (\Delta^3/2) \cos(p)/p [\theta \sin(p) \sin \theta + p \cos(p) - \sin(p)], \end{aligned}$$

$$k_{\theta} = (\Delta^2/2) \sin(p) \cos(p)/pR. \quad (5.12)$$

It is seen that the strain $\gamma_{x\theta}$ can be neglected with respect to ϵ_{θ} and k_{θ} . The curvature k_{θ} gives a maximum circumferential strain of about ' $t \cdot \Delta^2/4R$ ', which can be neglected for large R/t ratios.

The maximum value of ϵ_{θ} occurs at $\theta = \pm p$. The circumferential strain can be expressed by ' $d \cdot (-\Delta^2/2)$ ', where d is a factor depending on NP and the angle θ . For example with $NP=4$, d is 0.36 and converges to zero with increasing NP .

This rotation is equivalent to the derivative of the tangential displacement v with respect to the longitudinal coordinate x , calculated at the element origin. At the side elements at the cylinder ends we obtain:

$$\begin{aligned} \Delta &= \beta \cos(\pi/2NP) \cdot (1-1/2NX) \text{ if } NP \text{ is even,} \\ &\cong \beta \cos(\pi/2NP) \quad \text{for } NX \gg 1. \end{aligned} \quad (5.13)$$

Letting β be the critical elastic buckling rotation β_{cr} and $\nu=0.3$ the induced circumferential strain, ϵ_{θ}^* can be defined as

$$\epsilon_{\theta}^* = d \epsilon_{cr} tL^2/13.22R^3 \cos^2(\pi/2NP),$$

where ϵ_{cr} is the longitudinal strain corresponding to the classical buckling stress.

Table 5.4: Circumferential Strain Induced by Rotation around the \bar{z} -Axis.

NP	2	4	6	8	10
$\frac{-\epsilon_{\theta^*} \cdot R^3}{\epsilon_{cr} \cdot tL^2}$	0.0275	0.0075	0.0034	0.0019	0.0012

5.4.4 Summary of the Rigid Body Rotations

It was demonstrated that a rigid body motion around the \bar{x} -axis does not induce spurious strains.

The strains induced by rotations around the other two axes are reduced approximately quadratically for an increase in the number of circumferential elements. Except for the case with NP=2 the strains due to rotations around the \bar{y} -axis are larger than those of the \bar{z} -axis.

Table 5.5: Maximum of Induced Strains from Rigid Body Motions.

		Long Cylinder	Short Cylinder	Cylinder of Stephens <i>et al.</i>
L		2500	1829	2000
R		90	764.5	100
t		1.1	5.13	1
tL^2/R^3		9.43	0.038	4
	NP			
$\frac{\epsilon_{\theta^*}}{\epsilon_{cr}}$	2	0.259	0.0011	0.110
	4	0.100	0.0004	0.042
	6	0.051	0.0002	0.022
	8	0.030	0.0001	0.013
	10	0.020	0.0001	0.008

Considering the induced strains described above, the analysis of cylinders with a high ratio tL^2/R^3 should be done with some care using the present element. The short cylinder has a very low tL^2/R^3 ratio when compared to the other cylinders and therefore is less affected by strains from rigid body motions.

The induced negative circumferential strains cause the element to develop compressive stresses in the circumferential direction. These can be relieved by an increase of the circumference (that is an increase of the radius of the cylinder). With a larger radius the bending stiffness of the cylinder is increased. The short cylinder remains essentially unaffected but the induced strains for the long cylinders will tend to reduce the ovalization of the cross-section which thereby limits the reduction of the bending stiffness.

Compared with the arch and the barrel vault problem the geometric nonlinear bending of a cylinder is particularly difficult. The deflections of the barrel vault are in the order of the shell thickness t . The only rigid body rotation occurring for the circular arch is the rotation around the longitudinal axis which can be exactly represented by the element displacement functions. The circular cylinder under bending undergoes deformations in the order of 20 times the thickness and there are significant rigid body motions. In the finite element model these result in induced strains.

Although the induced circumferential strains are small compared to the longitudinal strains from bending they will tend to increase the diameter of the cylinder and thereby alter significantly the behaviour of the cylinder.

5.5 Cylinder under Bending

5.5.1 Review of Earlier Investigations

Flügge indicates in Ref. 26 for the buckling problem of a cylinder under bending that the bending stiffness for small displacements agrees with the linear theory of Donnell, but with increasing deflections (end rotation) the mid section of the cylinder ovalizes and the section modulus is reduced. As the end rotation increases the bending moment increases at a decreasing rate until it reaches a maximum (which is referred to as the buckling moment) after which it then decreases.

Stephens *et al.*^{3*} showed for cylinders with a ratio R/t of 100, that the buckling moment is equal to the classical buckling moment M_{cr} and decreases with increasing L/R ratio to Brazier's solution. Using a finite difference technique they showed the buckling mode that occurs to be a combination of longitudinal wrinkles and an ovalization of the cross-section. They defined the buckling moment to be the moment for which large deflections or ovalization occurs with increases in moment of the order of 0.01%. The ovalization is shown to depend largely on the L/R ratio. Since the development of longitudinal wrinkles is likely to occur only for thin cylinders, the ovalization effect should be studied with thick cylinders since otherwise a combination of both buckling modes may occur.

Fabian²⁴ investigated the nonlinear bending of infinite cylinders and separated the ovalization from the wrinkling effect by restricting the possible displacement functions. With longitudinal wrinkling prevented the bending moment was found to be linear up to stresses of 25 % of $\bar{\sigma}_{cr}$. Then the moment increased less than proportionally and reached a maximum of around 53 % of M_{cr} . This is only slightly less than predicted by the Brazier solution.

The results of structural tests are largely dependent on imperfections and material nonlinearities. Since most analytical studies include only geometrical nonlinearities and simplified imperfections, a discussion of structural tests is not done in this study. A review of these tests is given in Ref. 37.

5.5.2 Boundary Conditions and Their Representation

In many structures that incorporate cylinders, the cylinders have very complex boundary conditions. The ends are often attached to stiff plates to ensure that the cross-section is maintained. Often longitudinal or circumferential stiffeners are present to increase the load limits.

In most geometric nonlinear studies of cylinders under bending, the cylinder is idealized as a perfect tube. The end condition adopted depends on the type of cylinder investigated and the kind of analysis performed.

For infinitely long cylinders a complete torus has been considered (Flügge²⁵, Fabian²⁴). Seide and Weingarten²⁶ described the ends of finite cylinders by restricting the radial deflections to zero but allow a warping of the cross-section. Stephens *et al.*³⁸ investigated finite cylinders by applying stresses on the cylinder ends which were distributed according to the linear beam theory. In order to minimize the warping or distortion of the cross-section the cylinder end was stiffened with two cylindrical rings.

Although they state that a distortion of the cross-section was thereby prevented, the author believes that the rings allow a circumferential stretching as discussed in section 4.2.3. Otherwise an upward buckle near the cylinder end similar to Fig. 4.5 would be expected.

A third way to describe boundary conditions is to prescribe displacements at the cylinder ends, which is discussed in the following sections.

5.5.3 Prescribed Displacements at the Cylinder Ends

In prescribing the displacements at the cylinder ends the circular cross-section is retained and a warping or distortion of the cylinder end is prevented. However, one has to consider that rigid ends present a problem which is different from the infinite cylinder and might give rise to stresses or strains which deform the cylinder unexpectedly at the ends (e.g. Fig. 4.5).

5.5.3.1 Shortening of Cylinder due to Bending

If a cylinder is bent by applied moments (or end rotations as in the present study) the linear beam theory predicts a quadratic displacement function. Under finite deformations the cylinder stretches longitudinally because the deformed neutral axis describes an arc as opposed to a straight line. In the nonlinear analysis of cylinders, large end rotations give rise to a net axial force unless the cylinder ends are allowed to move axially. Using \bar{L} as the new cylinder length and \bar{R} as the radius of the curvature of the bent cylinder the elongation ΔL and the strain ϵ_x for fixed ends can be expressed.

$$\Delta L = \bar{L} - L, \quad (5.14)$$

Assuming the form of the bent cylinder is a circular arch, \bar{R} and L can be expressed by the end rotation β and the new cylinder length \bar{L} .

$$\begin{aligned} L &= 2 \bar{R} \sin \beta \\ &= \bar{L} \sin \beta / \beta. \end{aligned} \quad (5.15)$$

Inserting this into Eq. 5.14 we get

$$\begin{aligned} \Delta L &= \bar{L} (1 - \sin \beta / \beta), \\ \epsilon_x &\equiv \Delta L / \bar{L} = 1 - \sin \beta / \beta \\ &\equiv \beta^2 / 6 \quad \text{for } \beta \ll 1. \end{aligned} \quad (5.16)$$

A better insight of the effect of ϵ_x is gained if the induced stress $\bar{\sigma}$ is compared to the critical stress σ_{cr} .

$$\begin{aligned}\bar{\sigma} &= E \beta^2/6, \\ \sigma_{cr} &= \beta_{cr} E R/2L, \\ \beta_{cr} &= (t L/2R^2) \cdot [3(1-\nu^2)]^{-1/2}.\end{aligned}\tag{5.17}$$

Substituting β_{cr} for β we obtain:

$$\begin{aligned}\max \bar{\sigma}/\sigma_{cr} &= tL^2/24R^3 [3(1-\nu^2)]^{-1/2} \\ &= tL^2/39.65 R^3 \quad \text{for } \nu=0.3.\end{aligned}$$

The ratio of $\max \bar{\sigma}/\sigma_{cr}$ is given for three cylinders in Table 5.6.

Table 5.6: Ratio of $\max \bar{\sigma}/\sigma_{cr}$ for Three Cylinders.

	Long Cylinder	Short Cylinder	Cylinder of Stephens <i>et al.</i>
L	2500	1829	2000
R	90	764.5	100
t	1.1	5.13	1
L/R	27.18	2.392	20
t/R	0.0122	0.0067	0.01
$\max \bar{\sigma}/\sigma_{cr}$	0.238	0.001	0.101

As shown in Table 5.6 the axial stress $\bar{\sigma}$ is significant for large (L/R) and (t/R), that is for long thick cylinders. Therefore, for these problems care must be taken in dealing with axial boundary conditions.

In the program used for the present study, the axial force arising due to end restraint is treated similarly to an equilibrium force during the equilibrium iteration. Since the displacements at the cylinder end are prescribed, the application of nodal forces at the end is not possible. Instead, displacements are applied to the cylinder ends which approximate the displacements for free cylinder ends.

5.5.3.2 Nonlinear Boundary Conditions for End Rotation

The displacements prescribed at the cylinder end consist of two parts. First, the cross-section is rotated around the longitudinal axis with angle β , and second, if wanted, the circumferential stretching may be applied. The displacements and rotations at the cylinder end for a rotation about a horizontal axis while maintaining a rigid cross-section are given below.

$$u = -R \sin\beta \cos\bar{\theta}, \quad (5.18a)$$

$$v = R (1-\cos\beta) \sin\bar{\theta} \cos\bar{\theta}, \quad (5.18b)$$

$$w = -R (1-\cos\beta) \cos^2\bar{\theta}, \quad (5.18c)$$

$$\beta x = \sin\beta \cos\bar{\theta}, \quad (5.18d)$$

$$\beta\theta = (1-\cos\beta) \sin\bar{\theta} \cos\bar{\theta}. \quad (5.18e)$$

The angle $\bar{\theta}$ is the circumferential coordinate measured from the top fibre (Fig. 4.2) and β is the angular rotation of the cross-section.

For small rotations the trigonometric functions in β are approximated by the first term of the corresponding Taylor's series. This results in the following linear expressions which were used for the linear bending problem.

$$u = -R\beta \cos\bar{\theta}, \quad (5.19a)$$

$$v = 0, \quad (5.19b)$$

$$w = 0, \quad (5.19c)$$

$$\beta x = \beta \cos\bar{\theta}, \quad (5.19d)$$

$$\beta\theta = 0. \quad (5.19e)$$

In order to simulate the cylinder by Stephens *et al.*³⁸ points on the cylinder ends should be allowed to move in the circumferential direction. Otherwise stresses in the circumferential direction occur at the cylinder end, and an outward buckle similar to Fig. 4.5 would occur. In the linear analysis this effect was avoided by allowing v and $\beta\theta$ to be free.

In a nonlinear analysis, however, v and $\beta\theta$ cannot be let free since these degrees of freedom are needed to prescribe the rotation of the cylinder end (Eq. 5.18). Therefore displacements are applied which approximate a cylinder end with no circumferential stresses. The Donnell equation (Eq. 4.2) for zero circumferential stress is derived from the linear bending theory of cylinders. It is assumed that the nonlinear circumferential stretching is about as much as in the linear range.

In section 4.2 it is shown that the maximum displacement Δv for $\bar{\sigma}_x = \bar{\sigma}_{cr}$ is only 0.182 times the shell thickness t . For the derivation of the displacements it is therefore permissible, that $\sin(\Delta v/R)$ and $\cos(\Delta v/R)$ are approximated by $\Delta v/R$ and 1, respectively, for large R/t ratios.

The displacements due to this prescribed circumferential strain are as follows:

$$u = \bar{D} \beta \sin\beta \sin^2\bar{\theta}, \quad (5.20a)$$

$$v = \bar{D} \beta \sin\bar{\theta}, \quad (5.20b)$$

$$w = 0, \quad (5.20c)$$

$$\beta x = 0, \quad (5.20d)$$

$$\beta \theta = -\bar{D} \beta \sin\bar{\theta}/R, \quad (5.20e)$$

where \bar{D} equals to $2\sqrt{R^2/L}$.

5.5.4 Discussion of Test Results

The cylinders considered are the long cylinder by Stephens *et al.*¹¹ and the short cylinder by Stephens¹⁷, whose data are given in Table 5.6. As in the preceding nonlinear analysis the full Newton-Raphson-Method is used. The step size of the rotation of the cylinder end is chosen as 10 % of β_{cr} . The equilibrium iterations are stopped when the norm of the incremental displacements is smaller than 10^{-1} times the norm of the first displacements of the current load step. The CPU-time required for each load step is found to be approximately 0.9 seconds per element. The calculation of the three stiffness matrices takes about 48 seconds for one element type. This calculation is done only once. Due to these high computing costs only a limited number of runs were possible.

5.5.4.1 Rigid and Semi-Rigid Cylinder Ends

In order to study the effect of axial fixed ends and prescribed circumferential strain, three tests of the long cylinder ($L/R/t=2000/100/1$) were done with 4×2 elements. The results are given in Table 5.7 and are compared with the deflection and end moment of the linear beam theory.

Table 5.7: Effects of Axially Fixed Ends and Prescribed Circumferential Strain on the Long Cylinder by Stephens *et al.* with 4×2 Elements and $\beta = \beta_{cr}$.

	axial fixed	axial free, no Donnell strain	axial free, prescribed Donnell strain
w / w beam †	1.028	1.050	1.034
M / M beam	0.865	0.827	0.699
Δw (mm) ‡	7.27	7.50	7.35
(axial shortening or axial force) / beam theory	1.67	1.51	1.013
ϵ_x (top)/beam theory cylinder end cylinder middle	-1.28 -1.26	-1.50 -1.47	-1.35 -1.57
ϵ_x (bottom)/beam theory cylinder end cylinder middle	1.71 1.38	1.63 1.26	1.43 1.27

Comparing the two columns with no circumferential strain at the end, the following can be said: The axial force due to fixed ends increases the longitudinal strains in the cylinder and increases the end moment by about 5 %. The deflection is reduced by 3 % and the ovalization by 2.2 %. In prescribing Donnell's circumferential strain at the ends the deflection w and the ovalization Δw are slightly reduced. The bending moment drops by 16 % when compared to the cylinder with rigid ends. A similar effect

 † The deflection w is the mean of top and bottom deflection.
 ‡ The ovalization or flattening Δw is measured as the difference of top and bottom fibre deflection.

has been observed already in section 4.2.3 where deflections and moments of a long cylinder decreased when circumferential strains were allowed to develop.

The longitudinal strains vary significantly. For the cylinder with Donnell's strain the stresses vary less than in the two other cases. A significant improvement is the calculation of the axial shortening which shows only a 1.3 % difference from the beam solution. Because of the effect of the prescribed Donnell strain on the computation of the axial shortening and the increased bending stiffness for axial fixed ends the next tests are done with axial free ends and the prescription of Donnell's circumferential strain at the cylinder ends.

5.5.4.2 The Short Cylinder

The finite element gridwork chosen for the cylinder by Stephens¹¹ is $NP \times NX = 3 \times 8$ elements. It was chosen to have approximately equilateral elements. The cylinder data are given in Table 5.6. For the first load step ($\Delta\beta = 0.1 \beta_{cr}$) four equilibrium iterations were needed and only two iterations were necessary for further loadings. This fast convergence is possible because of the small displacements of the cylinder. The calculation could not however be continued beyond the first iteration of the fifth load step since the determinant of the tangent stiffness matrix was found to be negative. The results of Stephens *et al.*¹¹ indicate that the buckling moment for the present cylinder would be around $0.98 M_{cr}$. The results of the present study are given in the table below.

Table 5.8: Nonlinear Results of Short Cylinder under Bending.

Load Step, (β/β_{cr})	$\frac{ K^T }{ K^0 }$	Δw (mm)	Mean Deflection (mm)	Shortening of Cylinder (mm)
0.0	1.0000	0.0000	0.0000	0.000000
0.1	0.8669	0.0018	0.2194	0.000145
0.2	0.6289	0.0072	0.4388	0.000580
0.3	0.3041	0.0164	0.6583	0.001305
0.4	0.0359	0.0288	0.8779	0.002321
0.5	-0.1031	—	—	—

The mean value of the top and bottom deflection is almost proportional to the end rotation β and is 1.2 % less than predicted by beam theory ($w=0.222136$ mm). The bending moments found are almost proportional to the rotation β . The increase in the bending moment between the third and fourth load step is only 0.005 % smaller than the value of the first load step. The insignificant nonlinearities for deflection and the bending moment can be explained by the very small geometric differences between the loaded and the unloaded cylinder. The ovalization, for example, at $\beta = 0.4 \beta_{cr}$ is only 3.3 % of the deflections or 0.56 % of the thickness t . The flattening Δw increases quadratically with respect to the end rotation. The results by Stephens *et al.*³⁸ show the same trend; the ovalization grows approximately quadratically to the bending moment, which is, as found in the present study, almost proportional to the end rotation. A numerical comparison is difficult, since the smallest L/R ratio in Ref. 38 is 3.4 (as opposed to 2.4 in the present study) and the parameter Δw is hardly visible in the graphical representation of the results. Unfortunately Stephens *et al.* did not give the end rotation, shortening, or the circumferential stresses, which should be compared with the results obtained in this study.

The shortening of the cylinder is about double as much as Eq. 5.17 predicts. This discrepancy may be due to the small number of elements in the longitudinal direction and the relative low L/R ratio. However, a satisfactory explanation is still not available.

The stresses of the mid-section after the fourth load step are shown in Fig. 5.6. The stresses of the cylinder end are omitted since the differences are too small to be shown.

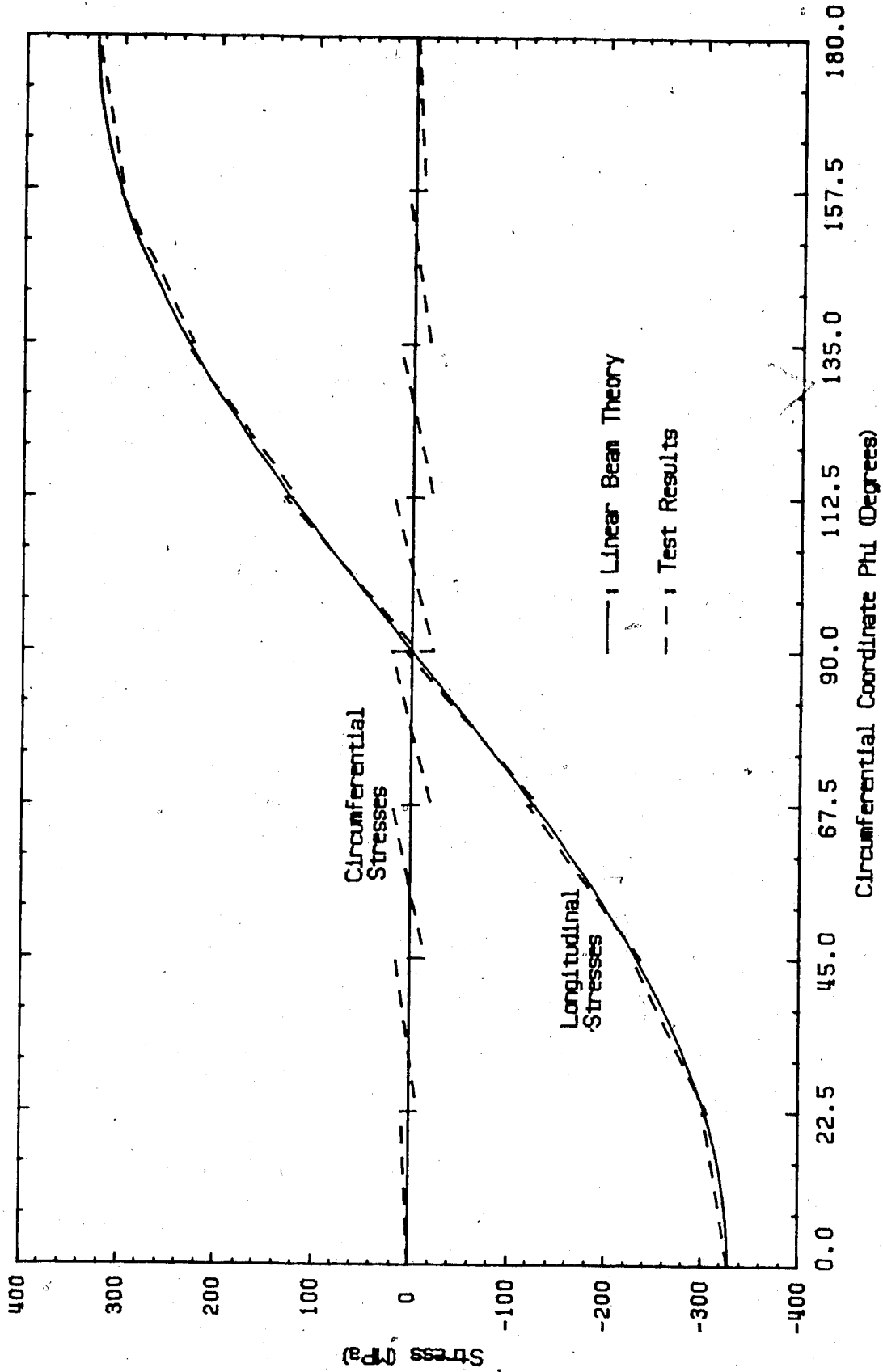


Fig. 5.6: Stresses for Short Cylinder at Mid-Section for $\beta = 0.4 \beta_{cr}$.

The longitudinal stresses approximate the beam solution quite well, since the deflections are very close to the beam theory.

The circumferential stresses approximate Donnell's theory that σ_θ should be zero. The stress σ_θ for each element ($p=22.5^\circ$) varies almost linearly, which is an effect of the lack of a continuous θ -term in the strain function for ϵ_θ .

At the cylinder middle the longitudinal stress of the top fibre is 0.05 % above the beam stress and the bottom stress is 0.03 % less than the beam theory. At the top fibre of the cylinder end σ_x has about the same value as predicted by the beam theory, while the longitudinal stress at the bottom fibre is about 0.4 % larger.

5.5.4.3 The Long Cylinder

The data for this cylinder are:

$$L = 2000 \text{ mm,}$$

$$R = 100 \text{ mm,}$$

$$t = 1 \text{ mm,}$$

$$E = 6895 \text{ MPa,}$$

$$\nu = 0.3.$$

Stephens *et al.* found the buckling moment to be $0.636 M_{cr}$ and observed a maximum ovalization of about 16 times the cylinder thickness. As in the preceding problem the cylinder is tested with prescribed circumferential strain at the ends and axial free ends. The finite element mesh chosen is $NX \times NP = 13 \times 4$ elements, which gives an element aspect ratio of 0.98. The cylinder is tested up to an end rotation of $\beta = \beta_{cr}$ with a load step size of $\beta = 0.1 \beta_{cr}$. The results are given in Table 5.9 below.

Table 5.9: Nonlinear Results of Long Cylinder under Bending.

Load Step	Increase of Moment (Nmm)	Increase in Mean Deflection (mm)	Increase in Δw (mm)
1	123156	3.0331	0.33
2	122158	3.0735	0.92
3	120650	3.1075	1.17
4	119235	3.1125	1.16
5	117974	3.1125	1.08
6	116819	3.1110	0.98
7	115699	3.1090	0.83
8	114659	3.1082	0.77
9	113743	3.1100	0.77
10	112739	3.1045	0.73

Despite a recalculation of the tangent stiffness matrix, the convergence was rather slow. Four to five equilibrium iterations were necessary for each load step. The axial movement of the cylinder end was found to be in good agreement with the prediction by Eq. 5.17. The difference lies between 1.1 % for $\beta = 0.1 \beta_{cr}$ and 4.2 % for $\beta = 1.0 \beta_{cr}$. The moment for the first load step is 93.9 % of the beam theory and for the tenth load step 86.0 %. The decrease in the difference between the moments at two successive load steps has an average of 0.8 % and is largest at the third load step. After the third load step the change in moment per load step decreases at a slower rate. It is interesting to note that the rate of increase in ovalization decreases after the third load step and that the additional mean deflections have their maximum at the fourth load step.

If one compares the end rotation with the ovalization and the deflection, a geometric stiffening of the cylinder after $\beta = 0.3 \beta_{cr}$ is observed. An explanation for this stiffening is that the induced stresses reduce the ovalization and thereby limit the reduction of the bending stiffness.

The relative increase of the bending stiffness is especially seen in the determinant $|K^T|$ which increases steadily from 1.5×10^{10} at $\beta = 0.1 \beta_{cr}$ to 1.2×10^{11} after the last load step.

Table 5.10 shows the ovalizations calculated by Stephens *et al.* and the present study.

Table 5.10: Ovalization of Long Cylinder under Bending

Moment / M_{cr}	Ovalization $\Delta w/t$ Stephens <i>et al.</i> †	Ovalization $\Delta w/t$ present study
0.1	0.3	0.4
0.2	1.0	1.4
0.3	2.3	2.7
0.4	4.5	4.0
0.5	8.7	5.1
0.6	13.5	6.1
0.636	16.0	6.5

Up to a moment of $0.3 M_{cr}$ the present study gives a larger ovalization than Stephens *et al.*. This can be partly explained by the calculation of the bending moment which for $\beta = 0.1 \beta_{cr}$ is 6 % lower than predicted by beam theory

† Approximate values obtained from graphical results.

(131000 Nmm). The present results compare reasonably well with those of Stephens up to 0.3 Mcr. Beyond that moment, Stephens' solution predicts a much larger rate of increase in Δw .

To illustrate the development of cross-section ovalization the incremental deflections for the first three and the last load step are illustrated in Fig 5.7. The curves above the dashed line are the deflections for the bottom fibre, and the deflections of the top fibre are shown below the dashed line. The fourth increment, which is almost identical with the third one and the increments of step 5 to 9 are omitted for clarity of the other curves.

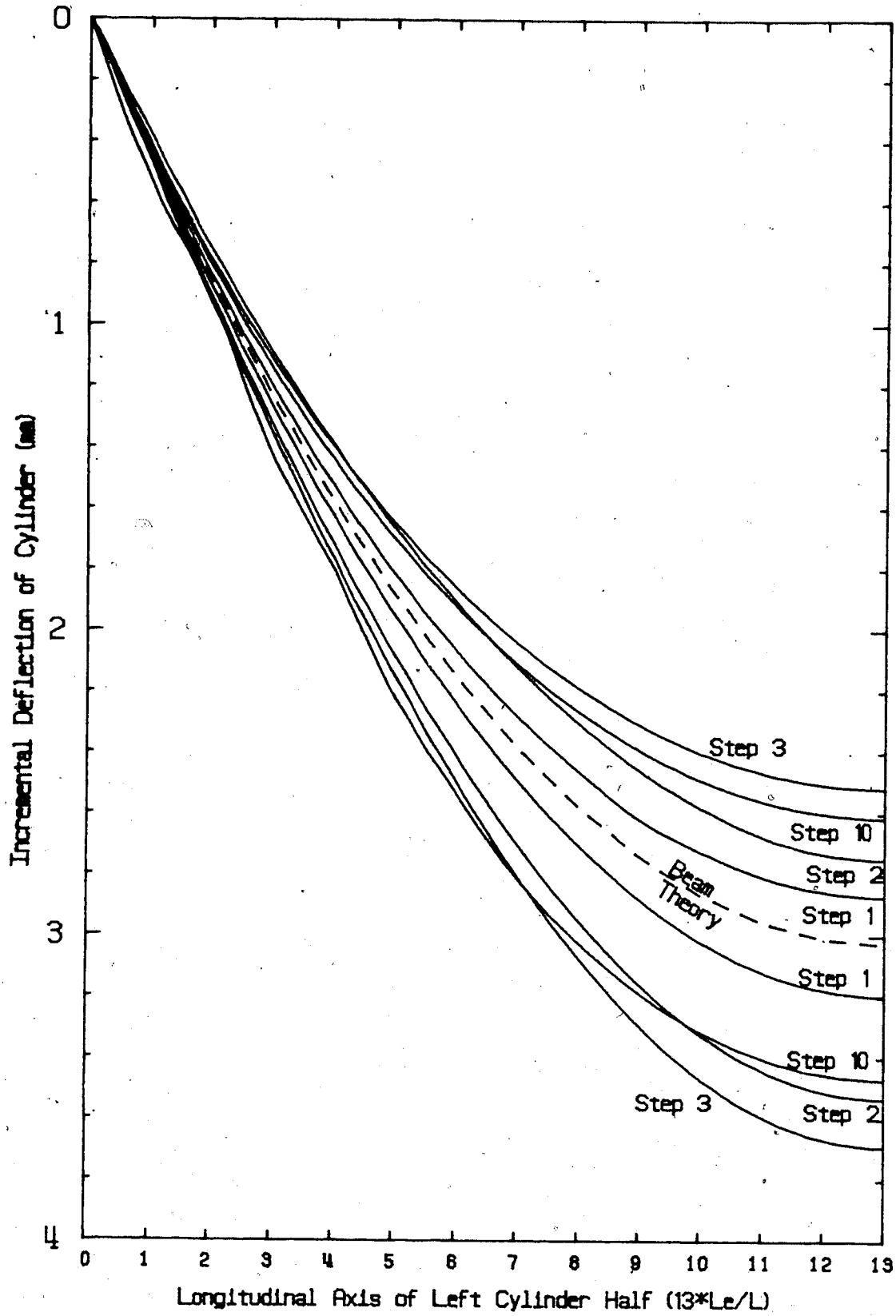


Fig. 5.7 : Incremental Deflections of Long Cylinder under Bending.

With increasing end rotation the ovalization is reduced at the cylinder middle but still increases near the cylinder end. The wave-like differences of the tenth step might be interpreted as the beginning of a longitudinal wrinkling. In order to find the buckling mode occurring an element refinement in the circumferential direction is appropriate so that the stresses induced by rigid body motions are kept small. Unfortunately Stephens *et al.* did not present the moment end rotation and moment-deflection relationship which should be compared to the present results.

Lastly the longitudinal and circumferential stresses for $\beta = 0.3 \beta_{cr}$ are presented in Fig. 5.8 and compared to the beam theory and the results of Stephens *et al.*.

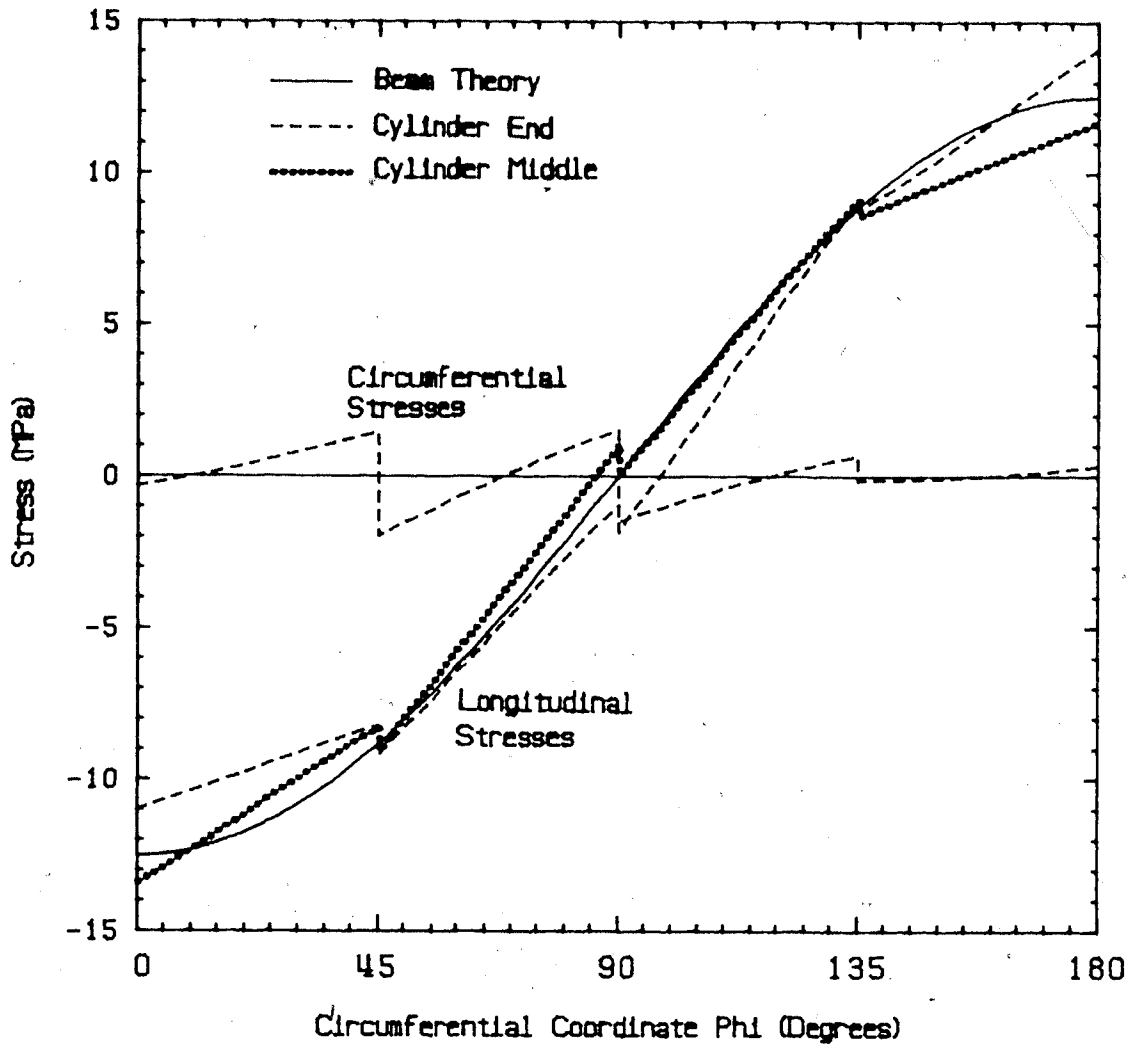


Fig. 5.8: Stresses of Long Cylinder at $\beta = 0.3 \beta_{cr}$.

Despite the surprisingly coarse stress distribution an effect is observed which Stephens *et al.* found also. In the middle of the bent cylinder the stresses at the top and the bottom fibre decreases. In order to maintain equilibrium of horizontal forces the neutral axis shifts by about 5° towards the top fibre.

The stresses at the cylinder end are shifted in the reverse sense. The neutral axis is about 7.5° lower than the middle fibre of the beam. The circumferential stresses at the cylinder end are in the average about zero. The more positive σ_θ from the top fibre to 45° is in accordance with the quite low σ_x : The circumferential strains prescribed are based on the longitudinal stresses of the beam theory. A positive increase in σ_x without changing the circumferential strain results in an increase in σ_θ . Near the bottom fibre the longitudinal stresses approximate the beam theory quite well; correspondingly the circumferential stress tends towards zero as expected.

6. Summary and Conclusions

In the foregoing a modified finite element is developed for geometric nonlinear behaviour of thin cylindrical shells. The element is proven to be at least equal in performance when compared to other elements for the linear pinched cylinder problem. The bending of a cylinder under end moments shows that the element gives the exact beam deflection if points at the cylinder ends are allowed to move in the circumferential direction. Otherwise an upward lifting is observed. Despite the good results for deflections the cylinder moment and the circumferential strain predicted are very poor unless approximately equilateral elements are used.

In the nonlinear range the element is successfully applied to the barrel vault problem with concentrated loads and successfully follows the nonlinear load-deflection path with horizontal tangents. In another test problem, the pinched circular arch, the element gives loads slightly higher than the results by Sabir and Lock. One reason for the different performance is the difference in the magnitude of the deflections in the two problems. The barrel vault was tested up to $w=0.011 R$ while the circular arch had a deflection of $0.137 R$.

In the context of nonlinear problems, the element is tested for spurious strains arising from rigid body motions. It is shown that the element remains strain-free for translations in all directions as well as for a rotation

around the longitudinal axis. However, rotations around the two other axes induce strains in the element. In the nonlinear bending problem, cylinders with a high ratio tL^2/R^3 are apt to develop compressive circumferential stresses as a result. These stresses enlarge the diameter of the cylinder and reduce the flattening or ovalization of the cross-section.

Due to high computing costs only a limited number of runs were done for the nonlinear bending problem. It was shown that the ends of the cylinder move axially due to second order effects and that a rigid cross-section at the cylinder end causes circumferential stresses which in turn influence the middle of the cylinder. In order to assess the influence of various boundary conditions it seems necessary that the element be refined near the cylinder end and that there be enough elements in the circumferential direction to obtain a uniform stress distribution for δx .

Two cylinders with quite different values of tL^2/R^3 were tested. The short cylinder showed good results except that the determinant of the tangent stiffness matrix became negative at the fifth load step. The reason for this behaviour is not clear. With an element gridwork of 3×8 elements the representation of the bent cylinder might be too coarse and might cause numerical problems during the triangularization of the stiffness matrix.

A very long cylinder showed the problem with induced strains. After a rotation of $\beta = 0.3 \beta_{cr}$ the ovalization and

the deflection did not increase very much and neither the determinant of the stiffness matrix nor the displacements indicated a buckling behaviour.

The success of the element for nonlinear problems with small deflections suggests that the element works best when strains arising from rigid body motions are kept small compared to the strains due to the structural loading. The rigid body motions which rotate perpendicular to the longitudinal axis are responsible for these strains.

In order to avoid these induced stresses one should either change the tangent stiffness matrix of an element by a subtraction of rigid body motions or change the displacement functions to include the rigid element displacements.

As shown, the element works well for most linear and nonlinear problems. However, the bending of cylinders appears to be particularly difficult. Besides the problems of representing the boundary conditions at the cylinder end, the element itself can only approximate the displacements of a cylinder under bending. With restrictions due to the high computing time involved, a detailed study of the various problems with the cylinder under bending has been only started and further research is necessary to solve the problem adequately.

References

1. B. O. Almroth and J. H. Starnes, Jr.,
"The Computer in Shell Stability Analysis",
ASCE Journal, Vol. 101, EM6, 1975, pp. 837-888.
2. J. H. Argyris and P. C. Dunne,
"Post-Buckling Finite Element Analysis of
Circular Cylinders under End Load",
Acta Technica, Vol. 87, 1978, Nr. 1-2, pp. 5-16.
3. D. G. Ashwell and R. H. Gallagher,
Finite Elements for Thin Shells and Curved
Members,
John Wiley & Sons, 1976.
4. D. G. Ashwell and A. B. Sabir,
"A New Cylindrical Shell Element Based on Simple
Independent Strain Functions", *International
Journal of Mechanical Science*, Vol. 4, 1972,
pp. 171-183.
5. D. G. Ashwell and A. B. Sabir,
"A Corrected Assessment of the Cylindrical Shell
Element of Bogner, Fox and Schmidt when Applied
to Arches", *International Journal of Mechanical
Sciences*, Vol. 15, 1973, pp. 325-327.
6. D. G. Ashwell, A. B. Sabir and T. M. Roberts,
"Further Studies in the Application of Curved
Finite Elements to Circular Arches",
International Journal of Mechanical Sciences,
Vol. 13, 1971, pp. 507-517.
7. K.-J. Barthe und E. L. Wilson,
Numerical Methods in Finite Element Analysis,
Prentice-Hall, 1976.
8. Budiansky (Editor),
Buckling of Structures, Symposium Cambridge
(USA), June 17-21 1974, Springer Verlag, Berlin,
1976.

9. F. K. Bogner, R. L. Fox and L. A. Schmidt,
"A Cylindrical Shell Discrete Element",
AIAA Journal, Vol. 5, 1967, Part 1, pp. 745-756.
10. L. G. Brazier,
"On the Flexure of Thin Cylindrical Shells and
Other "Thin" Sections", *Proceedings of the Royal
Society*, London, Series A, Vol. 116, 1927,
pp. 104-114.
11. F. A. Brogan and B. O. Almroth,
"Practical Methods for Elastic Collapse Analysis
for Shell Structures", *AIAA Journal*, Vol. 9,
Part 2, 1971, pp. 2321-2325.
12. D. O. Brush and B. O. Almroth,
Buckling of Bars, Plates and Shells,
McGraw-Hill, 1975.
13. G. Cantin,
"Rigid Body Motions in Curved Finite Elements",
AIAA Journal, Vol. 8, 1970, Part 2,
pp. 1252-1255.
14. G. Cantin and R. W. Clough,
"A Curved, Cylindrical-Shell, Finite Element",
AIAA Journal, Vol 6., 1968, pp. 1057-1062.
15. G. F. Carey,
"A Unified Approach to Three Finite Element
Theories for Geometric Nonlinearity", *Computer
Methods in Applied Mechanics and Engineering*,
Vol. 4, 1974, pp. 69-79.
16. Y. K. Cheung,
Finite Strip Method in Structural Analysis,
Pergamon Press, New-York, 1976.
17. J. J. Connor and C. Brebbia,
"Stiffness Matrix for Shallow Rectangular Shell
Element", *ASCE Proceedings, Engineering
Mechanics Division*, Vol. 93, 1967, EM5,
pp. 43-65.

18. G. R. Cowper, G. M. Lindberg and M. D. Olson,
"A Shallow Shell Finite Element of Triangular
Shape", *International Journal of Solids and
Structures*, Vol. 6, 1970, Part 2, pp. 1133-1156.
19. M. A. Crisfield,
"A Faster Modified Newton-Raphson Iteration",
*Computer Methods in Applied Mechanics and
Engineering*, Vol. 20, 1979, pp. 267-278.
20. D. J. Dawe,
"High Order Triangular Finite Element for Shell
Analysis", *International Journal of Solids and
Structures*, Vol. 11, 1975, pp. 1097-1110.
21. D. J. Dawe,
"Static Analysis of Diaphragm-Supported
Cylindrical Shells Using a Curved Finite Strip",
*International Journal for Numerical Methods in
Engineering*, Vol. 11, 1977, pp. 1347-1364.
22. L. H. Donnell,
Beams, Plates, and Shells,
McGraw-Hill, New-York, 1976.
23. C. L. Dym,
Introduction to the Theory of Shells,
Pergamon Press, Glasgow, 1974.
24. O. Fabian,
"Collapse of Cylindrical, Elastic Tubes under
Combined Bending, Pressure and Axial Loads",
International Journal of Solids and Structures,
Vol. 13, 1977, Part 2, pp. 1257-1270.
25. W. Flügge,
"Die Stabilität der Kreiszyllinderschale",
Ingenieurarchiv, Bd. 3, 1932, pp. 463-506.
26. W. Flügge,
Stresses in Shells, 2nd Edition,
Springer Verlag, New-York, 1973.

27. R. H. Gallagher,
"A Discrete Element Procedure for Thin-Shell Instability Analysis", *AIAA Journal*, Vol. 5, Part 1, 1967, pp. 138-145.
28. G. Horrigmoe,
"Hybrid Stress Finite Element Model for Non-linear Shell Problems", *International Journal of Numerical Methods in Engineering*, Vol. 12, 1978, pp. 1819-1838.
29. T. M. Hrudý,
"The Application of a Refined Shallow Shell Finite Element to Geometric Nonlinear Structures", *C.A.S.I. Transactions*, Vol. 6, No. 2, Sept. 1973.
30. W. Kanok-Nukulchai,
"A Simple and Efficient Finite Element for General Shell Analysis", *International Journal for Numerical Methods in Engineering*, Vol. 14, 1979, pp. 179-200.
31. E. Ramm,
Strategies for Tracing Nonlinear Response Near Limit Points, Europe - US Workshop: Nonlinear Finite Element Analysis in Structural Mechanics, July 28-31 1980, Bochum.
32. E. Ramm,
Geometrisch nichtlineare Elastostatik und finite Elemente, Bericht Nr. 76-2, Institut für Baustatik der Universität Stuttgart, 1976.
33. A. B. Sabir and A. C. Lock,
"A Curved Cylindrical Shell Finite Element", *International Journal of Mechanical Sciences*, Vol. 14, 1972, pp. 125-135.
34. A. B. Sabir and A. C. Lock,
"Large Deflection, Geometrically Non-linear Finite Element Analysis of Circular Arches", *International Journal of Mechanical Sciences*, Vol. 15, 1973, Part 1, pp. 37-47.

35. A. B. Sabir and A. C. Lock,
"The Application of Finite Elements to the Large Deflection Geometrically Non-linear Behaviour of Cylindrical Shells", Variational Methods in Engineering, Vol. 2, Department of Civil Engineering, University of Southampton, Southampton University Press, 1973, pp. 7/66-7/75.
36. P. Seide and V. I. Weingarten,
"On the Buckling of Circular Cylindrical Shells under Pure Bending", *Journal of Applied Mechanics*, Vol. 28, 1961, pp. 112-116.
37. M. Stephens,
"The Local Buckling of Thin-Walled Tubular Steel Members", thesis, Spring Convocation 1982, University of Alberta, Edmonton, Canada.
38. W. B. Stephens, J. H. Starnes, Jr., and B. O. Almroth,
"Collapse of Long Cylindrical Shells under Combined Bending and Pressure Loads", *AIAA Journal*, Vol. 13, 1975, Part 1, pp. 20-25.
39. J. R. Tillerson, J. A. Stricklin and W. C. Haisler,
Numerical Methods for the Solution of Nonlinear Problems in Structural Engineering, published in: Numerical Solutions of Nonlinear Structural Problems, pp. 67-101, edited by R. H. Hartung.
40. S. Timoshenko and S. Woinoisky-Kreiger,
Theory of Plates and Shells, Maple Press, York (Pa.), 1959.
41. S. Timoshenko and J. M. Gere,
Theory of Elastic Stability, McGraw-Hill, New-York, 1961.
42. J. R. Westlake,
A Handbook of Numerical Matrix Inversion and Solution of Linear Equations, John Wiley & Sons, New-York, 1968.

43. R. H. Wu and E. A. Witmer,
Analytical and Experimental Studies of Nonlinear
Transient Responses of Stiffened Cylindrical
Panels, *AIAA Journal*, Vol. 13, 1975,
pp. 1171-1178.
44. O. C. Zienkiewicz,
The Finite Element Method, 3rd Edition,
McGraw-Hill, London, 1977.
45. O. C. Zienkiewicz and E. Hinton,
"Reduced Integration, Function Smoothing and
Non-conformity in Finite Element Analysis (with
Special Reference to Thick Plates)", *Journal of
the Franklin Institute*, 302, Nos 5 & 6,
Nov./Dec. 1976, pp. 443-461.

$$s = \sin(p)$$

$$c = \cos(p)$$

$$\alpha = cp - s$$

$$A1 = 0.25$$

$$A2 = 1/4R$$

$$A3 = 1/4l$$

$$A4 = 1/4s$$

$$A5 = 1/4\alpha$$

$$A6 = 1/4ls$$

$$A7 = 1/4Rp$$

$$A8 = -1/4lp$$

$$A9 = -1/4lRp$$

$$B1 = 1/8R^2p$$

$$B2 = -1/16R^2p$$

$$B3 = 1/4l\alpha$$

$$B4 = -1/8R$$

$$B5 = 3/8Rl$$

$$B6 = 3/4l^3$$

$$B7 = -3/4l^2$$

$$B8 = 3/4pl^3$$

$$B9 = -3/4pl^2$$

$$C1 = c/4Rs$$

$$C2 = c/4lRs$$

$$C3 = -c/4R^2\alpha$$

$$C4 = s/4R^2\alpha$$

$$C5 = s/4R\alpha$$

$$C6 = s/4lR^2\alpha$$

$$C7 = s/4Rl\alpha$$

$$C8 = \alpha/4ps$$

$$C9 = \alpha/4lps$$

$$D1 = -p^2s/12l\alpha$$

$$D2 = -p^2s/9.6Rl\alpha$$

$$D3 = -1/8R$$

$$D4 = -1/8Rs$$

$$D5 = 1/8R^2p$$

$$D6 = 1/8R^2p$$

$$D7 = -p/24$$

$$D8 = -p/4\alpha$$

$$D9 = -p/4l\alpha$$

$$E1 = R/4s$$

$$E2 = R/4ls$$

$$E3 = -pR/4\alpha$$

$$E4 = -pR/4l\alpha$$

$$E5 = -Rc/4ls$$

$$E6 = -pl/16R$$

$$E7 = -pl/16$$

$$E8 = -R^2(2c+sp)/8sl$$

$$E9 = -s(2+p^2)/8\alpha$$

$$F1 = c(2+p^2)/8\alpha$$

$$F2 = -pR(2c+sp)/8\alpha$$

$$F3 = [(6\alpha+p^2(3cp-s)]/24lp\alpha$$

$$F4 = -R(3\alpha+sp^2)/12l\alpha$$

$$F5 = (s-3cp)/8lR^2p\alpha$$

$$F6 = [5p^2(3cp-s)-18\alpha]/96lp\alpha$$

$$F7 = (12-5p^2)/96pR$$

$$F8 = (-5p^2s-9\alpha)/48l\alpha$$

Appendix A.2

Linear Strain Fields in Terms of Nodal Displacements

$(s+\underline{s})K1$	K2	K8	$(ps-\underline{ps})/4L$	L7	$-(4x+1)N4$
0	$K3(1+x)$	-K9	0	$(1+x)/L8$	N5
0	$K4(21+3x)-K5(p+\underline{p})$	L1	$3x(p+\underline{p})L5$	-L9-N1	N6
0	$K6(x+1)$	-L2	$-(p+\underline{p})(1+3x)L6$	$(1+x)N3$	$N8-(21+3x)N7$
0	$K7(1+x)$	-L3	0	$(1+x)(\underline{p}ps-\alpha)N2$	-N9+M1
$-(s+\underline{s})K1$	-K2	K8	$-(\underline{ps}-\underline{ps})/4L$	-L7	$(4x-1)N4$
0	$K3(1-x)$	K9	0	$(1-x)/L8$	-N5
0	$-K4(21-3x)+K5(p+\underline{p})$	-L1	$-3x(p+\underline{p})L5$	-L9+N1	-N6
0	$K6(x-1)$	-L2	$(p+\underline{p})(1-3x)L6$	$-(1-x)N3$	$N8+(21-3x)N7$
0	$K7(1-x)$	L3	0	$(1-x)(\underline{p}ps-\alpha)N2$	N9-M1
$-(s-\underline{s})K1$	-K2	-K8	$(\underline{ps}-\underline{ps})/4L$	L7	$-(4x-1)N4$
0	$-K3(1-x)$	K9	0	$(1-x)/L8$	-N5
0	$K4(21-3x)-K5(p-\underline{p})$	L1	$-3x(p-\underline{p})L5$	L9-N1	N6
0	$K6(x-1)$	L2	$(p-\underline{p})(1-3x)L6$	$(1-x)N3$	$-N8-(21-3x)N7$
0	$-K7(1-x)$	L3	0	$(1-x)(\underline{p}ps+\alpha)N2$	-N9-M1
$(s-\underline{s})K1$	K2	-K8	$-(\underline{ps}-\underline{ps})/4L$	-L7	$(4x+1)N4$
0	$-K3(1+x)$	-K9	0	$(1+x)/L8$	N5
0	$K4(21+3x)-K5(p-\underline{p})$	-L1	$3x(p-\underline{p})L5$	L9+N1	-N6
0	$K6(x+1)$	L2	$-(p-\underline{p})(1+3x)L6$	$-(1-x)N3$	$-N8+(21+3x)N7$
0	$-K7(1+x)$	-L3	0	$(1+x)(\underline{p}ps+\alpha)N2$	N9+M1

- <θx>
- <θp>
- <θxθp>
- <αx>
- <αp>
- <αxαp>

=

$$s = \sin(p)$$

$$c = \cos(p)$$

$$\underline{s} = \sin(\varnothing)$$

$$\alpha = cp - s$$

$$K1 = 1/4ls$$

$$K2 = x^2\varnothing/8lpR^2$$

$$K3 = c/4lRs$$

$$K4 = 1/8Rl$$

$$K5 = x^3/8Rpl^3$$

$$K6 = (x^2 - 1^2)/8Rl^2 + \varnothing x^2/8Rpl^2$$

$$K7 = \alpha/4lsp$$

$$K8 = 1/4Rp$$

$$K9 = sp^2/12l\alpha$$

$$L1 = 1/4pl + p(3cp - s)/24l\alpha$$

$$L2 = p/24$$

$$L3 = R(sp^2 + 3\alpha)/12l\alpha$$

$$L4 = 1/4Rlps$$

$$L5 = 1/4pl^3$$

$$L6 = 1/4pl^2$$

$$L7 = x\varnothing/8R^3\varnothing$$

$$L8 = s\varnothing/4R^2l\alpha$$

$$L9 = c\varnothing/4R^2\alpha$$

$$N1 = x\varnothing(3cp - s)/8R^2pl\alpha$$

$$N2 = \varnothing/8R^2p$$

$$N3 = l\varnothing/8R^3p$$

$$N4 = 1/4R^2pl$$

$$N5 = s(6\varnothing^2 - 5p^2)/48Rl\alpha$$

$$N6 = (3cp - s)(5p^2 - 6\varnothing^2) + 18(2x^2 - 1^2)$$

$$N7 = x/8Rpl^2$$

$$N8 = (6\varnothing + 12 - 5p^2)/96Rp$$

$$N9 = \varnothing/4lp$$

$$M1 = (6s\varnothing^2 - 9\alpha - 5p^2s)/48l\alpha$$

Appendix B.1

Listing of the Finite Element Program

The finite element program used is given with subroutines ordered alphabetically. All computations were done at the Computing Centre of the University of Alberta on an Amdahl 470/V7 and later on Amdahl 470/V8. The equation solver VBSOLV is not given as it was not developed during this study. The functions COST and GUINFO are utility functions of the Department of Computing Services.

```

1 C *****
2 C *
3 C *      FINITE ELEMENT PROGRAM FOR GEOMETRIC NONLINEAR *
4 C *      ANALYSIS OF THIN-WALLED CIRCULAR STRUCTURES *
5 C *
6 C *****
7 C
8 C ( THIS PROGRAM CALLS THE PROGRAMS MAIN1 OR MAIN4 )
9 C
10 C      IMPLICIT REAL*8(A-H,O-Z)
11 C      READ(5,10) M
12 C      10 FORMAT(G5)
13 C      IF (M.EQ.1) CALL MAIN1
14 C      IF (M.EQ.2) CALL ASTART
15 C      IF (M.EQ.4) CALL MAIN4
16 C      STOP
17 C      END
18 C      SUBROUTINE ASOKT(NOEL,OD,OKT,IX)
19 C
20 C      ASSEMBLAGE OF THE (TANGENT) STIFFNESS MATRIX
21 C
22 C      IMPLICIT REAL*8(A-H,O-Z)
23 C      COMMON / EIK /E2K(20,20),E3K(1540),E4K(8855)
24 C      COMMON / WHOLE /IBC(2),INR,IN(50),IS,IT,IXCH,LCH,NBAND,NEC,
25 C      1 NEL,NINTP,NINTS,NINTX,NL,NMAX,NN,NNC,NN5,NPD,NX,NX1,NP,NP1,
26 C      2 N2P,N2X,NX2
27 C      COMMON / ETANK /ETK(20,20),V(20)
28 C      DIMENSION NOEL(4,NEL),OD(NN5),OKT(NBAND,NN5),IX(NN5),INS(121)
29 C
30 C      DO 10 J=1,NN5
31 C      DO 10 I=1,NBAND
32 C      10 OKT(I,J)=0.DO
33 C      DO 40 I=1,NEL
34 C      IF (IN(12).EQ.0) GOTO 30
35 C      DO 20 J=1,4
36 C      J5=(NOEL(J,I)-1)*5
37 C      L=(J-1)*5
38 C      DO 20 K=1,5
39 C      20 V(L+K)=OD(J5+K)
40 C      30 CALL KT
41 C      40 CALL STUFF(OKT,NBAND,NN5,INS,ETK,NOEL,NEL,NN,I,IX)
42 C      IF (IN(7).EQ.1) CALL PRMAT(OKT,NBAND,1,1,NBAND,NN5,'OKT,FREE')
43 C      RETURN
44 C      END
45 C      SUBROUTINE ASSEM(NOEL,OKT,IX,OD)
46 C
47 C      STIFFNESS MATRICES
48 C
49 C      IMPLICIT REAL*8(A-H,O-Z)
50 C      COMMON / EIK /E2K(20,20),E3K(1540),E4K(8855)
51 C      COMMON / WHOLE /IBC(2),INR,IN(50),IS,IT,IXCH,LCH,NBAND,NEC,
52 C      1 NEL,NINTP,NINTS,NINTX,NL,NMAX,NN,NNC,NN5,NPD,NX,NX1,NP,NP1,
53 C      2 ISTART,IHALF,IDUMMY(7),NCONV
54 C      COMMON / PART /BETA,BETA2,CBETA,CED,DB,DEG,DELTA,DELTA1,DELTA2,E,ED,
55 C      1 EN,E2,FLEX,PEL,PEL2,PI,R,RL,RM,RN,RNU,DNORM,PREC,TH,XEL,TIME,
56 C      2 XD,REDUCE,FLOAD,FSTEP
57 C      DIMENSION OKT(NBAND,NN5),OD(NN5),NOEL(4,NEL),IX(NN5)
58 C
59 C      DAS=COST(0)
60 C      WRITE(7,10) DAS
61 C      10 FORMAT(/' BEFORE ASSEM:',F10.2)
62 C      IS=IS+1
63 C      FLOAD=FLOAD+FSTEP
64 C      IT=-1
65 C      IF ((IS+IHALF).GT.1) GOTO 40
66 C      CALL GTCPL(TIME)
67 C      IF (IN(12).EQ.0) IS=-1
68 C      CALL TMAT
69 C      DO 20 I=1,NN5
70 C      20 OD(I)=0.DO
71 C      WRITE(12) OD
72 C      IF (IN(11).NE.1) GOTO 30

```



```

73      READ(11) E2K
74      IF (IN(12).EQ.0) GOTO 40
75      READ(11) E3K,E4K
76      GOTO 40
77      30 CALL CYLSTF
78      IN(11)=1
79      40 CALL ASOKT(NOEL,OD,OKT,IX)
80      RETURN
81      END
82      SUBROUTINE ASTART
83      C
84      C      ARRANGING ARRAYS FOR SUBROUTINE RSTART
85      C
86      IMPLICIT REAL*8(A-H,O-Z)
87      COMMON / WHOLE /IBC(2),INR,IN(50),IS,IT,IXCH,LCH,NBAND,NEC,
88      1 NEL,NINTP,NINTS,NINTX,NL,NMAX,NN,NNC,NN5,NPD,NX,NX1,NP,NP1,
89      2 ISTART,IHALF,NEXTIT,LCAUSE,NEXTIS,NEXTOV,ITOV,ITOVIT,NOVA
90      DIMENSION OKT(65,605),NOEL(4,100),P(605),IV(605),IH(605),
91      1 IX(605),OD(605),DV(53),ID(605),OF(605),VL(605),NPL(605),
92      2 IXNEW(605)
93      C
94      READ(10) IBC,INR,IN,IS,IT,IXCH,LCH,NBAND,NEC,NEL,NEXTIT,
95      1 LCAUSE,NINTP,NINTS,NINTX,NL,NMAX,NN,NNC,NN5,NPD,NX,NX1,NP,
96      2 NP1,IHALF,NEXTIS,NEXTOV,ITOV,ITOVIT,NOVA
97      ISTART=1
98      CALL RSTART(OKT,P,OD,NOEL,OF,IX,DV,IV,IH,VL,NPL,IXNEW)
99      STOP
100     END
101     SUBROUTINE BC1(IX)
102     C
103     C      GENERATION OF BOUNDARY CONDITIONS FOR (A-)SYMMETRY OF THE
104     C      TOP AND BOTTOM EDGE AND THE MID-SECTION OF THE CYLINDER
105     C
106     IMPLICIT REAL*8(A-H,O-Z)
107     COMMON / WHOLE /IBC(2),INR,IN(50),IS,IT,IXCH,LCH,NBAND,NEC,
108     1 NEL,NINTP,NINTS,NINTX,NL,NMAX,NN,NNC,NN5,NPD,NX,NX1,NP,NP1,
109     2 N2P,N2X,NX2
110     DIMENSION IX5(5,121),N(5),IX(NN5)
111     C
112     DO 10 J=1,NN
113     DO 10 I=1,5
114     10 IX5(I,J)=1
115     IF (IBC(1)-1) 30,30,20
116     20 N(1)=2
117     N(2)=5
118     GOTO 40
119     30 N(1)=3
120     N(2)=4
121     40 IF (IBC(2)-1) 60,60,50
122     50 K=4
123     N(3)=1
124     N(4)=4
125     GOTO 70
126     60 K=5
127     N(3)=2
128     N(4)=3
129     N(5)=5
130     70 CONTINUE
131     DO 80 I=1,2
132     DO 80 J=1,NX1
133     IX5(N(I),J*NP1)=0
134     80 IX5(N(I),J*NP1-NP)=0
135     J1=NX*NP1+1
136     J2=J1+NP
137     DO 90 I=3,K
138     DO 90 J=J1,J2
139     90 IX5(N(I),J)=0
140     DO 100 I=1,NN
141     K=5*(I-1)
142     DO 100 J=1,5
143     100 IX(K+J)=IX5(J,I)
144     RETURN

```

```

145      END
146      SUBROUTINE BXP(X,P)
147      C
148      C      COEFFICIENTS OF 'B.X', 'B.PHI', 'B3', AND 'B4'
149      C      (BX3,BP3,BX2,BP1)
150      C
151      IMPLICIT REAL*8(A-H,O-Z)
152      COMMON / WHOLE /IBC(2),INR,IN(50)
153      COMMON / PART /BETA,BETA2,CBETA,CED,DB,DEG,DELTA,DELTAT,E,ED,
154      1 EN,E2,FLEX,PEL,PEL2,PI,R,RL,RM,RN,RNU,RNU1,SIGMA,TH,XEL
155      COMMON / TMINUS/T(20,20)
156      COMMON / BF /BPF(20),BXF(20),B3F(20),B4F(20)
157
158      DS=DSIN(P)
159      DC=DCOS(P)
160      R2=R*R
161      X2=X*X/2.DO
162      XDR=X/R
163      P2=P*P/2.DO
164      XP=X*P
165      XDR4=XDR/4.DO
166      XDRS=XDR*DS
167      RP=R*P
168      X2DR=X2/R
169      X3DR=X2*XDR/3.DO
170      RXP=RP*X
171      R1=R*(1.DO+P2)
172      RXP2=R*X*P2
173      PX2=P*X2
174      PR2=P*R2
175      DO 10 I=1,20
176      BXF(I)=-T(2,I)*DC-T(4,I)*DS-T(8,I)*XDRS+T(10,I)*R-T(12,I)*X-
177      1 T(13,I)*X2-T(14,I)*XP-T(15,I)*PX2-T(17,I)*R2-T(19,I)*PR2
178      10 BPF(I)=-T(6,I)/R-T(11,I)*XDR4-T(14,I)*X2DR-T(15,I)*X3DR-
179      1 T(16,I)*RP-T(17,I)*RXP-T(18,I)*R1-T(19,I)*RXP2-T(20,I)*X
180      IF (IN(31).LT.1) RETURN
181      C
182      DO 20 I=1,20
183      B3F(I)=T(2,I)*DS-T(4,I)*DC-T(8,I)*XDR*DC+T(11,I)/4.DO+
184      1 T(17,I)*PR2+T(19,I)*R2*(P2-1.DO)+T(20,I)*R
185      20 B4F(I)=-T(2,I)*DS+T(4,I)*DC+T(8,I)*XDR*DC+T(11,I)*0.75DO-
186      1 T(17,I)*PR2-T(19,I)*R2*(P2-1.DO)-T(20,I)*R
187      RETURN
188      END
189      SUBROUTINE CHANGE(IXNEW,IX,NPL,VL)
190      C
191      C      INPUT OF LOAD, DISPLACEMENTS AND CORESPONDING FLAGS,
192      C      SHOWING IF A LOAD (DISPLACEMENT) IS TO BE HELD CONSTANT,
193      C      OR TO BE INCREASED AFTER EACH LOAD STEP
194      C
195      C      INPUT
196      C      K: DEGREE OF FREEDOM TO BE CHANGED
197      C      L: NEW BOUNDARY CONDITION (1 TO 6)
198      C      F: APPLYING FORCE OR DISPLACEMENT
199      C
200      IMPLICIT REAL*8(A-H,O-Z)
201      COMMON / WHOLE /IBC(2),INR,IN(50),IS,IT,IXCH,LCH,NBAND,NEC,
202      1 NEL,NINTP,NINTS,NINTX,NL,NMAX,NN,NNC,NN5,NPD,NX,NX1,NP,NP1,
203      2 N2P,N2X,NX2
204      COMMON / PART /BETA,BETA2,CBETA,CED,DB,DEG,DELTA,DELTAT,E,ED,
205      1 EN,E2,FLEX,PEL,PEL2,PI,R,RL,RM,RN,RNU,RNU1,SIGMA,TH,XEL,TIME
206      DIMENSION IX(NN5),VL(NN5),NPL(NN5),IXNEW(605)
207      C
208      NPD=2*NNC
209      IF (IXCH.EQ.0) GOTO 30
210      DO 20 I=1,IXCH
211      READ(5,10) K,L
212      10 FORMAT(3G20.10)
213      IF (IX(K).EQ.2) NPD=NPD-1
214      IF (L.EQ.2) NPD=NPD+1
215      20 IX(K)=L
216      30 NL=6

```

```

217         IF (LCH.EQ.0) GOTO 60
218         DO 40 I=1,6
219           NPL(I)=0
220     40    IXNEW(I)=0
221         DO 50 I=1,LCH
222         READ(5,10) K,L,F
223         IF (IX(K).EQ.0) CALL ERROR(7,K,K)
224         NL=NL+1
225         NPL(L)=NPL(L)+1
226         IXNEW(NL)=L
227         NPL(NL)=K
228     50    VL(NL)=F
229         NPL(1)=NPL(3)+NPL(4)
230         NPL(2)=NPL(5)+NPL(6)
231     60    READ (5,10,END=70)L
232         CALL ERROR(4,L,L)
233     70    RETURN
234         END
235         SUBROUTINE CYLSTF
236     C
237     C     CALCULATION OF THE THREE STIFFNESS MATRICES
238     C
239         IMPLICIT REAL*8(A-H,O-Z)
240         COMMON / WHOLE /IBC(2),INR,IN(50),IS,IT,IXCH,LCH,NBAND,NEC,
241     1    NEL,NINTP,NINTS,NINTX,NL,NMAX,NN,NNC,NN5,NPD,NX,NX1,NP,NP1,
242     2    N2P,N2X,NX2
243         COMMON / PART /BETA,BETA2,CBETA,CED,DB,DEG,DELTA,DELTAT,E,ED,
244     1    EN,E2,FLEX,PEL,PEL2,PI,R,RL,RM,RN,RNU,DNORM,SIGMA,TH,XEL,TIME
245         COMMON / EIK /E2K(20,20),E3K(1540),E4K(8855)
246         COMMON / AF /AXF(20),APF(20),APXF(20)
247         COMMON / TF /TXF(20),TPF(20),TPXF(20)
248         COMMON / BF /BPF(20),BFX(20),B3F(20),B4F(20)
249         DIMENSION X(24),WX(24),P(24),WP(24),T1(20),T2(20),
250     1    BX2(20,20),BP2(20,20),BXP(20,20),B32(20,20),B42(20,20),
251     2    BX32(20,20),BP42(20,20),B342(20,20),B432(20,20),
252     3    BX31(20,20),BP41(20,20)
253     C
254         IF (IN(31).NE.2) GOTO 10
255         CALL NEWCYL
256         RETURN
257     10    CONTINUE
258         CALL GAUSS(X,WX,24,XEL,NINTX)
259         CALL GAUSS(P,WP,24,PEL,NINTP)
260         IF (IN(25).EQ.1) CALL TMAT
261         DO 20 I=1,20
262         DO 20 J=1,20
263     20    E2K(J,I)=0.DO
264         DO 30 I=1,1540
265     30    E3K(I)=0.DO
266         DO 40 I=1,8855
267     40    E4K(I)=0.DO
268     C
269         C=E*TH/(1.DO-RNU*RNU)
270         D=C*TH*TH/12.DO
271         RNU1=(1.DO-RNU)/2.DO
272         RNU2=RNU1+RNU1
273         RNU4=RNU2+RNU2
274     C
275         DO 150 INX=1,NINTX
276         DO 150 INP=1,NINTP
277         CALL SALF(X(INX),P(INP))
278         CALL STH(X(INX),P(INP))
279         DO 50 I=1,20
280         T1(I)=TXF(I)+RNU*TPF(I)
281     50    T2(I)=TPF(I)+RNU*TXF(I)
282     C
283     C     STIFFNESS MATRIX OF SECOND ORDER
284     C
285         WXWPR=WX(INX)*WP(INP)*R
286         W2C=WXWPR*C
287         W2D=WXWPR*D
288         DO 60 I=1,20

```

```

289      DO 60 J=I,20
290      60 E2K(I,J)=E2K(I,J)+
291      1 W2C*(TXF(I)*T1(J)+TPF(I)*T2(J)+RNU1*TPXF(I)*TPXF(J))+
292      2 W2D*(AXF(I)*(AXF(J)+RNU*APF(J))+APF(I)*(APF(J)+RNU*AXF(J))+
293      3 RNU4*APXF(I)*APXF(J))
294      IF (IN(12).EQ.O).GOTO 150
295      C
296      C      PRECALCULATIONS FOR NONLINEAR TERMS
297      C
298      CALL BXP(X(INX),P(INP))
299      DO 80 I=1,20
300      DO 70 J=1,20
301      BX2(J,I)=BXF(I)*BXF(J)
302      70 BP2(J,I)=BPF(I)*BPF(J)
303      DO 80 J=1,20
304      80 BXP(J,I)=BXF(J)*BPF(I)
305      DO 90 J=1,20
306      DO 90 I=1,20
307      BX31(I,J)=BX2(I,J)
308      90 BP41(I,J)=BP2(I,J)
309      IF (N(31).NE.1) GOTO 110
310      C
311      C      PRECALCULATIONS FOR EXTENDED STRAIN EXPRESSIONS
312      C
313      C
314      DO 100 J=1,20
315      DO 100 I=1,20
316      B32(I,J)=B3F(I)*B3F(J)
317      B42(I,J)=B4F(I)*B4F(J)
318      BX31(I,J)=BX31(I,J)+B32(I,J)
319      BP41(I,J)=BP41(I,J)+B42(I,J)
320      B342(I,J)=B32(I,J)+RNU*B42(I,J)
321      B432(I,J)=B42(I,J)+RNU*B32(I,J)
322      BX32(I,J)=2.DO*BX2(I,J)+B32(I,J)
323      100 BP42(I,J)=2.DO*BP2(I,J)+B42(I,J)
324      C
325      C      STIFFNESS MATRIX OF THIRD ORDER
326      C
327      110 CONTINUE
328      W3=W2C
329      W4=W2C*1.5D0
330      N=0
331      DO 120 I=1,20
332      N=N+1
333      E3K(N)=E3K(N)+W3*3.DO*(T1(I)*BX31(I,I)+T2(I)*BP41(I,I)+
334      1 RNU2*(TPXF(I)*BXP(I,I)))
335      IF (I.EQ.20) GOTO 120
336      I1=I+1
337      DO 120 J=I1,20
338      N=N+1
339      E3K(N)=E3K(N)+W3*(2.DO*T1(I)*BX31(I,J)+T1(J)*BX31(I,I)+
340      1 2.DO*T2(I)*BP41(I,J)+T2(J)*BP41(I,I)+
341      2 RNU2*(TPXF(I)*(BXP(I,J)+BXP(J,I))+TPXF(J)*BXP(I,I)))
342      N=N+1
343      E3K(N)=E3K(N)+W3*(2.DO*T1(J)*BX31(I,J)+T1(I)*BX31(J,J)+
344      1 2.DO*T2(J)*BP41(I,J)+T2(I)*BP41(I,I)+
345      2 RNU2*(TPXF(J)*(BXP(I,J)+BXP(J,I))+TPXF(I)*BXP(J,I)))
346      IF (J.EQ.20) GOTO 120
347      J1=J+1
348      DO 120 K=J1,20
349      N=N+1
350      E3K(N)=E3K(N)+W3*(T1(I)*BX31(J,K)+T1(J)*BX31(I,K)+T1(K)*BX31(I,J)
351      1 +T2(I)*BP41(J,K)+T2(J)*BP41(I,K)+T2(K)*BP41(I,J)+
352      2 RNU1*(TPXF(I)*(BXP(J,K)+BXP(K,J))+TPXF(J)*(BXP(I,K)+
353      3 BXP(K,I))+TPXF(K)*(BXP(I,J)+BXP(J,I))))
354      120 CONTINUE
355      C
356      C      STIFFNESS MATRIX OF FOURTH ORDER
357      C
358      N=0
359      DO 130 I=1,20
360      N=N+1
361      E4K(N)=E4K(N)+W4*(BX2(I,I)+BP2(I,I))*(BX2(I,I)+BP2(I,I))

```

```

361      IF (I.EQ.20) GOTO 130
362      I1=I+1
363      DO 130 J=I1,20
364      N=N+1
365      E4K(N)=E4K(N)+W4*(BX2(I,I)+BP2(I,I))*(BX2(I,J)+BP2(I,J))
366      N=N+1
367      E4K(N)=E4K(N)+W4*(BX2(I,I)*BX2(J,J)+BP2(I,I)*BP2(J,J)+
368      1 (BX2(I,I)*BP2(J,J)+BX2(J,J)*BP2(I,I)+4.DO*BX2(I,J)*
369      2 BP2(I,J))/3.DO)
370      N=N+1
371      E4K(N)=E4K(N)+W4*(BX2(I,J)+BP2(I,J))*(BX2(J,J)+BP2(J,J))
372      IF (J.EQ.20) GOTO 130
373      J1=J+1
374      DO 130 K=J1,20
375      N=N+1
376      E4K(N)=E4K(N)+W4*(BX2(I,I)*BX2(J,K)+BP2(I,I)*BP2(J,K)+
377      1 (BX2(I,I)*BP2(J,K)+2.DO*BX2(I,J)*BP2(I,K)+
378      2 2.DO*BX2(I,K)*BP2(I,J)+BX2(J,K)*BP2(I,I))/3.DO)
379      N=N+1
380      E4K(N)=E4K(N)+W4*(BX2(I,J)*BX2(J,K)+BP2(I,J)*BP2(J,K)+
381      1 (2.DO*BX2(I,J)*BP2(J,K)+BX2(J,J)*BP2(I,K)+
382      2 2.DO*BX2(J,K)*BP2(I,J)+BX2(I,K)*BP2(J,J))/3.DO)
383      N=N+1
384      E4K(N)=E4K(N)+W4*(BX2(I,J)*BX2(K,K)+BP2(I,J)*BP2(K,K)+
385      1 (BX2(I,J)*BP2(K,K)+2.DO*BX2(I,K)*BP2(J,K)+
386      2 2.DO*BX2(J,K)*BP2(I,K)+BX2(K,K)*BP2(I,J))/3.DO)
387      IF (K.EQ.20) GOTO 130
388      K1=K+1
389      DO 130 L=K1,20
390      N=N+1
391      E4K(N)=E4K(N)+W4*(BX2(I,J)*BX2(K,L)+BP2(I,J)*BP2(K,L)+
392      1 (BX2(I,J)*BP2(K,L)+BX2(I,K)*BP2(J,L)+BX2(I,L)*BP2(J,K)+
393      2 BX2(J,K)*BP2(I,L)+BX2(J,L)*BP2(I,K)+BX2(K,L)*BP2(I,J))/3.DO)
394      130 CONTINUE
395      IF (IN(31).NE.1) GOTO 150
396      C
397      C      CONTRIBUTIONS OF EXTENDED STRAIN EXPRESSION FOR EK4(I,J,K,L)
398      C
399      N=0
400      DO 140 I=1,20
401      N=N+1
402      E4K(N)=E4K(N)+W4*(B342(I,I)*BX32(I,I)+B432(I,I)*BP42(I,I))
403      IF (I.EQ.20) GOTO 140
404      I1=I+1
405      DO 140 J=I1,20
406      N=N+1
407      E4K(N)=E4K(N)+W4*((B342(I,I)*BX32(I,J)+B432(I,I)*BP42(I,J))+
408      1 B342(I,J)*BX32(I,I)+B432(I,J)*BP42(I,I))/7.DO)
409      N=N+1
410      E4K(N)=E4K(N)+W4*(B342(I,I)*BX32(J,J)+B432(I,I)*BP42(J,J)+
411      1 B342(J,J)*BX32(I,I)+B432(J,J)*BP42(I,I)+
412      2 (B342(I,J)*BX32(I,J)+B432(I,J)*BP42(I,J))*4.DO)/6.DO)
413      N=N+1
414      E4K(N)=E4K(N)+W4*(B342(I,J)*BX32(J,J)+B432(I,J)*BP42(J,J)+
415      1 B342(J,J)*BX32(I,J)+B432(J,J)*BP42(I,J))/2.DO)
416      IF (J.EQ.20) GOTO 140
417      J1=J+1
418      DO 140 K=J1,20
419      N=N+1
420      E4K(N)=E4K(N)+W4*(B342(I,I)*BX32(J,K)+B432(I,I)*BP42(J,K)+
421      1 B342(J,K)*BX32(I,I)+B432(J,K)*BP42(I,I)+
422      2 (B342(I,J)*BX32(I,K)+B432(I,J)*BP42(I,K)+
423      3 B342(I,K)*BX32(I,J)+B432(I,K)*BP42(I,J))*2.DO)/6.DO)
424      N=N+1
425      E4K(N)=E4K(N)+W4*((B342(I,J)*BX32(J,K)+B432(I,J)*BP42(J,K))*2.DO+
426      1 B342(I,K)*BX32(J,J)+B432(I,K)*BP42(J,J)+
427      2 (B342(J,K)*BX32(I,J)+B432(J,K)*BP42(I,J))*2.DO+
428      3 B342(J,J)*BX32(I,K)+B432(J,J)*BP42(I,K))/6.DO)
429      N=N+1
430      E4K(N)=E4K(N)+W4*(B342(I,J)*BX32(K,K)+B432(I,J)*BP42(K,K)+
431      1 B342(K,K)*BX32(I,J)+B432(K,K)*BP42(I,J)+
432      2 (B342(I,K)*BX32(J,K)+B432(I,K)*BP42(J,K)+

```

```

433      3 B342(J,K)*BX32(I,K)+B432(J,K)*BP42(I,K))*2.DO)/6.DO
434      IF (K.EQ.20) GOTO 140
435      K1=K+1
436      DO 140 L=K1,20
437      N=N+1
438      E4K(N)=E4K(N)+W4*(B342(I,J)*BX32(K,L)+B432(I,J)*BP42(K,L)+
439      1 B342(I,K)*BX32(J,L)+B432(I,K)*BP42(J,L)+
440      2 B342(I,L)*BX32(J,K)+B432(I,L)*BP42(J,K)+
441      3 B342(J,K)*BX32(I,L)+B432(J,K)*BP42(I,L)+
442      4 B342(J,L)*BX32(I,K)+B432(J,L)*BP42(I,K)+
443      5 B342(K,L)*BX32(I,J)+B432(K,L)*BP42(I,J))/6.DO
444      140 CONTINUE
445      C
446      C      STORAGE OF STIFFNESS MATRICES
447      C
448      150 CONTINUE
449      WRITE(11) E2K
450      IF (IN(12).EQ.0) GOTO 160
451      WRITE(11) E3K,E4K
452      160 IF (IN(25).EQ.1) STOP
453      REWIND 11
454      RETURN
455      END
456      SUBROUTINE DATA(TITLE)
457      C
458      C      INPUT OF: GEOMETRY, MATERIAL PROPERTIES,
459      C      ELEMENT SUBDIVISION,
460      C      SYMMETRY AND ASYMMETRY,
461      C      ORDER OF INTEGRATION,
462      C      ANGLE AT ENDS,
463      C      OUTPUT AND ITERATION PARAMETERS.
464      C
465      IMPLICIT REAL*8(A-H,O-Z)
466      COMMON / WHOLE /IBC(2),INR,IN(50),IS,IT,IXCH,LCH,NBAND,NEC,
467      1 NEL,NINTP,NINTS,NINTX,NL,NMAX,NN,NNC,NN5,NPD,NX,NX1,NP,NP1,
468      2 N2P,N2X,NX2
469      COMMON / PART /BETA,BETA2,CBETA,CED,DB,DEG,DELTA,DELTAT,E,ED,
470      1 EN,E2,FLEX,PEL,PEL2,PI,R,RL,RM,RN,RNU,RNU1,PREC,TH,XEL,TIME
471      REAL TITLE(50)
472      C
473      READ(5,10) TITLE
474      10 FORMAT(50A4)
475      READ(5,20) RL,R,TH,E,RNU
476      READ(5,20) NX,NP
477      READ(5,20) (IBC(I),I=1,2)
478      READ(5,20) NINTX,NINTP,NINTS
479      READ(5,20) CBETA,CED
480      READ(5,20) INL,INL1,INN
481      READ(5,20) (IN(I),I=1,INL)
482      READ(5,20) (IN(I),I=INL1,INN)
483      READ(5,20) IXCH,LCH
484      20 FORMAT(20G20)
485      RETURN
486      END
487      SUBROUTINE EQ(OD,OF,NOEL)
488      C
489      C      CALCULATION OF NEGATIVE INTERNAL EQUILIBRIUM FORCES
490      C
491      IMPLICIT REAL*8(A-H,O-Z)
492      COMMON / EIK /E2K(20,20),E3K(1540),E4K(8855)
493      COMMON / WHOLE /IBC(2),INR,IN(50),IS,IT,IXCH,LCH,NBAND,NEC,
494      1 NEL,NINTP,NINTS,NINTX,NL,NMAX,NN,NNC,NN5,NPD,NX,NX1,NP,NP1,
495      2 N2P,N2X,NX2
496      DIMENSION V(20),F(20),OF(NN5),NOEL(4,NEL),VV(20,20),OD(NN5)
497      C
498      DO 10 I=1,NN5
499      10 OF(I)=0.DO
500      DO 80 M=1,NEL
501      DO 20 I=1,4
502      K=5*(NOEL(I,M)-1)
503      I5=(I-1)*5
504      DO 20 J=1,5

```

```

505         F(I5+J)=0.DO
506     20 V(I5+J)=0D(K+J)
507     C
508     C     QUADRATIC PART
509     C
510         DO 30 I=1,20
511         F(I)=F(I)+E2K(I,I)*V(I)
512         IF (I.EQ.20) GOTO 30
513         I1=I+1
514         DO 30 J=I1,20
515         F(I)=F(I)+E2K(I,J)*V(J)
516         F(J)=F(J)+E2K(I,J)*V(I)
517     30 CONTINUE
518     C
519     C     QUBIC PART
520     C
521         DO 40 I=1,20
522         DO 40 J=I,20
523     40 VV(I,J)=V(I)*V(J)
524         N=0
525         DO 50 I=1,20
526         N=N+1
527         F(I)=F(I)+E3K(N)*VV(I,I)/2.DO
528         IF (I.EQ.20) GOTO 50
529         I1=I+1
530         DO 50 J=I1,20
531         N=N+1
532         W=E3K(N)
533         F(I)=F(I)+W*VV(I,J)
534         F(J)=F(J)+W*VV(I,I)/2.DO
535         N=N+1
536         W=E3K(N)
537         F(I)=F(I)+W*VV(J,J)/2.DO
538         F(J)=F(J)+W*VV(I,J)
539         IF (J.EQ.20) GOTO 50
540         J1=J+1
541         DO 50 K=J1,20
542         N=N+1
543         W=E3K(N)
544         F(I)=F(I)+W*VV(J,K)
545         F(J)=F(J)+W*VV(I,K)
546         F(K)=F(K)+W*VV(I,J)
547     50 CONTINUE
548     C
549     C     QUARTIC PART
550     C
551         N=0
552         DO 60 I=1,20
553         N=N+1
554         F(I)=F(I)+E4K(N)*VV(I,I)*V(I)/3.DO
555         IF (I.EQ.20) GOTO 60
556         I1=I+1
557         DO 60 J=I1,20
558         N=N+1
559         W=E4K(N)
560         F(I)=F(I)+W*VV(I,I)*V(J)
561         F(J)=F(J)+W*VV(I,I)*V(I)/3.DO
562         N=N+1
563         W=E4K(N)
564         F(I)=F(I)+W*VV(I,J)*V(J)
565         F(J)=F(J)+W*VV(I,I)*V(J)
566         N=N+1
567         W=E4K(N)
568         F(I)=F(I)+W*VV(J,J)*V(J)/3.DO
569         F(J)=F(J)+W*VV(I,J)*V(J)
570         IF (J.EQ.20) GOTO 60
571         J1=J+1
572         DO 60 K=J1,20
573         N=N+1
574         W=E4K(N)
575         F(I)=F(I)+W*VV(I,J)*V(K)*2.DO
576         F(J)=F(J)+W*VV(I,I)*V(K)

```

```

577      F(K)=F(K)+W*VV(I,I)*V(J)
578      N=N+1
579      W=E4K(N)
580      F(I)=F(I)+W*VV(J,J)*V(K)
581      F(J)=F(J)+W*VV(I,J)*V(K)*2.DO
582      F(K)=F(K)+W*VV(I,J)*V(J)
583      N=N+1
584      W=E4K(N)
585      F(I)=F(I)+W*VV(J,K)*V(K)
586      F(J)=F(J)+W*VV(I,K)*V(K)
587      F(K)=F(K)+W*VV(I,J)*V(K)*2.DO
588      IF (K.EQ.20) GOTO 60
589      K1=K+1
590      DO 60 L=K1,20
591      N=N+1
592      W=2.DO*E4K(N)
593      F(I)=F(I)+W*VV(J,K)*V(L)
594      F(J)=F(J)+W*VV(I,K)*V(L)
595      F(K)=F(K)+W*VV(I,J)*V(L)
596      F(L)=F(L)+W*VV(I,J)*V(K)
597      60 CONTINUE
598      DO 70 I=1,4
599      IS=(I-1)*5
600      K=5*(NOEL(I,M)-1)
601      DO 70 J=1,5
602      70 OF(K+J)=OF(K+J)-F(I5+J)
603      80 CONTINUE
604      RETURN
605      END
606      SUBROUTINE ERROR(I,K,L)
607      C
608      C      ERROR DIAGNOSIS OF INPUT
609      C
610      IF (I.EQ.1) WRITE(6,10) K,L
611      10 FORMAT(' '// NUMBER OF ELEMENTS =',I5,' ALLOWED ONLY',I4)
612      IF (I.EQ.2) WRITE(6,20) K,L
613      20 FORMAT(' '// NUMBER OF CHANGES IN BOUNDARY CONDITIONS =',
614      1 I5,' POSSIBLE ONLY',I4)
615      IF (I.EQ.3) WRITE(6,30) K,L
616      30 FORMAT(' '// NUMBER OF LOAD CHANGES =',I5,' POSSIBLE ONLY',I4)
617      IF (I.EQ.4) WRITE(6,40) K
618      40 FORMAT(' '// NOT ALL DATA IN UNIT 5 IS NEEDED: FIRST SURPLUS
619      1 DATA IS',I5)
620      IF (I.EQ.5) WRITE(6,50) K,L
621      50 FORMAT(' '// NUMBER OF ELEMENTS IN THE LONGITUDINAL DIRECTION
622      1 =',I5,' ALLOWED ONLY',I3)
623      IF (I.EQ.6) WRITE(6,60) L,K
624      60 FORMAT(' '// NUMBER OF ELEMENTS IN THE CIRCUMFERENTIAL
625      1 DIRECTION =',I5,' ALLOWED ONLY',I3)
626      IF (I.EQ.7) WRITE(6,70) K
627      70 FORMAT(' '// DISPLACEMENT NUMBER',I4,' IS ASSIGNED LOAD,
628      1 BUT DEFINED AS FIXED')
629      IF (I.EQ.8) WRITE(6,80) K
630      80 FORMAT(' '// NUMBER OF LOAD STEPS =',I4,' ALLOWED ONLY',I4)
631      IF (I.EQ.9) WRITE(6,90) K,L
632      90 FORMAT(' '// NO SUCCESS IN VBSOLV AT LOAD STEP',I3,
633      1 ' , ITERATION',I3)
634      IF (I.EQ.10) WRITE(6,100) L,K
635      100 FORMAT(' '// DISPLACEMENT NORM OF ITERATION',I3,' IN LOAD',
636      1 ' STEP',I3,' IS GREATER THAN '// 1.001 TIMES THE FIRST',
637      2 ' DISPLACEMENT NORM OF THE CURRANT LOAD STEP.')
638      IF (I.EQ.11) WRITE(6,110) K
639      110 FORMAT(' '// CYLINDER FORCES CANNOT BE COMPUTED BY NODAL
640      1 FORCES '// WHEN CROSS SECTION IS ALLOWED TO DISTORT.')
641      STOP
642      END
643      SUBROUTINE FORCE1(NOEL,DD)
644      C
645      C      CALCULATION OF AXIAL FORCE AND BENDING MOMENT OF CYLINDER
646      C      BY CONSIDERING ELEMENT STRESSES
647      C
648      IMPLICIT REAL*8(A-H,O-Z)

```



```

649      COMMON / TMINUS/T(20,20)
650      COMMON / WHOLE /IBC(2),INR,IN(50),IS,IT,IXCH,LCH,NBAND,NEC,
651      1 NEL,NINTP,NINTS,NINTX,NL,NMAX,NN,NNC,NN5,NPD,NX,NX1,NP,NP1
652      COMMON / PART /BETA,BETA2,CBETA,CED,DB,DEG,DELTA,DELTA1,E,ED,
653      1 EN,E2,FLEX,PEL,PEL2,PI,R,RL,RM,RN,RNU,RNU1,PREC,TH,XEL,TIME
654      COMMON / AF /AXF(20),APF(20),APXF(20)
655      COMMON / TF /BX1(20),BP2(20),TPXF(20)
656      COMMON / BF /BP3(20),BX3(20),BX2(20),BP1(20)
657      COMMON / DELVW /RV(20),RW(20)
658      DIMENSION V(20),NOEL(4,NEL),PS(24),WS(24),OD(NN5)
659
660      C
661      RN=0.DO
662      RM=0.DO
663      PHI=PEL
664      X=XEL
665      IA=1
666      IE=NEC
667      IF (IN(16).EQ.2) GOTO 10
668      CALL GAUSS(PS,WS,24,XEL,NINTS)
669      X=PS(NINTS)
670      10 IF (IN(30).EQ.0) GOTO 20
671      X=-X
672      IA=NEL-NP+1
673      IE=NEL
674      20 CALL GAUSS(PS,WS,24,PEL,NINTS)
675
676      C
677      LINEAR STRESSES
678
679      DO 110 I=IA,IE
680      DO 30 J=1,4
681      L1=(J-1)*5
682      L2=(NOEL(J,I)-1)*5
683      DO 30 L=1,5
684      30 V(L1+L)=OD(L2+L)
685      DO 100 J=1,NINTS
686      S=PS(J)
687      PT=PHI+S
688      DS=DSIN(PT)
689      DC=DCOS(PT)
690      DCOSN=DC
691      DCOSM=DC
692      CALL STH(X,S)
693      CALL SALF(X,S)
694      VM=0.DO
695      VN=0.DO
696      T1=0.DO
697      T2=0.DO
698      T3=0.DO
699      T4=0.DO
700      DO 40 K=1,20
701      W=V(K)
702      T1=T1+BX1(K)*W
703      T2=T2+BP2(K)*W
704      T3=T3+AXF(K)*W
705      40 T4=T4+APF(K)*W
706      VN=VN+RNU*T2
707      VM=VM+RNU*T4
708      IF (IN(15).EQ.0) GOTO 90
709
710      C
711      NONLINEAR STRESS CONTRIBUTIONS
712
713      BETAX3=0.DO
714      BETAP3=0.DO
715      BETAX2=0.DO
716      BETAP2=0.DO
717      BETAX1=0.DO
718      BETAP1=0.DO
719      CALL BXP(X,S)
720      DO 50 K=1,20
721      BETAX3=BETAX3+BX3(K)*V(K)
722      50 BETAP3=BETAP3+BP3(K)*V(K)
723      IF (IN(31).LT.1) GOTO 70

```

```

721 C
722 DO 60 K=1,20
723 BETAX2=BETAX2+BX2(K)*V(K)
724 60 BETAP1=BETAP1+BP1(K)*V(K)
725 IF (IN(31).NE.2) GOTO 70
726 C
727 BETAX1=T1
728 BETAP2=T2
729 C
730 70 VN=VN+(BETAX1*BETAX1+BETAX2*BETAX2+BETAX3*BETAX3+
731 1 RNU*(BETAP1*BETAP1+BETAP2*BETAP2+BETAP3*BETAP3))/2.DO
732 IF (IN(30).EQ.O) GOTO 90
733 C
734 C INFLUENCE OF OVALIZATION OR STRETCHING
735 C OF CYLINDER CROSS SECTION
736 C
737 CALL UVW(X,S)
738 TV=O.DO
739 TW=O.DO
740 DO 80 K=1,20
741 W=V(K)
742 TV=TV+RV(K)*W
743 80 TW=TW+RW(K)*W
744 WB=(OD(NN5-2)-OD(NN5-NP*5-2))/2.DO
745 DCOSM=DCOSM+DS*BETAP3
746 DCOSN=DC+(TW*DC+WB-TV*DS)/R
747 C
748 90 RN=RN+VN*WS(J)
749 100 RM=RM-WS(J)*(VN*DCOSN+VM*DCOSM*E2)
750 110 PHI=PHI+PEL2
751 RN=RN*EN
752 RM=RM*EN*R
753 IF (IN(30).EQ.O) RN=RN*DCOS(BETA2)
754 IF (IN(1).EQ.O) RETURN
755 RM=RM+RM
756 RN=RN+RN
757 RETURN
758 END
759 SUBROUTINE FORCE2(OF,OD)
760 C
761 C CALCULATION OF AXIAL FORCE AND BENDING MOMENT OF CYLINDER
762 C BY CONSIDERING THE NODAL FORCES
763 C
764 IMPLICIT REAL*8(A-H,O-Z)
765 COMMON / WHOLE /IBC(2),INR,IN(50),IS,IT,IXCH,LCH,NBAND,NEC,
766 1 NEL,NINTP,NINTS,NINTX,NL,NMAX,NN,NNC,NN5,NPD,NX,NX1,NP,NP1,
767 2 N2P,N2X,NX2
768 COMMON / PART /BETA,BETA2,CBETA,CED,DB,DEG,DELTA,DELTAT,E,ED,
769 1 EN,E2,FLEX,PEL,PEL2,PI,R,RL,RM,RN,RNU,RNU1,PREC,TH,XEL,TIME
770 DIMENSION OF(NN5),OD(NN5)
771 C
772 IF (IN(30).GT.O) CALL ERROR(11,IN(30),O)
773 RN=O.DO
774 RM=O.DO
775 PHI=O.DO
776 DC=DCOS(BETA2)
777 DO 10 I=1,NNC
778 I5=I*5-4
779 RN=RN+OF(I5)
780 RM=RM+DCOS(PHI)*(OD(I5)*OF(I5+2)+OF(I5+3)-OF(I5)*R*DC)
781 10 PHI=PHI+PEL2
782 IF (IN(1).EQ.O) GOTO 20
783 RN=RN+RN
784 RM=RM+RM
785 20 CONTINUE
786 RETURN
787 END
788 SUBROUTINE GAUSS(X,WT,NDIM,A,NORDER)
789 C
790 C*****
791 C
792 C THIS SUBROUTINE RETURNS TO THE CALLING PROGRAM THE ABSCISSAS

```

```

793 C AND WEIGHT FACTORS FOR VARIOUS ORDERS OF GAUSSIAN INTEGRATION.
794 C
795 C INPUT:
796 C NORDER= THE ORDER OF THE GAUSSIAN INTEGRATION FORMULA WHICH
797 C IS WANTED. VALUES WHICH NORDER CAN TAKE ARE 2 TO
798 C 10, 12, AND 16.
799 C A= THE LOWER AND UPPER LIMIT FOR THE INTEGRATION VARIABLE X
800 C OUTPUT:
801 C X= A VECTOR CONTAINING THE X COORDINATES OF THE INTEGRATION
802 C POINTS
803 C WT= A VECTOR CONTAINING THE WEIGHT FACTORS
804 C NDIM= THE DIMENSION OF X AND WT
805 C
806 C THE INTEGRAL OF F(X) FROM X=-A TO X=A IS THUS EQUAL TO
807 C SUM( WT(I)*F(X(I)) ), I=1, NORDER
808 C
809 C*****
810 C IMPLICIT REAL*8 (A-H,O-Z)
811 C DIMENSION X(NDIM), WT(NDIM), XX(24,24), WWT(24,24)
812 C DATA WWT/24*0.DO, 1.DO, 23*0.DO,
813 C 1 0.888888888888889DO, 0.555555555555555DO, 22*0.DO,
814 C 2 0.652145154862546DO, 0.347854845137454DO, 22*0.DO,
815 C 3 0.568888888888889DO, 0.478628670499366DO, 0.236926885056189DO,
816 C 4 21*0.DO, 0.467913934572691DO, 0.360761573048139DO,
817 C 5 0.171324492379170DO, 21*0.DO, 0.417959183673469DO,
818 C 6 0.381830050505119DO, 0.279705391489277DO, 0.129484966168870DO,
819 C 7 20*0.DO, 0.362683783378362DO, 0.313706645877887DO,
820 C 8 0.222381034453374DO, 0.101228536290376DO, 20*0.DO,
821 C 9 0.330239355001260DO, 0.312347077040003DO, 0.260610696402935DO,
822 C * 0.180648160694857DO, 0.081274388361574DO, 19*0.DO,
823 C 1 0.295524224714753DO, 0.269266719309996DO, 0.219086362515982DO,
824 C 2 0.149451349150581DO, 0.066671344308688DO, 43*0.DO,
825 C 3 0.24914704581340278DO, 0.23349253653835480DO,
826 C 4 0.20316742672306592DO, 0.16007832854334622DO,
827 C 5 0.10693932599531843DO, 0.047175336386511828DO,
828 C 6 90*0.DO, 0.18945061045506850DO, 0.18260341504492359DO,
829 C 7 0.16915651939500254DO, 0.14959598881657673DO,
830 C 8 0.12462897125553387DO, 0.095158511682492785DO,
831 C 9 0.062253523938647893DO, 0.027152459411754095DO, 208*0.DO,
832 C DATA XX/24*0.DO, 0.577350269189626DO, 23*0.DO,
833 C 1 0.DO, 0.774596669241483DO, 22*0.DO,
834 C 2 0.339981043584856DO, 0.861136311594053DO, 22*0.DO,
835 C 3 0.DO, 0.538469310105683DO, 0.906179845938664DO, 21*0.DO,
836 C 4 0.238619186083197DO, 0.661209386466265DO, 0.932469514203152DO,
837 C 5 21*0.DO, 0.405845151377397DO, 0.741531185599394DO,
838 C 6 0.949107912342759DO, 20*0.DO, 0.183434642495650DO,
839 C 7 0.525532409916329DO, 0.796666477413627DO, 0.960289856497536DO,
840 C 8 21*0.DO, 0.324253423403809DO, 0.613371432700590DO,
841 C 9 0.836031107326636DO, 0.968160239507626DO, 19*0.DO,
842 C * 0.148874338981631DO, 0.433395394129247DO, 0.679400568299024DO,
843 C 1 0.865063366688985DO, 0.97390652851172DO, 43*0.DO,
844 C 2 0.12523340851146916DO, 0.367831498181802DO,
845 C 3 0.58731795428661744DO, 0.76990267419430468DO,
846 C 4 0.90411725637047486DO, 0.98156063424671926DO,
847 C 5 90*0.DO, 0.09501250983763744DO, 0.28160355077925891DO,
848 C 6 0.45801677765722739DO, 0.61787624440264375DO,
849 C 7 0.75540440835500303DO, 0.86563120238783174DO,
850 C 8 0.94457502307323258DO, 0.98940093499164993DO, 208*0.DO,
851 C IF (NDIM.GE.NORDER) GOTO 20
852 C WRITE(3,10)
853 C 10 FORMAT('ODIMENSION FOR X AND WT IN SUBROUTINE GAUSS IS TOO SMALL
854 C 1 FOR THE SPECIFIED VALUE OF NORDER')
855 C STOP
856 C 20 XORDER=NORDER
857 C IODD=0
858 C IF ((XORDER/2.DO).GT.(NORDER/2)) IODD=1
859 C N=NORDER/2
860 C IF (IODD.EQ.1) N=(NORDER+1)/2
861 C DO 40 I=1,N
862 C IF (I.EQ.IODD) GOTO 30
863 C N1=N+1-I
864 C N2=N+I

```

```

865     IF (IODD.EQ.1) N2=N2-1
866     X(N1)=-XX(I,NORDER)*A
867     X(N2)=-X(N1)
868     WT(N1)=WWT(I,NORDER)*A
869     WT(N2)=WT(N1)
870     GOTO 40
871 30 X(N)=O.DO
872     WT(N)=WWT(1,NORDER)*A
873 40 CONTINUE
874     RETURN
875     END
876     SUBROUTINE GTCPL(TIME)
877 C
878 C     REMAINING SECONDS OF CPU-TIME
879 C
880     REAL*8 TIME
881     CALL GUINFO('LOCCPUT',K1)
882     CALL GUINFO('GLOBCPU',K2)
883     TIME=(DFLOAT(MINO(K1,K2)))/76800.DO
884     RETURN
885     END
886     SUBROUTINE INOUT(NOEL,P,TITLE,L,IX,NPL,VL,IXNEW)
887 C
888 C     OUTPUT OF INPUT INFORMATION
889 C
890     IMPLICIT REAL*8(A-H,O-Z)
891     COMMON / WHOLE /IBC(2),INR,IN(50),IS,IT,IXCH,LCH,NBAND,NEC,
892     1 NEL,NINTP,NINTS,NINTX,NL,NMAX,NN,NNC,NN5,NPD,NX,NX1,NP,NP1,
893     2 N2P,N2X,NX2
894     COMMON / PART /BETA,BETA2,CBETA,CED,DB,DEG,DELTA,DELTA1,E,E,
895     1 EN,E2,FLEX,PEL,PEL2,PI,R,RL,RM,RN,RNU,RNU1,PREC,TH,XEL
896     DIMENSION NOEL(4,NEL),IX(NN5),P(NN5),NPL(NN5),VL(NN5),LT(5),
897     1 IXNEW(NL)
898     REAL TITLE(50)
899 C
900 C     OUTPLUT OF GEOMETRY AND CYLINDER IDEALIZATION
901 C
902     CALL TIME(6,O,LT)
903     IF (L.EQ.2) GOTO 120
904     IF (IN(26).GT.O) IN(26)=1
905     WRITE(7,10) LT,TITLE,RL,R,TH,E,RNU,(IN(I),I=1,35),NX,NP,PEL2,
906     1 BETA,NBAND
907 10 FORMAT('1',5A4/50A4//,'INPUT DATA'//10(' ')////'LENGTH',F13.3,
908     1 ' MM'/'RADIUS',F13.3,' MM'/'THICKNESS',F10.3,' MM' /
909     2 /'YOUNG',1H,'S MODULUS',F11.3,' MPA',
910     3 /'POISSON',1H,'S RATIO',F11.3,
911     4 /'PARAMETER LIST',7(/.5I4),
912     5 ///'NUMBER OF ELEMENTS',
913     6 ///'LONGITUDINAL:',I6,
914     7 /'CIRCUMFERENTIAL:',I3,
915     8 /'ANGLE PRESCRIBED PER ELEMENT =',F9.6,' RAD',
916     9 /'ANGLE (STEPSIZE) AT ENDS DUE TO MOMENT =',E14.8,
917     * /'HALF BANDWIDTH =',I3//
918     1 /'SYMMETRY PROPERTIES'///,'X-Z PLANE:')
919     DO 100 I=1,2
920     IF (IBC(I)-1) 20,40,60
921 20 WRITE(7,30)
922 30 FORMAT('+',11X,'NOT SPECIFIED')
923     GOTO 80
924 40 WRITE(7,50)
925 50 FORMAT('+',11X,'ASYMMETRY')
926     GOTO 100
927 60 WRITE(7,70)
928 70 FORMAT('+',11X,'SYMMETRY')
929 80 IF (I.EQ.1) WRITE(7,90)
930 90 FORMAT(' Y-Z PLANE:')
931 100 CONTINUE
932     WRITE(7,110) NINTX,NINTP,NINTS
933 110 FORMAT(' '///'ORDER OF GAUSSIAN INTEGRATION FOR STIFFNESS ',
934     1 'MATRIX'///,
935     2 ' DIRECTION ORDER'//5X,'X',I9/4X,'PHI',I8///,
936     3 'ORDER OF GAUSSIAN INTEGRATION FOR STRESS CALCULATION =',I3)

```

```

937         RETURN
938     C
939     C     OUTPUT OF NODE ELEMENT CONNECTION
940     C
941     120 WRITE(7,130)
942     130 FORMAT(' '///'NODE ELEMENT CONNECTIONS'
943     1 ///'ELEMENT          NODES'//)
944     DO 140 I=1,NEL
945     140 WRITE(7,150) I,(NOEL(J,I),J=1,4)
946     150 FORMAT(' ',I5,6X,4I4)
947     C
948     C     OUTPUT OF NODAL BOUNDARY CONDITIONS
949     C
950     WRITE(7,160)
951     160 FORMAT(' '///'FREEDOM OF DISPLACEMENTS (O=CONSTRAINT TO O,'
952     1 ' 1=FREE, 2=PRESCRIBED BY ANGLE AT END)'
953     2 ///'  NODE    U    V    W    W.X (W.PHI -V)/R'//)
954     DO 170 I=1,NN
955     170 WRITE(7,180) I,(IX((I-1)*5+J),J=1,5)
956     180 FORMAT(' ',I6,1X,4I4,I8)
957     IF (LCH.EQ.O) RETURN
958     190 WRITE(7,200) ((NPL(I),IXNEW(I),VL(I)),I=7,NL)
959     200 FORMAT(' '///' PRESCRIBED LOADS AND DISPLACEMENTS'
960     1 ///, ' NR. IXNEW  VALUE (N OR NMM)'//((I5,I4,E21.10))
961     RETURN
962     END
963     SUBROUTINE INPUT1(NOEL,P,IX,VL,NPL,IXNEW)
964     C
965     C     INPUT OF CYLINDER DATA AND INITIALIZING OF LOADING VARIABLES
966     C
967     IMPLICIT REAL*8(A-H,O-Z)
968     COMMON / WHOLE /IBC(2),INR,IN(50),IS,IT,IXCH,LCH,NBAND,NEC,
969     1 NEL,NINTP,NINTS,NINTX,NL,NMAX,NN,NNC,NN5,NPD,NX,NX1,NP,NP1,
970     2 ISTART,IHALF,NEXTIT,LCAUSE,NEXTIS,NEXTOV,ITOV,ITOVIT,NOVA,
971     3 NCONV
972     COMMON / PART /BETA,BETA2,CBETA,CED,DB,DEG,DELTA,DELTAT,E,ED,
973     1 EN,E2,FLEX,PEL,PEL2,PI,R,RL,RM,RN,RNU,DNORM,PREC,TH,XEL,TIME,
974     2 XD,REDUCE,FLOAD,FSTEP,FDELTA,DONM
975     DIMENSION IX(605),NOEL(4,100),P(605),NPL(605),VL(605),
976     1 IXNEW(605)
977     REAL TITLE(50)
978     C
979     CALL DATA(TITLE)
980     NEL=NX*NP
981     C     IF (NX.GT.10) CALL ERROR(5,NX,10)
982     IF (IN(17).GT.50) CALL ERROR(8,IN(18),50)
983     IF (NEL.GT.100) CALL ERROR(1,NEL,100)
984     NN5=(NX+1)*(NP+1)*5
985     IF (IXCH.GT.NN5) CALL ERROR(2,IXCH,NN5)
986     IF (LCH.GT.NN5) CALL ERROR(3,LCH,NN5)
987     C
988     C     INITIALIZATION OF VARIABLES AND FLAGS
989     C
990     ISTART=0
991     LCAUSE=0
992     PI=3.141592653589793D0
993     NX1=NX+1
994     NP1=NP+1
995     NN=NX1*NP1
996     NBAND=(NP1+2)*5
997     NEC=NP
998     NNC=NP1
999     XEL=RL/(4.DO*NX)
1000     PEL=PI/(2.DO*NP)
1001     IF (IN(26).NE.O) PEL=DFLOAT(IN(26))/1000000000.DO
1002     PEL2=PEL+PEL
1003     EN=E*TH*R/(1.DO-RNU*RNU)
1004     E2=TH*TH/R/12.DO
1005     WUR=DSQRT(3.DO*(1.DO-RNU*RNU))
1006     BETA=RL*TH/R/R/2.DO/WUR*CBETA
1007     DB=BETA
1008     ED=CED*(DMIN1((PI*PI*R*R/RL/2.DO),(RL*TH/WUR/R)))/2.DO

```

```

1009      DONM=2*RNU*R*R/RL
1010      IF (IN(30).EQ.0) DONM=0.DO
1011      IF (IN(25).EQ.1) CALL CYLSTF
1012      C
1013      C      INITIALIZATIONS FOR NONLINEAR PROBLEM
1014      C
1015      FLEX=-RL/EN/12.56637DO
1016      DELTA=0.DO
1017      IS=0
1018      RM=0.DO
1019      RN=0.DO
1020      IHALF=0
1021      FLOAD=0.DO
1022      FSTEP=1.DO
1023      REDUCE=0.56234DO
1024      IF (IN(29).GT.0) REDUCE=DFLOAT(IN(29))/10000.DO
1025      NEXTOV=0
1026      NCONV=0
1027      C
1028      C      DETERMINATION OF BOUNDARY CONDITIONS
1029      C
1030      CALL BC1(IX)
1031      IF (IN(12).EQ.1) GOTO 10
1032      CALL LINEND(P,IX)
1033      GOTO 30
1034      10 DO 20 I=1,NP1
1035          IS=(I-1)*5
1036          DO 20 J=1,5
1037      20 IX(I5+J)=2
1038      30 CALL CHANGE(IXNEW,IX,NPL,VL)
1039      IF (IN(22).EQ.1) CALL NORMD(DNORM,IX)
1040      C
1041      C      DETERMINATION OF ELEMENT NODE CONNECTIONS
1042      C
1043      DO 40 I=1,NX
1044          K=(I-1)*NP
1045          L=K+I-1
1046          DO 40 J=1,NP
1047              KJ=K+J
1048              LJ=L+J
1049              NOEL(1,KJ)=LJ+1
1050              NOEL(2,KJ)=LJ+NP1+1
1051              NOEL(3,KJ)=LJ+NP1
1052      40 NOEL(4,KJ)=LJ
1053      C
1054      IF (IN(5).EQ.1) CALL INOUT(NOEL,P,TITLE,1,IX,NPL,VL,IXNEW)
1055      IF (IN(6).EQ.1) CALL INOUT(NOEL,P,TITLE,2,IX,NPL,VL,IXNEW)
1056      RETURN
1057      END
1058      SUBROUTINE INPUT2
1059      C
1060      C      DATA CHANGES DURING RESTART
1061      C
1062      IMPLICIT REAL*8(A-H,O-Z)
1063      COMMON / WHOLE /IBC(2),INR,IN(50),IS,IT,IXCH,LCH,NBAND,NEC,
1064      1 NEL,NINTP,NINTS,NINTX,NL,NMAX,NN,NNC,NN5,NPD,NX,NX1,NP,NP1,
1065      2 ISTART,IHALF,NEXTIT,LCAUSE,NEXTIS,NEXTOV,ITOV,ITOVIT,NOVA,
1066      3 NCONV
1067      COMMON / PART /BETA,BETA2,CBETA,CED,DB,DEG,DELTA,DELTAT,E,ED,
1068      1 EN,E2,FLEX,PEL,PEL2,PI,R,RL,RM,RN,RNU,DNORM,PREC,TH,XEL,TIME,
1069      2 XD,REDUCE,FLOAD,FSTEP,FDELTA,DCNM,XDN
1070      C
1071      C      (IF NOT ENOUGH DATA IN FIRST INPUT LINE, NO CHANGES ARE MADE)
1072      C
1073      READ(5,10,END=50) NCHIN,NED,NDB,NREDUC,NEWIX,NLOAD
1074      10 FORMAT(10G20)
1075      20 IF (NCHIN.EQ.0) GOTO 30
1076      READ(5,10) I,J
1077      IN(I)=J
1078      NCHIN=NCHIN-1
1079      GOTO 20
1080      30 CONTINUE

```

```

1081      EDNEW=1.DO
1082      DBNEW=1.DO
1083      IF (NED.EQ.1) READ(5,10) EDNEW
1084      IF (NDB.EQ.1) READ(5,10) DBNEW
1085      ED=ED*EDNEW
1086      DB=DB*DBNEW
1087      FSTEP=FSTEP*(DMIN1(EDNEW,DBNEW))
1088      IF (NREDUC.EQ.1) READ(5,10) REDUCE
1089      IF ((NEWIX+NLOAD).EQ.0) GOTO 40
1090  C
1091  C      CHANGE OF LOADS AND BOUNDARY CONDITIONS NOT YET IMPLEMENTED
1092  C
1093      40 READ(5,10,END=50) L
1094      CALL ERROR(4,L,L)
1095      50 NCONV=0
1096      IF (XDN.LT.XD*10.DO**IN(19)) NCONV=1
1097      RETURN
1098      END
1099      SUBROUTINE ITERA(INDEX,DV,OD,VL)
1100  C
1101  C      REDUCTION OF LOAD STEP
1102  C
1103      IMPLICIT REAL*8(A-H,O-Z)
1104      COMMON / WHOLE /IBC(2),INR,IN(50),IS,IT,IXCH,LCH,NBAND,NEC,
1105      1 NEL,NINTP,NINTS,NINTX,NL,NMAX,NN,NNC,NN5,NPD,NX,NX1,NP,NP1,
1106      2 ISTART,IHALF
1107      COMMON / PART /BETA,BETA2,CBETA,CED,DB,DEG,DELTA,DELTAT,E,ED,
1108      1 EN,E2,FLEX,PEL,PEL2,PI,R,RL,RM,RN,RNU,DNORM,PREC,TH,XEL,TIME,
1109      2 XD,REDUCE,FLOAD,FSTEP,FDELTA
1110      DIMENSION DV(53),OD(NN5),VL(NL)
1111  C
1112      IF (INDEX.GT.1) GOTO 10
1113      REWIND 12
1114      WRITE(12) OD
1115      FDELTA=(DV(IS+2)-DELTAT)/2.DO
1116      IF (IHALF.GT.0) GOTO 30
1117      FDELTA=DELTA
1118      FLOAD=DFLOAT(IS)
1119      RETURN
1120  C
1121      10 IS=IS-1
1122      BETA2=BETA2-DB
1123      FLOAD=FLOAD-FSTEP
1124      IF (IHALF.EQ.0) WRITE(7,20)
1125      20 FORMAT('1',9('***'),' START OF LOAD STEP REFINEMENT ',9('***'))
1126      30 IHALF=IHALF+1
1127      REWIND 12
1128      READ(12) OD
1129      DB=DB*REDUCE
1130      ED=ED*REDUCE
1131      FSTEP=FSTEP*REDUCE
1132      IF (IS.EQ.0 .OR. IN(13).NE.2) FDELTA=0.DO
1133      FDELTA=FDELTA*REDUCE
1134      DELTA=FDELTA
1135      IF (LCH.EQ.0) GOTO 50
1136      DO 40 I=1,NL
1137      40 VL(I)=VL(I)*REDUCE
1138      50 WRITE(7,60)
1139      60 FORMAT(' .//. ' LOAD STEP IS REDUCED')
1140      RETURN
1141      END
1142      SUBROUTINE KT
1143  C
1144  C      CALCULATION OF THE ELEMENT TANGENT STIFFNESS MATRIX
1145  C      ( STORED IN A UPPER TRIANGLE )
1146  C
1147      IMPLICIT REAL*8(A-H,O-Z)
1148      COMMON / WHOLE /IBC(2),INR,IN(50),IS,IT,IXCH,LCH,NBAND,NEC
1149      COMMON / EIK /E2K(20,20),E3K(1540),E4K(8855)
1150      COMMON / ETANK /ETK(20,20),V(20)
1151      DIMENSION VV(20,20)
1152  C

```

```

1153 C QUADRATIC PART
1154 C
1155 DO 10 I=1,20
1156 DO 10 J=I,20
1157 10 ETK(I,J)=E2K(I,J)
1158 IF (IS.EQ.(-1)) GOTO 50
1159 C
1160 C QUBIC PART
1161 C
1162 N=0
1163 DO 20 I=1,20
1164 N=N+1
1165 ETK(I,I)=ETK(I,I)+E3K(N)*V(I)
1166 IF (I.EQ.20) GOTO 20
1167 I1=I+1
1168 DO 20 J=I1,20
1169 N=N+1
1170 W=E3K(N)
1171 ETK(I,I)=ETK(I,I)+W*V(J)
1172 ETK(I,J)=ETK(I,J)+W*V(I)
1173 N=N+1
1174 W=E3K(N)
1175 ETK(I,J)=ETK(I,J)+W*V(J)
1176 ETK(J,J)=ETK(J,J)+W*V(I)
1177 IF (J.EQ.20) GOTO 20
1178 J1=J+1
1179 DO 20 K=J1,20
1180 N=N+1
1181 W=E3K(N)
1182 ETK(I,J)=ETK(I,J)+W*V(K)
1183 ETK(I,K)=ETK(I,K)+W*V(J)
1184 ETK(J,K)=ETK(J,K)+W*V(I)
1185 20 CONTINUE
1186 C
1187 C QUARTIC PART
1188 C
1189 DO 30 I=1,20
1190 DO 30 J=I,20
1191 30 VV(I,J)=V(I)*V(J)
1192 N=0
1193 DO 40 I=1,20
1194 N=N+1
1195 ETK(I,I)=ETK(I,I)+E4K(N)*VV(I,I)
1196 IF (I.EQ.20) GOTO 40
1197 I1=I+1
1198 DO 40 J=I1,20
1199 N=N+1
1200 W=E4K(N)
1201 ETK(I,I)=ETK(I,I)+W*VV(I,J)*2.DO
1202 ETK(I,J)=ETK(I,J)+W*VV(I,I)
1203 N=N+1
1204 W=E4K(N)
1205 ETK(I,I)=ETK(I,I)+W*VV(J,J)
1206 ETK(I,J)=ETK(I,J)+W*VV(I,J)*2.DO
1207 ETK(J,J)=ETK(J,J)+W*VV(I,I)
1208 N=N+1
1209 W=E4K(N)
1210 ETK(I,J)=ETK(I,J)+W*VV(J,J)
1211 ETK(J,J)=ETK(J,J)+W*VV(I,J)*2.DO
1212 IF (J.EQ.20) GOTO 40
1213 J1=J+1
1214 DO 40 K=J1,20
1215 N=N+1
1216 W=E4K(N)*2.DO
1217 ETK(I,I)=ETK(I,I)+W*VV(J,K)
1218 ETK(I,J)=ETK(I,J)+W*VV(I,K)
1219 ETK(I,K)=ETK(I,K)+W*VV(I,J)
1220 ETK(J,K)=ETK(J,K)+W*VV(I,I)/2.DO
1221 N=N+1
1222 W=E4K(N)*2.DO
1223 ETK(I,J)=ETK(I,J)+W*VV(J,K)
1224 ETK(I,K)=ETK(I,K)+W*VV(J,J)/2.DO

```



```

1225     ETK(J,J)=ETK(J,J)+W*VV(I,K)
1226     ETK(J,K)=ETK(J,K)+W*VV(I,J)
1227     N=N+1
1228     W=E4K(N)*2.DO
1229     ETK(I,J)=ETK(I,J)+W*VV(K,K)/2.DO
1230     ETK(I,K)=ETK(I,K)+W*VV(J,K)
1231     ETK(J,K)=ETK(J,K)+W*VV(I,K)
1232     ETK(K,K)=ETK(K,K)+W*VV(I,J)
1233     IF (K.EQ.20) GOTO 40
1234     K1=K+1
1235     DO 40 L=K1,20
1236     N=N+1
1237     W=E4K(N)*2.DO
1238     ETK(I,J)=ETK(I,J)+W*VV(K,L)
1239     ETK(I,K)=ETK(I,K)+W*VV(J,L)
1240     ETK(I,L)=ETK(I,L)+W*VV(J,K)
1241     ETK(J,K)=ETK(J,K)+W*VV(I,L)
1242     ETK(J,L)=ETK(J,L)+W*VV(I,K)
1243     ETK(K,L)=ETK(K,L)+W*VV(I,J)
1244     40 CONTINUE
1245     50 CONTINUE
1246     RETURN
1247     END
1248     SUBROUTINE LINEND(P,IX)
1249     C
1250     C     BOUNDARY CONDITIONS FOR LINEAR CYLINDER PROBLEM
1251     C
1252     IMPLICIT REAL*8(A-H,O-Z)
1253     COMMON / WHOLE /IBC(2),INR,IN(50),IS,IT,IXCH,LCH,NBAND,NEC,
1254     1 NEL,NINTP,NINTS,NINTX,NL,NMAX,NN,NNC,NN5,NPD,NX,NX1,NX2,NP1,
1255     2 N2P,N2X,NX2
1256     COMMON / PART /BETA,BETA2,CBETA,CED,DB,DEG,DELTA,DELTAT,E,ED,
1257     1 EN,E2,FLEX,PEL,PEL2,PI,R,RL,RM,RN,RNU,RNU1,PREC,TH,XEL
1258     DIMENSION P(NN5),IX(NN5)
1259     C
1260     DO 10 I=1,NN5
1261     10 P(I)=0.DO
1262     BETA2=BETA
1263     PHI=0.DO
1264     K=NN5-NNC*5
1265     DO 30 I=1,NNC
1266     L=(I-1)*5
1267     BC=BETA*DCOS(PHI)
1268     IX(L+1)=2
1269     P(L+1)=-R*BC+ED
1270     IX(L+2)=0
1271     IX(L+3)=0
1272     IX(L+4)=2
1273     P(L+4)=BC
1274     IX(L+5)=0
1275     IF (IN(1).EQ.1) GOTO 30
1276     LK=L+K
1277     DO 20 J=1,5
1278     IX(LK+J)=0
1279     20 P(LK+J)=-P(L+J)
1280     30 PHI=PHI+PEL2
1281     RETURN
1282     END
1283     SUBROUTINE LOADS(IX,IV,P,OKT,VL,NPL,IXNEW,OD)
1284     C
1285     C     COMPUTATION OF LOAD VECTOR AND CHANGE OF STIFFNESS MATRIX
1286     C
1287     IMPLICIT REAL*8(A-H,O-Z)
1288     COMMON / WHOLE /IBC(2),INR,IN(50),IS,IT,IXCH,LCH,NBAND,NEC,
1289     1 NEL,NINTP,NINTS,NINTX,NL,NMAX,NN,NNC,NN5,NPD,NX,NX1,NX2,NP1,
1290     2 ISTART,IHALF,NEXTIT,LCAUSE,NEXTIS,NEXTOV,IT,IT1
1291     COMMON / PART /BETA,BETA2,CBETA,CED,DB,DEG,DELTA,DELTAT,E,ED,
1292     1 EN,E2,FLEX,PEL,PEL2,PI,R,RL,RM,RN,RNU,RNU1,SIGMA,TH,XEL,TIME
1293     DIMENSION OKT(NBAND,NN5),IV(NN5),IH(605),P(NN5),IX(NN5),
1294     1 H(605),VL(NL),NPL(NL),IXNEW(NL),OD(NN5),ID(605),IF(4)
1295     LOGICAL SUCCES
1296     C

```

```

1297 C      COMPUTATION OF LOAD VECTOR
1298 C
1299       IF (IS.GT.1 .OR. IT.GE.O) GOTO 20
1300 10 CALL SPARSE(IV,IH)
1301       IF (IN(12).EQ.O) GOTO 60
1302       GOTO 30
1303 20 REWIND 13
1304       READ(13) IV,(IH(I),I=1,NN5)
1305 30 DO 40 I=1,NN5
1306 40 P(I)=O.DO
1307       XED=ED+DELTA
1308       IF (IT.EQ.-1) CALL NONEND(P,XED,DB)
1309       IF (IN(13).NE.2 .OR. IT.LT.2) GOTO 60
1310       IF (NEXTOV.EQ.O) CALL NONEND(H,DELTA,O.DO)
1311       IF (NEXTOV.EQ.1) CALL OVAL(H,OD)
1312       DO 50 I=1,NN5
1313 50 P(I)=P(I)+H(I)
1314 60 IF (IT.EQ.-1 .AND. NPL(2).GT.O) CALL LOADS2(VL,P,NPL,IXNEW,2)
1315       IF (IN(22).NE.2) GOTO 170
1316 C
1317 C      COMPUTATION OF DETERMINANT WITHOUT NONZERO PRESCRIBED
1318 C      DISPLACEMENTS
1319 C
1320       WRITE(8) OKT,IV
1321       DO 70 I=1,NN5
1322       IF (IX(I).GT.O) GOTO 70
1323       IV(I)=1
1324       IH(I)=1
1325 70 CONTINUE
1326       DO 80 I=1,NN5
1327 80 H(I)=O.DO
1328       CALL VBSOLV(NBAND,-1,NN5,O.1D-15,NN5,H,OKT,ID,NBAND,DET,
1329 1 IEXDET,IV,TRUE,SUCCESS)
1330       IF (.NOT.SUCCESS) CALL ERROR(9,IS,IT)
1331 C
1332 C      OUTPUT OF THE DETERMINANT AND ITS RELATIVE CONDITION
1333 C
1334       KK=IDINT(DLOG10(DFLOAT(IABS(IEXDET))))+1
1335       WRITE(9,90) KK
1336 90 FORMAT(13H( 1H+.32X,I,I2.'))
1337       REWIND 9
1338       READ(9,100) IF(1),IF(2),IF(3),IF(4)
1339 100 FORMAT(4A4)
1340       WRITE(7,110) DET
1341 110 FORMAT(' DETERMINANT =',F10.6,' * 10 **')
1342       WRITE(7,IF) IEXDET
1343       IF (IN(22).EQ.1) CALL TEST(OKT,DET,IEXDET,DNORM)
1344       INN5=NN5
1345       DO 120 I=1,NN5
1346 120 INN5=INN5-ID(I)
1347       IF (INN5.EQ.O) GOTO 160
1348       WRITE(7,130)
1349 130 FORMAT(' NEGATIVE DIAGONAL ELEMENTS IN FOLLOWING ROWS:')
1350       DO 140 I=1,NN5
1351 140 IF (ID(I).EQ.-1) WRITE (7,150) I
1352 150 FORMAT(' ',I4)
1353 160 READ(8) OKT,IV
1354 C
1355 C      CHANGE OF STIFFNESS MATRIX
1356 C
1357 170 CONTINUE
1358       DO 180 I=1,NN5
1359 180 H(I)=P(I)
1360       DO 240 I=1,NN5
1361       IF (IX(I)-1) 230,240,190
1362 190 I1=IV(I)
1363       I2=I-1
1364       IF (I2.LT.I1) GOTO 210
1365       DO 200 J=I1,I2
1366       IZ=NBAND-I+J
1367       P(J)=P(J)-H(I)*OKT(IZ,I)
1368 200 OKT(IZ,I)=O.DO

```

```

1369      210 OKT(NBAND,I)=1.DO
1370          J1=I+1
1371          J2=IH(I)
1372          IF (J2.LT.J1) GOTO 230
1373          DO 220 J=J1,J2
1374          IZ=NBAND+I-J
1375          P(J)=P(J)-H(I)*OKT(IZ,J)
1376      220 OKT(IZ,J)=O.DO
1377      230 IV(I)=I
1378          IH(I)=I
1379      240 CONTINUE
1380          DO 250 I=1,NN5
1381      250 IF (IX(I).NE.1) P(I)=H(I)
1382          IF (IN(8).EQ.1 .OR. IN(8).EQ.3)
1383              1 CALL PRMAT(OKT,NBAND,1,1,NBAND,NN5,'OKT,LOAD')
1384          RETURN
1385      END
1386      SUBROUTINE LOADS2(VL,OF,NPL,IXNEW,LD)
1387  C
1388  C      ADDITION OF LOADS AND DISPLACEMENTS DESCRIBED IN INPUT-FILE
1389  C
1390          IMPLICIT REAL*8(A-H,O-Z)
1391          COMMON / WHOLE /IBC(2),INR,IN(50),IS,IT,IXCH,LCH,NBAND,NEC,
1392          1 NEL,NINTP,NINTS,NINTX,NL,NMAX,NN,NNC,NN5,NPD,NX,NX1,NP,NP1,
1393          2 N2P,N2X,NX2
1394          DIMENSION VL(NL),NPL(NL),IXNEW(NL),OF(NN5)
1395  C
1396  C      ADDITIONAL LOADS
1397  C
1398          IF (LD.NE.1 .OR. NPL(1).EQ.O) GOTO 40
1399          IE=6+NPL(3)
1400          IF (IE.EQ.6 .OR. (IT.EQ.O.AND.IS.GT.1)) GOTO 20
1401          DO 10 I=7,IE
1402              J=NPL(I)
1403          10 OF(J)=OF(J)+VL(I)
1404          20 IF (NPL(4).EQ.O) RETURN
1405              DIS=DFLOAT(IS)
1406              IF (IT.EQ.O) DIS=1.DO
1407              IA=IE+1
1408              IE=IA-1+NPL(4)
1409              DO 30 I=IA,IE
1410                  J=NPL(I)
1411          30 OF(J)=OF(J)+VL(I)*DIS
1412          RETURN
1413  C
1414  C      ADDITIONAL DISPLACEMENTS
1415  C
1416          40 IF (IT.GE.O) RETURN
1417          IF (NPL(2).EQ.O) RETURN
1418          IF (NPL(5).EQ.O .OR. IS.GE.2) GOTO 60
1419          IA=7+NPL(1)
1420          IE=IA-1+NPL(5)
1421          DO 50 I=IA,IE
1422          50 OF(NPL(I))=VL(I)
1423          60 IF (NPL(6).EQ.O) RETURN
1424          IA=7+NPL(1)+NPL(5)
1425          IE=IA-1+NPL(6)
1426          DO 70 I=IA,IE
1427          70 OF(NPL(I))=VL(I)
1428          RETURN
1429      END
1430      SUBROUTINE LONGER(OD,DELTA)
1431  C
1432  C      APPROXIMATE NODAL DISPLACEMENTS FOR AXIAL FORCE CA. ZERO
1433  C
1434          IMPLICIT REAL*8(A-H,O-Z)
1435          COMMON / WHOLE /IBC(2),INR,IN(50),IS,IT,IXCH,LCH,NBAND,NEC,
1436          1 NEL,NINTP,NINTS,NINTX,NL,NMAX,NN,NNC,NN5,NPD,NX,NX1,NP,NP1,
1437          2 N2P,N2X,NX2
1438          DIMENSION OD(NN5)
1439  C
1440          DO 10 I=1,NX

```

```

1441      K=(I-1)*NNC-4
1442      DR=DELTA*DFLOAT(NX1-1)/DFLOAT(NX)
1443      DO 10 J=1,NNC
1444 10 OD(J*5+K)=OD(J*5+K)+DR
1445      IF (IN(1).NE.O) GOTO 30
1446      NX2=NX+2
1447      N2X=NX+NX
1448      DO 20 I=NX2,N2X
1449      K=(I-1)*NNC-4
1450      DR=DELTA*DFLOAT(I-NX1)/DFLOAT(NX)
1451      DO 20 J=1,NNC
1452 20 OD(J*5+K)=OD(J*5+K)-DR
1453 30 CONTINUE
1454      RETURN
1455      END
1456      SUBROUTINE MAIN1
1457      C
1458      C      ONE QUARTER OF THE CYLINDER IS CONSIDERED
1459      C
1460      C      IMPLICIT REAL*8(A-H,O-Z)
1461      COMMON / WHOLE / IBC(2), INR, IN(50), IS, IT, IXCH, LCH, NBAND, NEC,
1462 1 NEL, NINTP, NINTS, NINTX, NL, NMAX, NN, NNC, NNS, NPD, NX, NX1, NP, NP1,
1463 2 ISTART, IHALF, NEXTIT, LCAUSE, NEXTIS
1464      DIMENSION OKT(65,605), NOEL(4,100), P(605), IV(605), IX(605),
1465 1 OD(605), DV(53), OF(605), VL(605), NPL(605), IXNEW(605)
1466      C
1467      CALL INPUT1(NOEL,P,IX,VL,NPL,IXNEW)
1468      C
1469 10 CALL ASSEM(NOEL,OKT,IX,OD)
1470      C
1471      CALL LOADS(IX,IV,P,OKT,VL,NPL,IXNEW,OD)
1472      C
1473      CALL SOLVE(OKT,P,IV,OD,NOEL,IX,DV,OF,VL,NPL,IXNEW)
1474      C
1475      IF (NEXTIS.GT.O) GOTO 10
1476      C
1477      STOP
1478      END
1479      SUBROUTINE MAINR(OKT,P,OD,NOEL,OF,IX,DV,IV,VL,NPL,IXNEW)
1480      C
1481      C      MAIN SUBROUTINE FOR RESTART FACILITY
1482      C
1483      C      IMPLICIT REAL*8(A-H,O-Z)
1484      COMMON / WHOLE / IBC(2), INR, IN(50), IS, IT, IXCH, LCH, NBAND, NEC,
1485 1 NEL, NINTP, NINTS, NINTX, NL, NMAX, NN, NNC, NNS, NPD, NX, NX1, NP, NP1,
1486 2 ISTART, IHALF, NEXTIT, LCAUSE, NEXTIS
1487      DIMENSION OKT(NBAND,NNS), NOEL(4,NEL), P(NNS), IV(NNS),
1488 1 IX(NNS), OD(NNS), DV(53), OF(NNS), VL(NL), NPL(NL), IXNEW(NL)
1489      C
1490      CALL INPUT2
1491      C
1492      GOTO 20
1493      C
1494 10 CALL ASSEM(NOEL,OKT,IX,OD)
1495      C
1496      CALL LOADS(IX,IV,P,OKT,VL,NPL,IXNEW,OD)
1497      C
1498 20 CALL SOLVE(OKT,P,IV,OD,NOEL,IX,DV,OF,VL,NPL,IXNEW)
1499      C
1500      IF (NEXTIS.GT.O) GOTO 10
1501      C
1502      STOP
1503      END
1504      SUBROUTINE NEWCYL
1505      C
1506      C      CALCULATION OF THE THREE STIFFNESS MATRICES
1507      C
1508      C      IMPLICIT REAL*8(A-H,O-Z)
1509      COMMON / WHOLE / IBC(2), INR, IN(50), IS, IT, IXCH, LCH, NBAND, NEC,
1510 1 NEL, NINTP, NINTS, NINTX, NL, NMAX, NN, NNC, NNS, NPD, NX, NX1, NP, NP1,
1511 2 N2P, N2X, NX2
1512      COMMON / PART / BETA, BETA2, CBETA, CED, DB, DEG, DELTA, DELTAT, E, ED,

```

```

1513      1 EN,E2,FLEX,PEL,PEL2,PI,R,RL,RM,RN,RNU,DNORM,SIGMA,TH,XEL,TIME
1514      COMMON / EIK /E2K(20,20),E3K(1540),E4K(8855)
1515      COMMON / AF /AXF(20),APF(20),APXF(20)
1516      COMMON / TF /BX1(20),BP2(20),TPXF(20)
1517      COMMON / BF /BP3(20),BX3(20),BX2(20),BP1(20)
1518      DIMENSION X(24),WX(24),P(24),WP(24),T1(20),T2(20),
1519      1 BX12(20,20),BX22(20,20),BX32(20,20),BXX(20,20),
1520      2 BP12(20,20),BP22(20,20),BP32(20,20),BPP(20,20),
1521      3 BXP2(20,20),BXNBP(20,20),BPNBX(20,20)
1522      C
1523      CALL GAUSS(X,WX,24,XEL,NINTX)
1524      *CALL GAUSS(P,WP,24,PEL,NINTP)
1525      IF (IN(25).EQ.1) CALL TMAT
1526      DO 10 I=1,20
1527      DO 10 J=1,20
1528      10 E2K(J,I)=0.DO
1529      DO 20 I=1,1540
1530      20 E3K(I)=0.DO
1531      DO 30 I=1,8855
1532      30 E4K(I)=0.DO
1533      C
1534      C=E*TH/(1.DO-RNU*RNU)
1535      D=C*TH*TH/12.DO
1536      RNU1=(1.DO-RNU)/2.DO
1537      RNU2=RNU1+RNU1
1538      RNU4=RNU2+RNU2
1539      RNU4D3=RNU4/3.DO
1540      C
1541      DO 110 INX=1,NINTX
1542      DO 110 INP=1,NINTP
1543      CALL SALF(X(INX),P(INP))
1544      CALL STH(X(INX),P(INP))
1545      DO 40 I=1,20
1546      T1(I)=BX1(I)+RNU*BP2(I)
1547      40 T2(I)=BP2(I)+RNU*BX1(I)
1548      C
1549      C STIFFNESS MATRIX OF SECOND ORDER
1550      C
1551      WXWPR=WX(INX)*WP(INP)*R
1552      W2C=WXWPR*C
1553      W2D=WXWPR*D
1554      DO 50 I=1,20
1555      DO 50 J=I,20
1556      50 E2K(I,J)=E2K(I,J)+
1557      1 W2C*(BX1(I)*T1(J)+BP2(I)*T2(J)+RNU1*TPXF(I)*TPXF(J))+
1558      2 W2D*(AXF(I)*(AXF(J)+RNU*APF(J))+APF(I)*(APF(J)+RNU*AXF(J))+
1559      3 RNU4*APXF(I)*APXF(J))
1560      IF (IN(12).EQ.0) GOTO 110
1561      C
1562      C PRECALCULATIONS FOR NONLINEAR TERMS
1563      C
1564      CALL BXP(X(INX),P(INP))
1565      DO 70 I=1,20
1566      DO 60 J=1,20
1567      BX12(I,J)=BX1(I)*BX1(J)
1568      BX22(I,J)=BX2(I)*BX2(J)
1569      BX32(I,J)=BX3(I)*BX3(J)
1570      BP12(I,J)=BP1(I)*BP1(J)
1571      BP22(I,J)=BP2(I)*BP2(J)
1572      BP32(I,J)=BP3(I)*BP3(J)
1573      BXX(I,J)=BX12(I,J)+BX22(I,J)+BX32(I,J)
1574      BPP(I,J)=BP12(I,J)+BP22(I,J)+BP32(I,J)
1575      BXP2(I,J)=BX1(I)*BP1(J)+BX2(I)*BP2(J)+BX3(I)*BP3(J)
1576      BXNBP(I,J)=BXX(I,J)+RNU*BPP(I,J)
1577      BPNBX(I,J)=BPP(I,J)+RNU*BXX(I,J)
1578      60 CONTINUE
1579      70 CONTINUE
1580      DO 80 I=1,19
1581      I1=I+1
1582      DO 80 J=I1,20
1583      80 BXP2(I,J)=(BXP2(I,J)+BXP2(J,I))/2.DO
1584

```

```

1585 C
1586 C STIFFNESS MATRIX OF THIRD ORDER .
1587 C
1588 W3=W2C
1589 W4=W2C*1.5D0
1590 N=0
1591 DO 90 I=1,20
1592 N=N+1
1593 E3K(N)=E3K(N)+W3*3.DO*(BX1(I)*BXNBP(I,I)+BP2(I)*BPNBX(I,I)+
1594 1 RNU2*(TPXF(I)*BXP2(I,I)))
1595 IF (I.EQ.20) GOTO 90
1596 I1=I+1
1597 DO 90 J=I1,20
1598 N=N+1
1599 E3K(N)=E3K(N)+W3*(2.DO*BX1(I)*BXNBP(I,J)+BX1(J)*BXNBP(I,I)+
1600 1 2.DO*BP2(I)*BPNBX(I,J)+BP2(J)*BPNBX(I,I)+
1601 2 RNU2*(TPXF(I)*BXP2(I,J)*2.DO+TPXF(J)*BXP2(I,I)))
1602 N=N+1
1603 E3K(N)=E3K(N)+W3*(2.DO*BX1(J)*BXNBP(I,J)+BX1(I)*BXNBP(J,J)+
1604 1 2.DO*BP2(J)*BPNBX(I,J)+BP2(I)*BPNBX(J,J)+
1605 2 RNU2*(TPXF(J)*BXP2(I,J)*2.DO+TPXF(I)*BXP2(J,J)))
1606 IF (J.EQ.20) GOTO 90
1607 J1=J+1
1608 DO 90 K=J1,20
1609 N=N+1
1610 E3K(N)=E3K(N)+W3*
1611 1 (BX1(I)*BXNBP(J,K)+BX1(J)*BXNBP(I,K)+BX1(K)*BXNBP(I,J)
1612 2 +BP2(I)*BPNBX(J,K)+BP2(J)*BPNBX(I,K)+BP2(K)*BPNBX(I,J)+
1613 3 RNU2*(TPXF(I)*BXP2(J,K)+TPXF(J)*BXP2(I,K)+TPXF(K)*BXP2(I,J)))
1614 90 CONTINUE
1615 C
1616 C STIFFNESS MATRIX OF FOURTH ORDER
1617 C
1618 N=0
1619 DO 100 I=1,20
1620 N=N+1
1621 E4K(N)=E4K(N)+W4*(BXX(I,I)*BXNBP(I,I)+BPP(I,I)*BPNBX(I,I)+
1622 1 RNU4*BXP2(I,I)*BXP2(I,I))
1623 IF (I.EQ.20) GOTO 100
1624 I1=I+1
1625 DO 100 J=I1,20
1626 N=N+1
1627 E4K(N)=E4K(N)+W4*((BXX(I,I)*BXNBP(I,J)+BPP(I,I)*BPNBX(I,J)+
1628 1 BXX(I,J)*BXNBP(I,I)+BPP(I,J)*BPNBX(I,I))/2.DO+
1629 2 RNU4*BXP2(I,I)*BXP2(I,J))
1630 N=N+1
1631 E4K(N)=E4K(N)+W4*((BXX(I,I)*BXNBP(J,J)+BPP(I,I)*BPNBX(J,J)+
1632 1 BXX(J,J)*BXNBP(I,I)+BPP(J,J)*BPNBX(I,I)+
1633 2 (BXX(I,J)*BXNBP(I,J)+BPP(I,J)*BPNBX(I,J))*4.DO)/6.DO+
1634 3 RNU4D3*(BXP2(I,I)*BXP2(J,J)+BXP2(I,J)*BXP2(I,J)*2.DO))
1635 N=N+1
1636 E4K(N)=E4K(N)+W4*((BXX(I,J)*BXNBP(J,J)+BPP(I,J)*BPNBX(J,J)+
1637 1 BXX(J,J)*BXNBP(I,J)+BPP(J,J)*BPNBX(I,J))/2.DO+
1638 2 RNU4*BXP2(I,J)*BXP2(J,J))
1639 IF (J.EQ.20) GOTO 100
1640 J1=J+1
1641 DO 100 K=J1,20
1642 N=N+1
1643 E4K(N)=E4K(N)+W4*((BXX(I,I)*BXNBP(J,K)+BPP(I,I)*BPNBX(J,K)+
1644 1 BXX(J,K)*BXNBP(I,I)+BPP(J,K)*BPNBX(I,I)+
1645 2 (BXX(I,J)*BXNBP(I,K)+BPP(I,J)*BPNBX(I,K)+
1646 3 BXX(I,K)*BXNBP(I,J)+BPP(I,K)*BPNBX(I,J))*2.DO)/6.DO+
1647 4 RNU4D3*(BXP2(I,I)*BXP2(J,K)+BXP2(I,J)*BXP2(I,K)*2.DO))
1648 N=N+1
1649 E4K(N)=E4K(N)+W4*((BXX(I,J)*BXNBP(J,K)+BPP(I,J)*BPNBX(J,K)+
1650 1 BXX(J,K)*BXNBP(I,J)+BPP(J,K)*BPNBX(I,J))*2.DO+
1651 2 BXX(I,K)*BXNBP(J,J)+BPP(I,K)*BPNBX(J,J)+
1652 3 BXX(J,J)*BXNBP(I,K)+BPP(J,J)*BPNBX(I,K))/6.DO+
1653 4 RNU4D3*(BXP2(J,J)*BXP2(I,K)+BXP2(I,J)*BXP2(J,K)*2.DO))
1654 N=N+1
1655 E4K(N)=E4K(N)+W4*((BXX(I,J)*BXNBP(K,K)+BPP(I,J)*BPNBX(K,K)+
1656 1 BXX(K,K)*BXNBP(I,J)+BPP(K,K)*BPNBX(I,J)+

```

```

1657      2 (BXX(I,K)*BXNBP(J,K)+BPP(I,K)*BPNBX(J,K)+
1658      3 BXX(J,K)*BXNBP(I,K)+BPP(J,K)*BPNBX(I,K))*2.DO)/6.DO+
1659      4 RNU4D3*(BXP2(I,J)*BXP2(K,K)+BXP2(I,K)*BXP2(J,K)*2.DO))
1660      IF (K.EQ.20) GOTO 100
1661      K1=K+1
1662      DO 100 L=K1,20
1663      N=N+1
1664      E4K(N)=E4K(N)+W4*((BXX(I,J)*BXNBP(K,L)+BPP(I,J)*BPNBX(K,L)+
1665      1 BXX(I,K)*BXNBP(J,L)+BPP(I,K)*BPNBX(J,L)+
1666      2 BXX(I,L)*BXNBP(J,K)+BPP(I,L)*BPNBX(J,K)+
1667      3 BXX(J,K)*BXNBP(I,L)+BPP(J,K)*BPNBX(I,L)+
1668      4 BXX(J,L)*BXNBP(I,K)+BPP(J,L)*BPNBX(I,K)+
1669      5 BXX(K,L)*BXNBP(I,J)+BPP(K,L)*BPNBX(I,J))/6.DO+
1670      6 RNU4D3*(BXP2(I,J)*BXP2(K,L)+BXP2(I,K)*BXP2(J,L)+
1671      7 BXP2(I,L)*BXP2(J,K)))
1672 100 CONTINUE
1673      C
1674      C      STORAGE OF STIFFNESS MATRICES
1675      C
1676 110 CONTINUE
1677      WRITE(11) E2K
1678      IF (IN(12).EQ.0) GOTO 120
1679      WRITE(11) E3K,E4K
1680 120 IF (IN(25).EQ.1) STOP
1681      REWIND 11
1682      RETURN
1683      END
1684      SUBROUTINE NONEND(P,D1,D2)
1685      C
1686      C      COMPUTATION OF NONLINEAR BOUNDARY CONDITIONS
1687      C      FOR RIGID CYLINDER ENDS
1688      C
1689      IMPLICIT REAL*8(A-H,O-Z)
1690      COMMON / WHOLE /IBC(2),INR,IN(50),IS,IT,IXCH,LCH,NBAND,NEC,
1691      1 NEL,NINTP,NINTS,NINTX,NL,NMAX,NN,NNC,NN5,NPD,NX,NX1,NP,NP1,
1692      2 N2P,N2X,NX2
1693      COMMON / PART /BETA,BETA2,CBETA,CED,DB,DEG,DELTA,DELTAT,E,ED,
1694      1 EN,E2,FLEX,PEL,PEL2,PI,R,RL,RM,RN,RNU,RNU1,PREC,TH,XEL,TIME,
1695      2 DUMMY(5),DONM
1696      DIMENSION P(NN5)
1697      C
1698      DO 10 I=1,NN5
1699 10 P(I)=0.DO
1700      IF (IS.EQ.1 .AND. IT.EQ.-1) BETA2=0.DO
1701      BETA1=BETA2
1702      BETA2=BETA1+D2
1703      PHI=0.DO
1704      C21=DCOS(BETA1)-DCOS(BETA2)
1705      S21=DSIN(BETA2)-DSIN(BETA1)
1706      DON1=DONM*D2
1707      DON2=DONM*(DSIN(BETA2)*BETA2-DSIN(BETA1)*BETA1)
1708      K=NN5-NNC*5
1709      DO 20 I=1,NNC
1710      L=(I-1)*5
1711      DC=DCOS(PHI)
1712      DS=DSIN(PHI)
1713      P(L+1)=D1-R*DC*S21+DON2*DS*DS
1714      P(L+2)=R*C21*DS*DC+DON1*DS
1715      P(L+3)=-R*C21*DC*DC
1716      P(L+4)=S21*DC
1717      P(L+5)=C21*DS*DC-DON1*DS/R
1718      IF (IN(1).EQ.1) GOTO 20
1719      LK=L+K
1720      P(LK+1)=-P(L+1)
1721      P(LK+2)=P(L+2)
1722      P(LK+3)=P(L+3)
1723      P(LK+4)=-P(L+4)
1724      P(LK+5)=P(L+5)
1725 20 PHI=PHI+PEL2
1726      RETURN
1727      END
1728      SUBROUTINE NORMD(DNORM,IX)

```

```

1729 C
1730 C CALCULATION OF THE NORMALIZED DETERMINANT OF A TRIANGULAR
1731 C STIFFNESS MATRIX WITH VALUES OF 1 FOR ALL NONZERO TERMS
1732 C
1733 REAL*8 DNORM
1734 COMMON / WHOLE / IBC(2), INR, IN(50), IS, IT, IXCH, LCH, NBAND, NEC,
1735 1 NEL, NINTP, NINTS, NINTX, NL, NMAX, NN, NNC, NN5, NPD, NX, NX1, NP, NP1,
1736 2 N2P, N2X, NX2
1737 DIMENSION IX(NN5)
1738 C
1739 IF (NX.EQ.1.AND.NP.EQ.1) X=ALOG10(2.)
1740 IF (NX.EQ.1.AND.NP.GE.2) X=ALOG10(16.)+(NP-2)*ALOG10(6.)
1741 IF (NX.GE.2.AND.NP.EQ.1) X=ALOG10(80.)+FLOAT(NX-2)*ALOG10(108.)
1742 IF (NX.GE.2.AND.NP.EQ.2) X=ALOG10(17472.)+FLOAT(NX-2)*ALOG10(3344.)
1743 IF (NX.GE.2.AND.NP.GE.3) X=ALOG10(2056320.)+FLOAT(NX-2)*
1744 1 ALOG10(85008.)+FLOAT(NP-3)*ALOG10(114.)+FLOAT((NX-2)*(NP-3))*
1745 2 ALOG10(25.)
1746 DNORM=X
1747 NMAX=0
1748 DO 10 I=1, NN5
1749 10 IF (IX(I).EQ.1) NMAX=NMAX+1
1750 RETURN
1751 END
1752 SUBROUTINE OVAL(H, OD)
1753 C
1754 C ADDING DISPLACEMENTS TO CYLINDRICAL ENDS TO OBTAIN
1755 C DEFORMATIONS EQUIVALENT TO THE MID-LENGTH OF CYLINDER
1756 C
1757 IMPLICIT REAL*8(A-H, O-Z)
1758 COMMON / WHOLE / IBC(2), INR, IN(50), IS, IT, IXCH, LCH, NBAND, NEC,
1759 1 NEL, NINTP, NINTS, NINTX, NL, NMAX, NN, NNC, NN5, NPD, NX, NX1, NP, NP1,
1760 2 ISTART, IHALF, NEXTIT, LCAUSE, NEXTIS, NEXTOV, ITOVAL
1761 COMMON / PART / BETA, BETA2, CBETA, CED, DB, DEG, DELTA, DELTAT, E, ED,
1762 1 EN, E2, FLEX, PEL, PEL2, PI, R, RL, RM, RN, RNU, DNORM, PREC, TH, XEL, TIME,
1763 2 XD, REDUCE, FLOAD, FSTEP
1764 DIMENSION H(NN5), OD(NN5)
1765 C
1766 ITOVAL=ITOVAL+1
1767 DELTA=O.DO
1768 WB=(OD(NN5-2)-OD(NN5-NP*5-2))/2.DO
1769 SB=DSIN(BETA2)
1770 CBM=1.DO-DCOS(BETA2)
1771 PHI=O.DO
1772 K=NN5-NNC*5
1773 C
1774 DO 10 I=1, NNC
1775 L=(I-1)*5
1776 DS=DSIN(PHI)
1777 DC=DCOS(PHI)
1778 VM=OD(L+K+2)
1779 WM=OD(L+K+3)
1780 VS=VM-WB*DS
1781 WS=WM+WB*DC
1782 S2=-WS*DC+VS*DS
1783 S3=DC*R-S2
1784 S4=S3*CBM
1785 H(L+1)=-S3*SB+DELTA-DELTAT/2.DO-OD(L+1)
1786 H(L+2)=VS+S4*DS-OD(L+2)
1787 H(L+3)=WS-S4*DC-OD(L+3)
1788 H(L+4)=O.DO
1789 H(L+5)=(DC*CBM*(R*DS+WS*DS+VS*DC)-VM)/R-OD(L+5)
1790 PHI=PHI+PEL2
1791 10 CONTINUE
1792 IA=L+6
1793 DO 20 I=IA, NN5
1794 H(I)=O.DO
1795 20 CONTINUE
1796 C
1797 NEXTOV=0
1798 RETURN
1799 END
1800 SUBROUTINE PRMAT(A, I1, IS, JS, NR, NC, ANAME)

```



```

1801 REAL*8 A(I1,NC), ANAME
1802 C
1803 JMAX=JS+NC-1
1804 IE=IS+NR-1
1805 JJS=JS
1806 JJE=JS+7
1807 10 IF (JJE.GT.JMAX) JJE=JMAX
1808 WRITE(8,20) ANAME
1809 20 FORMAT('1',20X,'MATRIX ',A8,/)
1810 WRITE(8,30)
1811 30 FORMAT(' * COLUMN',/, ' ',/, ' ',/, ' ',/, ' ',/, ' ',/, ' ')
1812 WRITE(8,40) (J,J=JJS,JJE)
1813 40 FORMAT(' ROW * ',8(6X,I3.6X))
1814 WRITE(8,50)
1815 50 FORMAT(7X,' ',/,8X,' ',/)
1816 DO 60 I=IS,IE
1817 60 WRITE(8,70) (I,(A(I,J),J=JJS,JJE))
1818 70 FORMAT(2X,I3.6X,8E15.7)
1819 IF (JJE.GE.JMAX) GOTO 80
1820 JJS=JJS+B
1821 JJE=JJE+B
1822 GOTO 10
1823 80 CONTINUE
1824 RETURN
1825 END
1826 SUBROUTINE RSTART(OKT,P,OD,NOEL,OF,IX,DV,IV,IH,VL,NPL,IXNEW)
1827 C
1828 C STORING AND READING OF DATA FOR RESTART
1829 C
1830 IMPLICIT REAL*8(A-H,O-Z)
1831 COMMON / EIK /E2K(20,20),E3K(1540),E4K(8855)
1832 COMMON / WHOLE /IBC(2),INR,IN(50),IS,IT,IXCH,LCH,NBAND,NEC,
1833 1 NEL,NINTP,NINTS,NINTX,NL,NMAX,NN,NNC,NN5,NPD,NX,NX1,NP,NP1,
1834 2 ISTART,IHALF,NEXTIT,LCAUSE,NEXTIS,NEXTOV,ITOVAL,ITOVIT,NOVA,
1835 3 NCONV
1836 COMMON / PART /BETA,BETA2,CBETA,CED,DB,DEG,DELTA,DELTAT,E,ED,
1837 1 EN,E2,FLEX,PEL,PEL2,PI,R,RL,RM,RN,RNU,DNORM,PREC,TH,XEL,TIME,
1838 2 XD,REDUCE,FLOAD,FSTEP,FDELTA,DONM,XDN,
1839 COMMON / TMINUS/ T(20,20)
1840 DIMENSION OKT(NBAND,NN5),P(NN5),OD(NN5),NOEL(4,NEL),OF(NN5),
1841 1 IX(NN5),DV(53),IV(NN5),IH(NN5),VL(NL),NPL(NL),IXNEW(NL)
1842 C
1843 CALL GTCPL(TMNEW)
1844 IF (ISTART.EQ.3) GOTO 20
1845 IF (ISTART.EQ.1) GOTO 40
1846 IF (IN(23).NE.1) RETURN
1847 TMMIN=(TIME-TMNEW)*1.1DO+10.DO
1848 WRITE(7,10) TMNEW,TMMIN
1849 10 FORMAT(// REMAINING CPU-TIME =',F8.3/' REQUIRED CPU-TIME =',
1850 1 F8.3)
1851 LCAUSE=1
1852 IF (TMNEW.LT.TMMIN) GOTO 30
1853 TIME=TMNEW
1854 RETURN
1855 C
1856 C STORING OF RESTART VARIABLES
1857 C
1858 20 IF (LCAUSE.EQ.3) GOTO 30
1859 LCAUSE=2
1860 30 REWIND 13
1861 READ(13) IV,IH
1862 REWIND 10
1863 WRITE(10) IBC,INR,IN,IS,IT,IXCH,LCH,NBAND,NEC,NEL,NEXTIT,
1864 1 LCAUSE,NINTP,NINTS,NINTX,NL,NMAX,NN,NNC,NN5,NPD,NX,NX1,NP,
1865 2 NP1,IHALF,NEXTIS,NEXTOV,ITOVAL,ITOVIT,NOVA,
1866 WRITE(10) BETA,BETA2,CBETA,CED,DB,DEG,DELTA,DELTAT,E,ED,
1867 1 EN,E2,FLEX,PEL,PEL2,PI,R,RL,RM,RN,RNU,DNORM,PREC,TH,XEL,
1868 2 REDUCE,FLOAD,FSTEP,FDELTA,DONM,XDN,NCONV,
1869 3 T,OD,NOEL,IX,IV,IH,P,OF,DV,PREC,TIME,XD,VL,NPL,IXNEW
1870 IF (IN(14).NE.2) WRITE(10) OKT
1871 STOP
1872 C

```

```

1873 C      READING OF RESTART VARIABLES
1874 C
1875 40 READ(10) BETA,BETA2,CBETA,CED,DB,DEG,DELTA,DELTAT,E,ED,
1876 1 EN,E2,FLEX,PEL,PEL2,PI,R,RL,RM,RN,RNU,ONORM,PREC,TH,XEL,
1877 2 REDUCE,FLOAD,FSTEP,FDELTA,DONM,XDN,NCONV,
1878 3 T,OD,NOEL,IX,IV,IH,P,OF,DV,PREC,TIME,XD,VL,NPL,IXNEW
1879 READ(11) E2K
1880 READ(11) E3K,E4K
1881 IF (IN(14).NE.2) READ(10) OKT
1882 REWIND 13
1883 WRITE(13) IV,(IH(I),I=1,NN5)
1884 REWIND 12
1885 WRITE(12) OD
1886 TIME=TMNEW
1887 CALL MAINR(OKT,P,OD,NOEL,OF,IX,DV,IV,VL,NPL,IXNEW)
1888 C
1889 STOP
1890 END
1891 SUBROUTINE WOLF(X,P)
1892 C
1893 C      COEFFICIENTS KAPPA FOR (LINEAR) OUT-OF-PLANE STRAINS
1894 C
1895 IMPLICIT REAL*8(A-H,O-Z)
1896 COMMON / TMINUS/T(20,20)
1897 COMMON / PART /BETA,BETA2,CBETA,CED,DB,DEG,DELTA,DELTAT,E,ED,
1898 1 EN,E2,FLEX,PEL,PEL2,PI,R,RL,RM,RN,RNU,RNU1,SIGMA,TH,XEL,TIME
1899 COMMON / AF /AXF(20),APF(20),APXF(20)
1900 C
1901 SDR=DSIN(P)/R
1902 XP=X*P
1903 XDR=X/R
1904 XX=XDR*X/2.DO
1905 RP=R*P
1906 R2P=RP*P/2.DO
1907 DO 10 I=1,20
1908 AXF(I)=T(8,I)*SDR+T(12,I)+T(13,I)*X+T(14,I)*P+T(15,I)*XP
1909 APF(I)=T(16,I)+T(17,I)*X+T(18,I)*P+T(19,I)*XP
1910 10 APXF(I)=T(14,I)*XDR+T(15,I)*XX+T(17,I)*RP+T(19,I)*R2P+T(20,I)
1911 RETURN
1912 END
1913 SUBROUTINE SHORT(DV,DELTA,DELTAT,IS)
1914 C
1915 C      ESTIMATE OF SHORTAGE OF CYLINDER FOR NEXT LOAD STEP
1916 C
1917 IMPLICIT REAL*8(A-H,O-Z)
1918 DIMENSION DV(53)
1919 C
1920 IF (IS.GT.2.) GOTO 30
1921 IF (IS.EQ.2) GOTO 10
1922 DV(2)=DELTAT
1923 DV(3)=0.DO
1924 DV(4)=DELTAT
1925 DV(5)=DELTAT*4.DO
1926 GOTO 40
1927 10 DV(1)=DELTAT
1928 DV(5)=DELTAT
1929 20 DV(6)=6.DO*DV(1)-15.DO*DV(2)
1930 GOTO 40
1931 30 DV(IS+3)=DELTAT
1932 DV(IS+4)=-DV(IS-2)+6.DO*DV(IS-1)-15.DO*DV(IS)+20.DO*DV(IS+1)-
1933 1 15.DO*DV(IS+2)+6.DO*DV(IS+3)
1934 40 DELTA=(DV(IS+3)-DV(IS+4))/2.DO
1935 RETURN
1936 END
1937 SUBROUTINE SOLVE(OKT,P,IV,OD,NOEL,IX,DV,OF,VL,NPL,IXNEW)
1938 C
1939 C      SOLVING OF "K * V = P" AND ITERATION CONTROL
1940 C
1941 IMPLICIT REAL*8(A-H,O-Z)
1942 COMMON / EIK /E2K(20,20),E3K(1540),E4K(8855)
1943 COMMON / WHOLE /IBC(2),INR,IN(50),IS,IT,IXCH,LCH,NBAND,NEC,
1944 1 NEL,NINTP,NINTS,NINTX,NL,NMAX,NN,NNC,NN5,NPD,NX,NX1,NP,NP1,

```

```

1945      2 ISTART, IHALF, NEXTIT, LCAUSE, NEXTIS, NEXTOV, ITOVAL, ITOVIT, NOVA,
1946      3 NCONV
1947      COMMON / PART / BETA, BETA2, CBETA, CED, DB, DEG, DELTA, DELTAT, E, ED,
1948      1 EN, E2, FLEX, PEL, PEL2, PI, R, RL, RM, RN, RNU, DNORM, PREC, TH, XEL, TIME,
1949      2 XD, REDUCE, FLOAD, FSTEP, FDELTA, DONM, XDN
1950      DIMENSION OKT(NBAND, NN5), P(NN5), IV(NN5), ID(605), IF(4), DV(53),
1951      1 OD(NN5), NOEL(4, NEL), OF(NN5), IX(NN5), IH(605), VL(NL), NPL(NL),
1952      2 IXNEW(NL)
1953      LOGICAL SUCCES
1954
1955      C
1956      NEXTIS=1
1957      IF (IS.LE.0) NEXTIS=0
1958      IF (LCAUSE.EQ.2) GOTO 470
1959      IF (LCAUSE.EQ.3) GOTO 260
1960      IF (ISTART.EQ.1) GOTO 470
1961      IF (IN(9).EQ.1) WRITE (7,10) (I,P(I),I=1,NN5)
1962      10 FORMAT(' '///10X,'LOAD VECTOR'//5X,'NR. (MM OR ANGLE)'//
1963      1 /((I7,E14.6))
1964      DO 20 I=1,NN5
1965      20 OF(I)=P(I)
1966      NEXTIT=1
1967      NOVA=0
1968      NEXTOV=0
1969      ITOVAL=0
1970      ITOVIT=0
1971      IF (IS.EQ.-1) NEXTIT=0
1972      PREC=0.1D-15
1973      DEG=BETA2*57.2957977509D0
1974      RMO=RM
1975      DELTA=0.D0
1976
1977      C
1978      C EQUILIBRIUM ITERATIONS
1979      C
1980      30 IT=IT+1
1981      RNO=RN
1982      TLOAD=CBETA*FLOAD
1983      CSTEP=CBETA*FSTEP
1984      WRITE(7,40) IS, IT, TLOAD, CSTEP, IHALF, DEG
1985      40 FORMAT(' '///',60('**')/' LOAD STEP =',I3/, ' ITERATION =',I3/,
1986      1 ' CURRANT LOAD FACTOR =',F9.6, ' OF CLASSICAL BUCKLING LOAD',/
1987      2 ' CURRANT STEP SIZE =',F9.6/,
1988      3 ' REFINEMENT=',I3/, ' ROTATION =',E14.6, ' DEGREES')
1989      IF (NOVA.EQ.0) GOTO 60
1990      IF (NEXTOV.EQ.1) ITPLUS=ITVAL+1
1991      IF (NEXTOV.EQ.1) ITOVIT=0
1992      IF (NEXTOV.EQ.0) ITOVIT=ITOVIT+1
1993      WRITE(7,50) ITPLUS, ITOVIT
1994      50 FORMAT(' OVALIZATION STEP',I3,', EQUILIBRIUM ITERATION',I3)
1995
1996      C
1997      C STIFFNESS MATRIX, LOAD VECTOR, AND DISPLACEMENT VECTOR
1998      C
1999      60 D1=COST(0)
2000      WRITE(7,70) D1
2001      70 FORMAT('/' BEFORE ASOKT:',F7.2)
2002      IF (IT.EQ.0) GOTO 120
2003      IF (IN(14).EQ.0 .OR. (IN(14).EQ.1.AND.IT.GT.1)) GOTO 90
2004      CALL ASOKT(NOEL,OD,OKT,IX)
2005      PREC=0.1D-15
2006      DAS=COST(0)
2007      WRITE(7,80) DAS
2008      80 FORMAT(' AFTER ASOKT:',F7.2)
2009      GOTO 100
2010      90 IF (IN(13).NE.2 .AND. NOVA.EQ.0) GOTO 120
2011      100 CALL LOADS(IX,IV,P,OKT,VL,NPL,IXNEW,OD)
2012      PREC=0.1D-15
2013      DO 110 I=1,NN5
2014      110 OF(I)=OF(I)+P(I)
2015      120 IF (LCH.GT.0) CALL LOADS2(VL,OF,NPL,IXNEW,1)
2016      CALL VBSOLV(NBAND-1,NN5,PREC,NN5,OF,OKT,ID,NBAND,DET, IEXDET,
2017      1 IV, .TRUE., SUCCES)
2018      IF (IN(8).GE.2) CALL PRTMAT(OKT,NBAND,1,1,NBAND,NN5,'L=OKT/LT')
2019      IF (.NOT.SUCCES) CALL ERROR(9,IS,IT)

```

```

2017      DVB=COST(O)
2018      IF (PREC.LT.O.DO) GOTO 210
2019      C
2020      C      OUTPUT OF THE DETERMINANT AND ITS RELATIVE CONDITION
2021      C
2022      KK=IDINT(DLOG10(DFLOAT(IABS(IEXDET))))+1
2023      WRITE(9,130) KK
2024      130  FORMAT(13H( 1H+,32X,I,I2,''))
2025      REWIND 9
2026      READ(9,140) IF(1),IF(2),IF(3),IF(4)
2027      140  FORMAT(4A4)
2028      WRITE(7,150) DVB,DET
2029      150  FORMAT(' AFTER VBSOLV:',F7.2//
2030      1 ' DETERMINANT =',F10.6,' * 10 **')
2031      WRITE(7,IF) IEXDET
2032      IF (IN(22).EQ.1) CALL TEST(OKT,DET,IEXDET,UNORM)
2033      INN5=NN5
2034      DO 160 I=1,NN5
2035      160  INN5=INN5-ID(I)
2036      IF (INN5.EQ.0) GOTO 200
2037      WRITE(7,170)
2038      170  FORMAT(' NEGATIVE DIAGONAL ELEMENTS IN FOLLOWING ROWS:')
2039      DO 190 I=1,NN5
2040      IF (ID(I).EQ.-1) WRITE(7,180) I
2041      180  FORMAT(' ',I4)
2042      190  CONTINUE
2043      GOTO 250
2044      200  PREC=-O.1D-15
2045      C
2046      C      CHECK OF CONVERGENCE OF DISPLACEMENTS
2047      C
2048      210  DO 220 I=1,NN5
2049      220  OD(I)=OD(I)+OF(I)
2050      IF (IS.EQ.-1) GOTO 310
2051      XDN=O.DO
2052      DO 230 I=1,NN5
2053      A=OF(I)
2054      230  XDN=XDN+OF(I)*A
2055      XDN=DSQRT(XDN)
2056      WRITE(7,240) XDN
2057      240  FORMAT('/ DISPLACEMENT NORM:',E11.4)
2058      IF (IT.EQ.O) XD=XDN
2059      IF (XDN.LE.XD*1.OO1DO) GOTO 280
2060      IF (IN(28).EQ.O) CALL ERROR(10,IS,IT)
2061      250  IF (IHALF.LT.IN(28)) GOTO 270
2062      LCAUSE=3
2063      ISTART=3
2064      CALL RSTART(OKT,P,OD,NOEL,OF,IX,DV,IV,IH,VL,NPL,IXNEW)
2065      260  CONTINUE
2066      LCAUSE=0
2067      ISTART=0
2068      270  CALL ITERA(3,DV,OD)
2069      RETURN
2070      C
2071      280  NCONV=0
2072      IF (XDN.LT.XD*1O.DO**IN(19)) NCONV=1
2073      WRITE(7,290,END=300) (OF(I),I=1,NN5)
2074      290  FORMAT('/ INCREMENTAL DISPLACEMENTS'/(10E12.4))
2075      300  CONTINUE
2076      C
2077      C      EQUILIBRIUM FORCES, AXIAL FORCE AND END MOMENT
2078      C
2079      310  IF (IN(16).GT.1) CALL FORCE1(NOEL,OD)
2080      IF (NCONV.GT.NOVA .OR. IS.EQ.-1) GOTO 380
2081      IF (IN(13).EQ.1) CALL LONGER(OD,DELTA)
2082      CALL EQ(OD,OF,NOEL)
2083      DEQ=COST(O)
2084      IF (IN(16).EQ.1) CALL FORCE2(OF,OD)
2085      WRITE(7,320) DEQ
2086      320  FORMAT('/ AFTER EQ:',F11.2)
2087      I=IN(27)
2088      IF (I.GT.O) WRITE(7,330) I,OF(I)

```

```

2089      330 FORMAT(/' INTERNAL FORCE NR. ',I4,' =',E14.6)
2090      IF (IN(21).EQ.1) WRITE(7,340) (OF(I),I=1,NN5)
2091      340 FORMAT(/' (NEGATIVE) INTERNAL FORCES'/(10E12.4))
2092      DO 350 I=1,NN5
2093      350 IF (IX(I).NE.1) OF(I)=0 DO
2094      XOF=0 DO
2095      DO 360 I=1,NN5
2096      360 XOF=XOF+OF(I)*OF(I)
2097      XOF=DSQRT(XOF)
2098      WRITE(7,370) XOF
2099      370 FORMAT(/' /' NORM OF FREE EQUILIBRIUM FORCES =',E14.6)
2100      GOTO 400
2101      380 DO 390 I=1,NN5
2102      390 OF(I)=0 DO
2103      400 IF (IN(13).EQ.0 .OR. IT.EQ.0 .OR. ITOVIT.LT.NOVA) GOTO 430
2104      IF ((IT.GT.1 .AND. NOVA.EQ.0) .OR. ITOVIT.GT.1) GOTO 410
2105      GOTO 420
2106      410 FLEX=DMAX1(DMIN1(DELTA/(RND-RN),FLEX*0.8D0),FLEX*1.25D0)
2107      420 DELTA=FLEX*RN
2108      430 DELTAT=-OD(1)-OD(NP*5+1)
2109      WRITE(7,440) RN,RM,DELTAT
2110      440 FORMAT(/' AXIAL FORCE =',E18.10,' N'/' MOMENT =',E18.10,
2111      1 ' NMM'/' SHORTENING =',E18.10,' MM')
2112      C
2113      C CHECK FOR MORE EQUILIBRIUM OR OVALIZATION ITERATIONS.
2114      C RESTART, OR OUTPUT
2115      C
2116      IF (IN(30).EQ.2 .AND. NCONV.EQ.1) NOVA=1
2117      IF ((ITOVAL.GE.IN(3) .AND. (ITOVIT.GE.IN(4) .OR. NCONV.EQ.1))
2118      1 .OR. IT.GE.IN(18)) NOVA=0
2119      IF (( (ITOVAL+ITOVIT).EQ.0 .OR. ITOVIT.GE.IN(4) .OR. NCONV.EQ.1)
2120      1 .AND. NOVA.EQ.1) NEXTOV=1
2121      IF (IT.GE.IN(18) .OR. (NCONV.EQ.1 .AND. NOVA.EQ.0)) NEXTIT=0
2122      IF (NEXTIT.GT.NCONV) GOTO 460
2123      C
2124      WRITE (7,450) (I,OD(I),I=1,NN5)
2125      450 FORMAT(/' ///10X,'RESULT-VECTOR'/'5X,'NR. ',
2126      1 ' (MM OR ANGLE)'/, (1X,5(I6,E16.8)))
2127      IF (IN(32).GT.0) CALL STRESS(NOEL,OD)
2128      460 IF (NEXTIT.EQ.1) GOTO 30
2129      IF (IS.EQ.IN(17) .OR. (RMO.GT.RM .AND. IN(20).GT.IHALF)
2130      1 .OR. (IHAF.GT.0 .AND. IHAF.GE. IN(28))) NEXTIS=0
2131      IF (IN(24).EQ.1 .AND. NEXTIS.EQ.0) ISTART=3
2132      C
2133      CALL RSTART(OKT,P,OD,NOEL,DF,IX,DV,IV,IH,VL,NPL,IXNEW)
2134      470 IF (ISTART.EQ.0) GOTO 480
2135      ISTART=0
2136      LCAUSE=0
2137      NEXTIT=1
2138      NEXTIS=1
2139      IF (IN(30).EQ.2 .AND. NCONV.EQ.1) NOVA=1
2140      IF ((ITOVAL.GE.IN(3) .AND. (ITOVIT.GE.IN(4) .OR. NCONV.EQ.1))
2141      1 .OR. IT.GE.IN(18)) NOVA=0
2142      IF ( ((ITOVAL+ITOVIT).EQ.0 .OR. ITOVIT.GE.IN(4) .OR. NCONV.EQ.1)
2143      1 .AND. NOVA.EQ.1) NEXTOV=1
2144      IF (IT.GE.IN(18) .OR. (NCONV.EQ.1 .AND. NOVA.EQ.0)) NEXTIT=0
2145      IF (NEXTIT.EQ.1) GOTO 30
2146      C
2147      C END OF EQUILIBRIUM ITERATION
2148      C
2149      480 IF (IS.EQ.IN(17) .OR. (RMO.GT.RM .AND. IN(20).GT.IHALF)
2150      1 .OR. (IHAF.GT.0 .AND. IHAF.GE. IN(28))) NEXTIS=0
2151      IF (IN(13).NE.0) CALL SHORT(DV,DELTA,DELTAT,IS)
2152      IF (IN(28).EQ.0) RETURN
2153      IF (INNS.EQ.0 .AND. XDN.LT.(XD*10.DO** (DFLOAT(IN(19))/2.DO)))
2154      1 GOTO 490
2155      CALL ITERA(2,DV,OD,VL)
2156      RETURN
2157      490 CALL ITERA(1,DV,OD,VL)
2158      RETURN
2159      END
2160      SUBROUTINE SPARSE(IV,IH)

```

```

2161 C
2162 C COMPUTATION OF FIRST ROW AND LAST COLUMN UNEQUAL ZERO OF
2163 C GLOBAL STIFFNESS MATRIX
2164 C
2165 C IMPLICIT REAL*8(A-H,O-Z)
2166 COMMON / WHOLE /IBC(2),INR,IN(50),IS,IT,IXCH,LCH,NBAND,NEC,
2167 1 NEL,NINTP,NINTS,NINTX,NL,NMAX,NN,NNC,NN5,NPD,NX,NX1,NP,NP1,
2168 2 N2P,N2X,NX2
2169 DIMENSION IV(NN5),IH(NN5)
2170 C
2171 DO 10 I=1,NBAND
2172 10 IV(I)=1
2173 IF (NP.EQ.1) GOTO 30
2174 DO 20 I=3,NP1
2175 I5=I*5-9
2176 K=I5+4
2177 DO 20 J=1,5
2178 20 IV(K+J)=I5
2179 30 IE=NN-1
2180 IA=NP1+2
2181 I5=1
2182 DO 40 I=IA,IE
2183 I5=I5+5
2184 K=I*5
2185 DO 40 J=1,5
2186 40 IV(K+J)=I5
2187 IF (NX.EQ.1) GOTO 60
2188 DO 50 I=2,NX
2189 I5=(I-1)*NP1*5+1
2190 K=I*NP1*5
2191 DO 50 J=1,5
2192 50 IV(K+J)=I5
2193 60 CONTINUE
2194 DO 70 I=1,NN5
2195 70 IH(I)=NN5+1-IV(NN5+1-I)
2196 WRITE(13) IV,IH
2197 REWIND 13
2198 RETURN
2199 END
2200 SUBROUTINE STH(X,P)
2201 C
2202 C COEFFICIENTS OF IN-PLANE STRESS FUNCTIONS
2203 C
2204 C IMPLICIT REAL*8(A-H,O-Z)
2205 COMMON / PART /BETA,BETA2,CBETA,CED,DB,DEG,DELTA,DELTA1,E,ED,
2206 1 EN,E2,FLEX,PEL,PEL2,PI,R,RL,RM,RN,RNU,RNU1,SIGMA,TH,XEL,TIME
2207 COMMON / TMINUS/T(20,20)
2208 COMMON / TF /TXF(20),TPF(20),TPXF(20)
2209 C
2210 S=DSIN(P)
2211 X2DR=X*X/2.DO/R
2212 X2PDR=X2DR*P
2213 X3DR=X2DR*X/3.DO
2214 X3PDR=X3DR*P
2215 DO 10 I=1,20
2216 TXF(I)=T(7,I)+T(8,I)*S
2217 TPF(I)=T(9,I)+T(10,I)*X-T(12,I)*X2DR-T(13,I)*X3DR-T(14,I)*
2218 1 X2PDR-T(15,I)*X3PDR
2219 10 TPXF(I)=T(11,I)
2220 RETURN
2221 END
2222 SUBROUTINE STRESS(NOEL,OD)
2223 C
2224 C CALCULATION OF STRESS DISTRIBUTION ALONG THE CIRCUMFERENCE
2225 C
2226 C IMPLICIT REAL*8(A-H,O-Z)
2227 COMMON / WHOLE /IBC(2),INR,IN(50),IS,IT,IXCH,LCH,NBAND,NEC,
2228 1 NEL,NINTP,NINTS,NINTX,NL,NMAX,NN,NNC,NN5,NPD,NX,NX1,NP,NP1
2229 COMMON / PART /BETA,BETA2,CBETA,CED,DB,DEG,DELTA,DELTA1,E,ED,
2230 1 EN,E2,FLEX,PEL,PEL2,PI,R,RL,RM,RN,RNU,RNU1,PREC,TH,XEL,TIME
2231 COMMON / TF /BX1(20),BP2(20),TPXF(20)
2232 COMMON / BF /BP3(20),BX3(20),BX2(20),BP1(20)

```

```

2233      DIMENSION V(24),V2(24),NOEL(4,NEL),OD(NN5)
2234      C
2235      IF (IN(33).LE.0) RETURN
2236      DP=PI/NP/DFLOAT(IN(33))
2237      ENU=EN/TH/R
2238      X=XEL
2239      C      IF (IN(32).EQ.1) GOTO 2
2240      C      CALL GAUSS(V,V2,24,XEL,NINTS)
2241      C      X=V(NINTS)
2242      C
2243      10 I1=1
2244      I2=NP
2245      WRITE(7,20)
2246      20 FORMAT(' '//, ' STRESSES AT THE CYLINDER END', '/')
2247      GOTO 50
2248      C
2249      30 X=-X
2250      I1=NEL-NP+1
2251      I2=NEL
2252      WRITE(7,40)
2253      40 FORMAT(' '//, ' STRESSES AT THE CYLINDER MIDDLE', '/')
2254      C
2255      50 DO 150 I=I1,I2
2256      WRITE(7,60) I
2257      60 FORMAT(' '//, ' ELEMENT NR.', 'I3,
2258      1      SIGMA X      SIGMA PHI      SIGMA X-PHI', '/')
2259      DO 70 J=1,4
2260      L1=(J-1)*5
2261      L2=(NOEL(J,I)-1)*5
2262      DO 70 L=1,5
2263      70 V(L1+L)=OD(L2+L)
2264      S=-PEL-DP
2265      C
2266      C      LINEAR STRESSES
2267      C
2268      IIE=IN(33)+1
2269      DO 140 II=1,IIE
2270      S=S+DP
2271      CALL STH(X,S)
2272      T1=O.DO
2273      T2=O.DO
2274      T3=O.DO
2275      DO 80 K=1,20
2276      W=V(K)
2277      T1=T1+BX1(K)*W
2278      T2=T2+BP2(K)*W
2279      80 T3=T3+TPXF(K)*W
2280      BETAX1=O.DO
2281      BETAX2=O.DO
2282      BETAX3=O.DO
2283      BETAP1=O.DO
2284      BETAP2=O.DO
2285      BETAP3=O.DO
2286      IF (IN(15).EQ.0) GOTO 120
2287      C
2288      C      NONLINEAR STRESS CONTRIBUTIONS
2289      C
2290      CALL BXP(X,S)
2291      DO 90 K=1,20
2292      BETAX3=BETAX3+BX3(K)*V(K)
2293      90 BETAP3=BETAP3+BP3(K)*V(K)
2294      IF (IN(31).LT.1) GOTO 120
2295      C
2296      DO 100 K=1,20
2297      BETAX2=BETAX2+BX2(K)*V(K)
2298      100 BETAP1=BETAP1+BP1(K)*V(K)
2299      IF (IN(31).NE.2) GOTO 120
2300      C
2301      BETAX1=T1
2302      110 BETAP2=T2
2303      C
2304      120 EPSX=T1+(BETAX1*BETAX1+BETAX2*BETAX2+BETAX3*BETAX3)/2.DO

```

```

2305      EPSP=T2+(BETAP1*BETAP1+BETAP2*BETAP2+BETAP3*BETAP3)/2.DO
2306      EPSXP=T3+(BETAP1*BETAX1+BETAP2*BETAX2+BETAP3*BETAX3)/2.DO
2307      SX=ENU*(EPSX+RNU*EPSP)
2308      SP=ENU*(EPSP+RNU*EPSX)
2309      SXP=E*EPSXP/(1.DO+RNU)
2310      WRITE(7,130) S,SX,SP,SXP
2311      130 FORMAT(F10.6,' ',3E14.6)
2312      140 CONTINUE
2313      150 CONTINUE
2314      IF (I1.EQ.1) GOTO 30
2315      RETURN
2316      END
2317      SUBROUTINE STUFF(OKT,NBAND,J1,INS,EK,ICD,J3,NTNODE,IEL,IX)
2318      C
2319      C*-----
2320      C
2321      C THIS SUBROUTINE INSERTS AN ELEMENT STIFFNESS MATRIX AND CONSISTENT
2322      C LOAD. ROWS AND COLUMNS ARE DELETED FOR THE ZERO BOUNDARY CONDITIONS.
2323      C
2324      C OKT = AN I1XJ1 MATRIX CONTAINING THE TRANSPOSE OF THE LOWER HALF
2325      C BAND OF THE STRUCTURE STIFFNESS MATRIX.
2326      C EK = AN I2X12 MATRIX CONTAINING THE UPPER HALF OF THE ELEMENT
2327      C STIFFNESS MATRIX
2328      C ICD = AN I3XJ3 MATRIX OF INTEGERS. THE (I,J)TH TERM CONTAINS
2329      C THE ITH NODE NUMBER OF THE JTH ELEMENT.
2330      C IEL = THE NUMBER OF THE ELEMENT BEING INSERTED
2331      C NTNODE= THE TOTAL NUMBER OF NODES IN THE ASSEMBLED STRUCTURE
2332      C NBAND = ( THE BANDWIDTH OF THE STRUCTURE STIFFNESS MATRIX )
2333      C IX = A VECTOR CONTAINING THE BOUNDARY CONDITION INFORMATION
2334      C IX(I) = 0 DEGREE OF FREEDOM I SET EQUAL TO ZERO
2335      C IX(I) = 1 DEGREE OF FREEDOM I FREE
2336      C
2337      C*-----
2338      C
2339      IMPLICIT REAL*8(A-H,O-Z)
2340      DIMENSION OKT(NBAND,J1),EK(20,20)
2341      DIMENSION ICD(4,J3),IX(J1),INS(NTNODE),IES(20)
2342      C
2343      IF (IEL.NE.1) GOTO 20
2344      DO 10 I=1,NTNODE
2345      10 INS(I)=(I-1)*5
2346      20 DO 30 I=1,4
2347      30 IES(I)=(I-1)*5
2348      DO 70 JN=1,4
2349      JJN=ICD(JN,IEL)
2350      KJ=INS(JJN)
2351      MJ=IES(JN)
2352      DO 70 IN=JN,4
2353      IIN=ICD(IN,IEL)
2354      KI=INS(IIN)
2355      MI=IES(IN)
2356      DO 70 J=1,5
2357      JJ=J+MJ
2358      JJJ=J+KJ
2359      IF ((IX(JJJ).EQ.0) .AND. (IN.NE.JN)) GOTO 70
2360      DO 60 I=1,5
2361      II=I+MI
2362      III=I+KI
2363      JO=III
2364      IO=NBAND-III+JJJ
2365      IF ((III.GE.JJJ) .OR. (IN.EQ.JN)) GOTO 40
2366      JO=JJJ
2367      IO=NBAND-JJJ+III
2368      40 IF (IX(III).EQ.0 .OR. IX(JJJ).EQ.0) GOTO 50
2369      IF (IO.GT.NBAND) GOTO 60
2370      OKT(IO,JO)=OKT(IO,JO)+EK(JJ,II)
2371      GOTO 60
2372      50 IF (III.EQ.JJJ) OKT(IO,JO)=1.DO
2373      60 CONTINUE
2374      70 CONTINUE
2375      RETURN
2376      END

```



```

2377       SUBROUTINE TEST(OKT,DET,IEXDET,DNORM)
2378       C
2379       C   THIS SUBROUTINE NORMALIZES THE DETERMINANT
2380       C   OF A LOWER TRIANGULAR MATRIX BY DIVIDING EACH J-TH ROW BY
2381       C   SQUARE ROOT ( SUM ( A ,IJ ) ) ; I=1,N
2382       C   AND MULTIPLICATION WITH THE NORMALIZED DETERMINANT OF A
2383       C   TRIANGULAR MATRIX WITH ONLY '1' VALUES
2384       C
2385       C   RELATIVE CONDITION = NMAX / NORMALIZED DETERMINANT
2386       C
2387       C   IMPLICIT REAL*8(A-H,O-Z)
2388       C   COMMON / WHOLE /IBC(2),INR,IN(50),IS,IT,IXCH,LCH,NBAND,NEC,
2389       C   1 NEL,NINTP,NINTS,NINTX,NL,NMAX,NN,NNC,NN5,NPD,NX,NX1,NP,NP1,
2390       C   2 N2P,N2X,NX2
2391       C   DIMENSION OKT(NBAND,NN5)
2392       C
2393       C   DO 20 I=1,NN5
2394       C   S=0.DO
2395       C   DO 10 J=1,NBAND
2396       C   SS=OKT(J,I)
2397       C   10 S=S+SS*SS
2398       C   DET=DET/S
2399       C   K=IDINT(DLOG10(DABS(DET)))
2400       C   DET=DET/10.DO**K
2401       C   20 IEXDET=IEXDET+K
2402       C   DEXDET=(DFLOAT(IEXDET)+DLOG10(DABS(DET))+DNORM)/2.DO
2403       C   RCOND=0.1DO**(DEXDET/DFLOAT(NMAX))
2404       C   WRITE(7,30) RCOND
2405       C   30 FORMAT(' RELATIVE CONDITION =',E14.6)
2406       C   RETURN
2407       C   END
2408       C   SUBROUTINE TMAT
2409       C
2410       C   EXPLICIT INVERSION OF MATRIX T (UNKNOWN DISPLACEMENT PARAMETERS)
2411       C
2412       C   IMPLICIT REAL*8(A-H,L,O-Z)
2413       C   COMMON / PART /BETA,BETA2,CBETA,CED,DB,DEG,DELTA,DELTAT,E,ED,
2414       C   1 EN,E2,FLEX,PEL,PEL2,PI,R,RL,RM,RN,RNU,RNU1,SIGMA,TH,XEL,TIME
2415       C   COMMON / TMINUS/T(20,20)
2416       C
2417       C   P=PEL
2418       C   L=XEL
2419       C   S=DSIN(P)
2420       C   C=DCOS(P)
2421       C   A=C*P-S
2422       C   DO 10 J=1,20
2423       C   DO 10 I=1,20
2424       C   10 T(I,J)=0.DO
2425       C
2426       C   H=.25DO/S
2427       C   T(1,2)=H
2428       C   T(1,7)=H
2429       C   T(1,12)=-H
2430       C   T(1,17)=-H
2431       C   H=H*R
2432       C   T(1,5)=H
2433       C   T(1,10)=H
2434       C   T(1,15)=-H
2435       C   T(1,20)=-H
2436       C   H=.25DO/L/S
2437       C   T(2,2)=H
2438       C   T(2,7)=-H
2439       C   T(2,12)=H
2440       C   T(2,17)=-H
2441       C   H=H*R
2442       C   T(2,5)=H
2443       C   T(2,10)=-H
2444       C   T(2,15)=H
2445       C   T(2,20)=-H
2446       C   H=-L/8.DO/R/S
2447       C   T(3,1)=H
2448       C   T(3,6)=-H

```

2449 $T(3, 11)=H$
 2450 $T(3, 16)=-H$
 2451 $H=-P/4 \cdot DO/A$
 2452 $T(3, 2)=H$
 2453 $T(3, 7)=H$
 2454 $T(3, 12)=H$
 2455 $T(3, 17)=H$
 2456 $H=.25DO/A$
 2457 $T(3, 3)=H$
 2458 $T(3, 8)=H$
 2459 $T(3, 13)=-H$
 2460 $T(3, 18)=-H$
 2461 $H=-P \cdot R/4 \cdot DO/A$
 2462 $T(3, 5)=H$
 2463 $T(3, 10)=H$
 2464 $T(3, 15)=H$
 2465 $T(3, 20)=H$
 2466 $H=-P/4 \cdot DO/L/A$
 2467 $T(4, 2)=H$
 2468 $T(4, 7)=-H$
 2469 $T(4, 12)=-H$
 2470 $T(4, 17)=H$
 2471 $H=.25DO/L/A$
 2472 $T(4, 3)=H$
 2473 $T(4, 8)=-H$
 2474 $T(4, 13)=H$
 2475 $T(4, 18)=-H$
 2476 $H=-H \cdot R \cdot P$
 2477 $T(4, 5)=H$
 2478 $T(4, 10)=-H$
 2479 $T(4, 15)=-H$
 2480 $T(4, 20)=H$
 2481 $H=.25DO$
 2482 $T(5, 1)=H$
 2483 $T(5, 6)=H$
 2484 $T(5, 11)=H$
 2485 $T(5, 16)=H$
 2486 $H=-R \cdot C/4 \cdot DO/L/S$
 2487 $T(5, 2)=H$
 2488 $T(5, 7)=-H$
 2489 $T(5, 12)=H$
 2490 $T(5, 17)=-H$
 2491 $H=-R \cdot R \cdot (2 \cdot DO \cdot C + S \cdot P)/8 \cdot DO/S/L$
 2492 $T(5, 5)=H$
 2493 $T(5, 10)=-H$
 2494 $T(5, 15)=H$
 2495 $T(5, 20)=-H$
 2496 $H=-P \cdot L/16 \cdot DO/R$
 2497 $T(6, 1)=H$
 2498 $T(6, 6)=-H$
 2499 $T(6, 11)=H$
 2500 $T(6, 16)=-H$
 2501 $H=-S \cdot (2 \cdot DO + P \cdot P)/8 \cdot DO/A$
 2502 $T(6, 2)=H$
 2503 $T(6, 7)=H$
 2504 $T(6, 12)=H$
 2505 $T(6, 17)=H$
 2506 $H=-H \cdot C/S$
 2507 $T(6, 3)=H$
 2508 $T(6, 8)=H$
 2509 $T(6, 13)=-H$
 2510 $T(6, 18)=-H$
 2511 $H=-P \cdot L/16 \cdot DO$
 2512 $T(6, 4)=H$
 2513 $T(6, 9)=-H$
 2514 $T(6, 14)=H$
 2515 $T(6, 19)=-H$
 2516 $H=-P \cdot R \cdot (2 \cdot DO \cdot C + S \cdot P)/8 \cdot DO/A$
 2517 $T(6, 5)=H$
 2518 $T(6, 10)=H$
 2519 $T(6, 15)=H$
 2520 $T(6, 20)=H$

2521 $H = .25DO/L$
 2522 $T(7,1) = H$
 2523 $T(7,6) = -H$
 2524 $T(7,11) = -H$
 2525 $T(7,16) = H$
 2526 $H = H/S$
 2527 $T(8,1) = H$
 2528 $T(8,6) = -H$
 2529 $T(8,11) = H$
 2530 $T(8,16) = -H$
 2531 $H = C/4 . DO/R/S$
 2532 $T(9,2) = H$
 2533 $T(9,7) = H$
 2534 $T(9,12) = -H$
 2535 $T(9,17) = -H$
 2536 $H = .25DO/R$
 2537 $T(9,3) = H$
 2538 $T(9,8) = H$
 2539 $T(9,13) = H$
 2540 $T(9,18) = H$
 2541 $H = -L/8 . DO/R$
 2542 $T(9,4) = H$
 2543 $T(9,9) = -H$
 2544 $T(9,14) = -H$
 2545 $T(9,19) = H$
 2546 $H = A/4 . DO/S/P$
 2547 $T(9,5) = H$
 2548 $T(9,10) = H$
 2549 $T(9,15) = -H$
 2550 $T(9,20) = -H$
 2551 $H = C/4 . DO/L/R/S$
 2552 $T(10,2) = H$
 2553 $T(10,7) = -H$
 2554 $T(10,12) = H$
 2555 $T(10,17) = -H$
 2556 $H = 0.375DO/R/L$
 2557 $T(10,3) = H$
 2558 $T(10,8) = -H$
 2559 $T(10,13) = -H$
 2560 $T(10,18) = H$
 2561 $H = -0.125DO/R$
 2562 $T(10,4) = H$
 2563 $T(10,9) = H$
 2564 $T(10,14) = H$
 2565 $T(10,19) = H$
 2566 $H = A/4 . DO/S/L/P$
 2567 $T(10,5) = H$
 2568 $T(10,10) = -H$
 2569 $T(10,15) = H$
 2570 $T(10,20) = -H$
 2571 $H = 0.25DO/P/R$
 2572 $T(11,1) = H$
 2573 $T(11,6) = H$
 2574 $T(11,11) = -H$
 2575 $T(11,16) = -H$
 2576 $H = -S * P * P / 12 . DO/L/A$
 2577 $T(11,2) = H$
 2578 $T(11,7) = -H$
 2579 $T(11,12) = -H$
 2580 $T(11,17) = H$
 2581 $H = 0.25DO/P/L + P * (3 . DO * C * P - S) / 24 . DO/L/A$
 2582 $T(11,3) = H$
 2583 $T(11,8) = -H$
 2584 $T(11,13) = H$
 2585 $T(11,18) = -H$
 2586 $H = -P / 24 . DO$
 2587 $T(11,4) = H$
 2588 $T(11,9) =$
 2589 $T(11,14)$
 2590 $T(11,19) = H$
 2591 $H = (-S * P * P - 3 . DO * A) * R / 12 . DO/L/A$
 2592 $T(11,5) = H$

2593	T(11,10)=-H
2594	T(11,15)=-H
2595	T(11,20)=H
2596	H=-0.25DO/L
2597	T(12,4)=H
2598	T(12,9)=-H
2599	T(12,14)=-H
2600	T(12,19)=H
2601	H=.75DO/L/L/L
2602	T(13,3)=H
2603	T(13,8)=-H
2604	T(13,13)=-H
2605	T(13,18)=H
2606	H=-0.75DO/L/L
2607	T(13,4)=H
2608	T(13,9)=H
2609	T(13,14)=H
2610	T(13,19)=H
2611	H=-0.25DO/L/R/P
2612	T(14,1)=H
2613	T(14,6)=-H
2614	T(14,11)=H
2615	T(14,16)=-H
2616	H=-0.25DO/P/L
2617	T(14,4)=H
2618	T(14,9)=-H
2619	T(14,14)=H
2620	T(14,19)=-H
2621	H=.75DO/P/L/L/L
2622	T(15,3)=H
2623	T(15,8)=-H
2624	T(15,13)=H
2625	T(15,18)=-H
2626	H=-H*L
2627	T(15,4)=H
2628	T(15,9)=H
2629	T(15,14)=-H
2630	T(15,19)=-H
2631	H=-0.25DO/R/P
2632	T(16,5)=H
2633	T(16,10)=H
2634	T(16,15)=-H
2635	T(16,20)=-H
2636	H=H/L
2637	T(17,5)=H
2638	T(17,10)=-H
2639	T(17,15)=H
2640	T(17,20)=-H
2641	H=L/8.DO/P/R/R/R
2642	T(18,1)=H
2643	T(18,6)=-H
2644	T(18,11)=H
2645	T(18,16)=-H
2646	H=S/4.DO/R/R/A
2647	T(18,2)=H
2648	T(18,7)=H
2649	T(18,12)=H
2650	T(18,17)=H
2651	H=-C/4.DO/R/R/A
2652	T(18,3)=H
2653	T(18,8)=H
2654	T(18,13)=-H
2655	T(18,18)=-H
2656	H=L/8.DO/P/R/R
2657	T(18,4)=H
2658	T(18,9)=-H
2659	T(18,14)=H
2660	T(18,19)=-H
2661	H=S/4.DO/R/A
2662	T(18,5)=H
2663	T(18,10)=H
2664	T(18,15)=H

```

2665      T(18,20)=H
2666      H=S/4.DO/L/R/R/A
2667      T(19,2)=H
2668      T(19,7)=-H
2669      T(19,12)=-H
2670      T(19,17)=H
2671      H=(S-3.DO*C*P)/8.DO/P/L/R/R/A
2672      T(19,3)=H
2673      T(19,8)=-H
2674      T(19,13)=H
2675      T(19,18)=-H
2676      H=0.125DO/P/R/R
2677      T(19,4)=H
2678      T(19,9)=H
2679      T(19,14)=-H
2680      T(19,19)=-H
2681      H=S/4.DO/R/L/A
2682      T(19,5)=H
2683      T(19,10)=-H
2684      T(19,15)=-H
2685      T(19,20)=H
2686      H=-0.0625DO/P/R/R
2687      T(20,1)=H
2688      T(20,6)=H
2689      T(20,11)=-H
2690      T(20,16)=-H
2691      H=-S*P*P/9.6DO/R/L/A
2692      T(20,2)=H
2693      T(20,7)=-H
2694      T(20,12)=-H
2695      T(20,17)=H
2696      H=(5.DO*P*P*(3.DO*C*P-S)-18.DO*A)/96.DO/R/P/L/A
2697      T(20,3)=H
2698      T(20,8)=-H
2699      T(20,13)=H
2700      T(20,18)=-H
2701      H=(12.DO-5.DO*P*P)/96.DO/P/R
2702      T(20,4)=H
2703      T(20,9)=H
2704      T(20,14)=-H
2705      T(20,19)=-H
2706      H=-(5.DO*P*P*S+9.DO*A)/48.DO/L/A
2707      T(20,5)=H
2708      T(20,10)=-H
2709      T(20,15)=-H
2710      T(20,20)=H
2711      RETURN
2712      END
2713      SUBROUTINE UVW(X,P)
2714      C
2715      C      COMPUTATION OF ELEMENT DISPLACEMENTS
2716      C
2717      IMPLICIT REAL*8(A-H,O-Z)
2718      COMMON / PART /BETA,BETA2,CBETA,CED,DB,DEG,DELTA,DELTAT,E,ED,
2719      1 EN,E2,FLEX,PEL,PEL2,PI,R,RL,RM,RN,RNU,RNU1,SIGMA,TH,XEL,TIME
2720      COMMON / TMINUS/T(20,20)
2721      COMMON / DELVW /RV(20),RW(20)
2722      C
2723      DS=DSIN(P)
2724      DC=DCOS(P)
2725      X2=X*X/2.DO
2726      RX=X*R
2727      XP=X*P
2728      P2=P*P/2.DO
2729      XD4=X/4.DO
2730      R2=R*R
2731      X2CR=X2*DC/R
2732      X2SR=X2*DS/R
2733      S=X*(P2-1.DO)
2734      DO 10 I=1,20
2735      RV(I)=(T(1,I)+T(2,I)*X)*DS-(T(3,I)+T(4,I)*X)*DC+T(6,I)-
2736      1 T(8,I)*X2CR+T(11,I)*XD4+

```

```
2737      2 R2*(T(16,I)*P+T(17,I)*XP+T(18,I)*P2+T(19,I)*S)+T(20,I)*RX
2738      RW(I)=- (T(1,I)+T(2,I))*DC-(T(3,I)+T(4,I)*X)*DS-T(8,I)*X2SR+
2739      1 R*(T(9,I)+T(10,I)*X)-
2740      2 X2*(T(12,I)+T(13,I)*X/3.DO+T(14,I)*P+T(15,I)*XP/3.DO)-
2741      3 R2*(T(16,I)+T(17,I)*X+T(18,I)*P+T(19,I)*XP)
2742 10 CONTINUE
2743     RETURN
2744     END
END OF FILE
```

Appendix B.2

Input Description

The input format for the program is given below with an example of the input for the pinched cylinder problem.

```

M,
TITLE
RL,R,TH,E,RNU,
NX,NP,
IBC(1),IBC(2),
NINTX,NINTP,NINTS,
CBETA,CED,
INL,INL1,INN,
IN(1), ..., IN(INL),           (INL values)
IN(INL1), ..., IN(INN),       (INN-INL1+1 values)
IXCH,LCH,
K,L,                           (IXCH lines)
K,L,F,                         (LCH lines)

```

Input data for the pinched cylinder problem

```

1,
TEST WITH THIN PINCHED CYLINDER
10.35,4.953,0.01548,10500000,0.3125,
1,1,
2,2,
16,16,16,
0,0,
12,16,33,
1,0,0,0,1, 1,0,0,0,1, 0,0,0,0,0,
0,1,0,0,0, 1,0,0,0,0, 785398164,0,0,0,0, 0,0,0,
10,1,
1,1,
3,1,
4,1,
6,1,
7,1,
8,1,
9,1,
11,1,
13,1,
14,1,
33,3,0.025,

```

Explanation of Input Variables

M computational indicator
 1: initial program run
 2: restart run

TITLE heading for output

RL length of cylinder

R radius of cylinder

TH thickness of cylinder

E Young's modulus

RNU Poisson's ratio

NX number of elements in the longitudinal direction

NP number of elements in the circumferential direction

IBC symmetry conditions
 about longitudinal axes, IBC(1): 1=asymmetry
 2=symmetry
 about axes at mid half, IBC(2): 1=asymmetry
 2=symmetry
 (as yet, the program is only tested for double symmetry)

NINTX gaussian integration order for the x-direction

NINTP gaussian integration order for the ϕ -direction

NINTS gaussian integration order for stress computation

CBETA ratio of (applied end rotation per load step) /
 (angle which causes classical cylinder-buckling stress)

CED ratio of (applied shortening of cylinder) /
 (shortening which causes the lesser of cylinder or column buckling stress)

INL,INL1,INN first and last indices to read array IN(I)

IN(I) parameter vector.
 if no values are given, the description is in effect for a value of '1' and not in effect for a value of '0'

- 1 one quarter of the cylinder is analyzed
- 2 print matrix 'E2K'
- 3 number of ovalization iterations
- 4 number of equilibrium iterations per ovalization
- 5 output of material properties and geometry
- 6 output of boundary condition etc.
- 7 print matrix 'OK, FIRST'
- 8 print matrix 'OK, +LOAD'
- 0 no output of matrix
 - 1 before VBSOLV
 - 2 after VBSOLV
 - 3 both, 1 and 2
- 9 print load vector
- 10 print deformation vector
- 11 element stiffness matrices are read from file 11
- 12 nonlinear analysis is performed
- 13 maintain a specified axial force

- 0 axial force is not maintained
- 1 adjustments of all u - displacements
- 2 load vector and boundary condition are changed
- 14 tangent stiffness matrix is recalculated
 - 0 before each load step
 - 1 as 0 and before each first iteration
 - 2 as 0 and before each equilibrium iteration
- 15 calculation of forces includes nonlinear terms (always included, if IN(16) = 1)
- 16 cylinder forces are calculated from
 - 0 (no calculation)
 - 1 equilibrium forces
 - 2 stress integration along boundary
 - 3 stress integration at integration points
- 17 maximum number of successful load steps
- 18 maximum number of equilibrium iterations
- 19 pivot number to control iteration (if $XD < XDN * 10 ** IN(19)$, stop iteration),
 XD is the vector norm of the first deflection increment,
 XDN is the vector norm of an increment during an equilibrium iteration
- 20 no load steps after decreasing end moment
- 21 output of out-of-balance forces
- 22 output of determinants
 - 0: output of determinant of altered stiffness matrix only
 - 1: compute normalized determinant
 - 2: compute determinant of unchanged stiffness matrix
- 23 restart: (local and global time limit is set)
- 24 restart: storage of variables without time limits being reached
- 25 only stiffness calculation
- 26 if $IN(26) > 0$, $PEL=IN(26)/10**9$
 PEL=half of angle subtended by element (for non-cylinder problems)
- 27 if $IN(27) > 0$, output of equilibrium force: IN(27)
- 28 number of refinements for buckling load (IN(20) is ignored)
- 29 if $IN(29) > 0$, $REDUCE=IN(29)/10**4$
- 30 boundary condition flag
 - 0: rigid cylinder ends
 - 1: include donnell-stretch in nonlinear boundary conditions
 - 2: iterate to cross-section of mid-length of cylinder
- 31 inclusion of nonlinear strain parts for the computation of nonlinear stiffness matrices
 - 0: simplest expression for nonlinear strains
 - 1: extended expression for nonlinear strains
 - 2: full expression for nonlinear strains

32 calculation of stresses at the circumference
 0: no calculation
 1: stresses at the boundaries of cylinder
 2: stresses at the nearest integration points for the longitudinal direction
 33 number of points for stress calculation
 34 to 50: not used

IXCH Number of changes of boundary conditions
 LCH Number of changes of loads
 K,L K: degree of freedom to be changed,
 L: new degree of freedom
 0: displacement restricted to a value of 0
 1: displacement is free, load may be prescribed
 2: displacement with value other than 0 is prescribed

K,L,F K: degree of freedom to be changed,
 L: description whether load or displacement is to be described, and whether it is held constant or increased with each load step
 3: constant load is prescribed
 4: additional load per load step
 5: constant displacement is specified
 6: additional displacement per load step
 F: value of prescribed load or displacement

The necessary data to restart the program is given below.

2,
 NCHIN,NED,NDB,NREDUC,0,0,
 I,J (NCHIN lines)
 EDNEW (if NED≠0),
 DBNEW (if NDB≠0),
 REDUCE 0 (if NREDUC≠0)

Hereby are

NCHIN number of changes for parameter vector "IN"
 NED factor for input variable "CED"
 NDB factor for input variable "CBETA"
 I,J parameter IN("I") is given the value "J"
 REDUCE factor with which the load step size is reduced if a negative determinant is detected

The following files are needed during the computation:

- 5 input data
- 6 error diagnosis
- 7 input echo, results
- 8 temporary storage for global stiffness matrix
- 9 temporary storage for format construction
- 10 storage for restart
- 11 storage of stiffness matrices
- 12 temporary storage during step size iteration
- 13 temporary storage of reference vectors